ABSTRACTS FROM THE 15TH CONGRESS OF THE INTERNATIONAL VETERINARY RADIOLOGY ASSOCIATION

BÚZIOS, RIO DE JANEIRO, BRAZIL
JULY 26-31, 2009

SERIAL POSTMORTEM ABDOMINAL RADIOGRAPHIC FINDINGS IN CANINE CADAVERS.

[1,2]H.G. Heng, [2]G. Thevi, [2]H.T. Lim, [2]J.S. Ong, [2]J. H. Lim, [2]J.T. Ooi.
[1]Department of Veterinary Clinical Sciences, Purdue University, 625 Harrison Street, West Lafayettem, IN 47907. USA. [2]Faculty of Veterinary Medicine, University Putra Malaysia, 43300 Serdang, Selangor Malaysia.

Introduction

Post mortem radiographic examinations of animals are often performed in judicial investigation to rule out gunshot and fractures due to cruelty. Literatures describing animal abdominal radiographic postmortem changes are rarely available.

Methods

Serial lateral and ventrodorsal abdominal radiographs of 6 recently euthanized dogs were performed in intervals of 8 hours at a tropical ambient temperature of 22 to 33ºC. All six had radiographs at 16 hours post-euthanasia and only 3 had radiographs at 24 hours post-euthanasia. Radiographic changes such as presence of gas and/or fluid in the peritoneal cavity and retroperitoneal space and gas in the blood vessels were observed. The size of the stomach was estimated and the diameter of the small intestines and colon were measured.

Results

Gradual increment of gas accumulation in the gastrointestinal tract, liver, spleen, kidney and blood vessels were observed. Increased amount of gas in the gastrointestinal tract was detected as early as 8 hours post-euthanasia and continuously increased throughout the study. Gas was seen in the portal vein and caudal vena cava of all cadavers at 16 hours post-euthanasia. The presence of gas in the aorta occurred at a later stage. Tubular branching gas pattern in the liver and spleen was first observed and progressed to vesicular gas pattern due to tissue decomposition.

Discussion

This study shows that gradual gas production and accumulation in the peritoneal cavity, abdominal organs and blood vessels is a consequence of putrefaction. The abdominal radiographic postmortem changes occurred most rapidly between 8 and 16 hours post-euthanasia at the ambient temperature of 22 to 33ºC. Interpretation of postmortem radiographs should be taken into consideration of the normal postmortem changes as described in this study.

Radiographic Interpretations of Some Cardiac Affections in Dogs

Torad, F.A. Department of Surgery, Anesthesiology & Radiology , Faculty of Veterinary Medicine, Cairo University, Egypt.

Abstract

Radiographic examination is still a valuable routine procedure for diagnosing cardiopulmonary diseases and assessing their response to treatment.

Methodology: In the present study, thoracic radiography was carried out on 47 clinical cases of dogs that suffered from cardiac problem- and five apparently healthy mongrel dogs that were used as a control for normal radiography of the canine heart. The diseased dogs were of both sexes and of ages that ranged between 45 days and 12 years.

Results: The recorded affections were; persistent right aortic arch (2), microcardia (2), left atrial dilatation (6), right ventricular dilatation (9), generalized cardiomegaly (18), pericardial effusion (8), hypertrophic cardiomyopathy (1) and pneumopericardium (1). All radiographic findings of both normal and diseased canine hearts were described.

Conclusion: thoracic radiography still constitutes the cornerstone for diagnosing and evaluating cardiopulmonary diseases through providing direct and immediate information about cardiac size and shape, and indirectly through assessing the cardiopulmonary circulation which reflects the degree of heart failure.

The Role of Radiography in Diagnosing Some Canine Thoracic Affections

Torad, F.A.; Abu Sieda, A. and El-Tookhy, O. Department of Surgery, Anesthesiology & Radiology , Faculty of Veterinary Medicine, Cairo University, Egypt.

Abstract

Radiographic images of the thorax are important for evaluating patients with known or suspected thoracic diseases. Thoracic radiography provides direct information about lesions or abnormalities in lung parenchyma, airways, and plural and mediastinal spaces.

Methodology: The present study was carried out between October 2005 and December 2008. Plain thoracic radiography was done on 82 clinical cases of dogs diagnosed clinically as having respiratory disease. Contrast media was used where indicated.

Results: The recorded affections were; pectus excaratum (2), tracheal collapse (5), oesophegeal dilatation (9), mediastinal foreign body (2), pneumomediastinum (2), tension pneumothorax (5), pneumothorax (12), hydropneumothorax (1), plural effusion –mild- (4), moderate (9), severe (15), primary lung neoplasm (3), focal metastatic pulmonary neoplasia (7), metastatic trachobroncheal lymphadenopathy (2), metastatic rib neoplasm (1), and pulmonary bullae (3).

Conclusion: Thoracic radiography serves to verify the diagnosis, document the extent and location of the lesion, assist in detecting complication and also helpsl in classifying the lesions.

THE EFFECT OF POSITIONING ON THE APPEARANCE OF CAUDODORSAL CANINE MEDIASTINAL MASSES. R.M. Kirberger, E. Dvir, L.L. van der Merwe. Faculty of Veterinary Science, University of Pretoria, Private Bag X04, Onderstepoort 0110, Republic of South Africa.

Introduction

The effect of various radiographic views on the visibility or position of normal and pathologic thoracic structures in the dog is well described. Mediastinal pathology is better delineated on a DV or VD but no specific positioning recommendations are available for caudodorsal mediastinal pathology. This prospective study was undertaken to determine the effect of positioning on the visibility and size of caudodorsal mediastinal pathology, and in particular, cases with endoscopically confirmed intraluminal *Spirocerca lupi* nodules in the terminal esophagus.

Methods

Twenty eight dogs with endoscopically confirmed *Spirocerca lupi* were evaluated. Each dog had 4 standard radiographic thoracic views made (DV, VD, RLR and LLR) which were examined independently from each other to avoid interpretation bias due to known mass on another view. On each view mass visibility was evaluated as definitely not present; possibly present, likely to be present and definitely present. Additionally the length of the mass was measured in mm on all views**.** The nodules were endoscopically assessed for number and individual length as well as confluent length of esophageal involvement. Visibility of the masses between the 4 views were compared using the chi square test. The difference in the nodule mean length was compared between views. Length measurements in the different views were also tested for correlation with endoscopic length. The significance level for all tests was $P<0.05$.

Results

Masses were seen equally well in left *versus* right recumbency as well as in DV *versus* VD positions. However the latter identified 86% (24/28) of masses whereas lateral views only identified 50% (14/28) of masses, the difference being statistically significant. In 10 dogs masses were only seen on DV and VD radiographs. While DV or VD views were superior for detection, the lateral recumbent views were superior for measurement, with RLR view showing the best linear correlation with endoscopic measurement ($r^2=0.84$).

Discussion

Subtle or early pathology of the mediastinum is often difficult to assess. This study proves that DV/VD radiographs are more reliable to detect a caudodorsal mediastinal mass than lateral radiographs. As there were no significant difference between the visibility indices between VD and DV or RLR and LLR other factors should be taken into consideration when deciding which view to make. In spirocercosis endemic areas the left lateral border of the descending aorta is evaluated for evidence of aneurysms and as the aorta is better defined on the DV view, this view should thus take preference. On a LLR view a normal esophagus may be seen in large breed dogs so a RLR view should preferably be made and this view also resulted in the most accurate dimension of the pathology.

RADIOGRAPHIC EVALUATION OF LIVER SIZE IN PEKINGESE DOGS

J.H. Choi[1], S.Y. Keh[1], H.W. Kim[1], M.E. Kim[2], M.C. Choi[2], J.H. Yoon[2]
[1]Haemaru Referral Animal Hospital, Seongnam, Gyeonggi-do, 463-050, South Korea.
[2]College of Veterinary Medicine and BK21 Program for Veterinary Science, Seoul National University, Seoul, 151-742, South Korea.

Introduction: Survey radiography of the abdomen may produce useful information in animals with suspected hepatobiliary disease, particularly on the view of liver size. The authors have observed that a large number of clinically healthy Pekingese dogs showed cranially displaced gastric axis during practice. Thus we speculated that the gastric axis has the limit as a reliable criterion to determine normal or altered liver size in Pekingese.

Methods: ANIMALS: 61 clinically healthy Pekingese dogs, 45 brachycephalic breed dogs, and 71 non-brachycephalic breed dogs; and 22 Pekingese dogs with liver disease (all dogs > 1 year old). PROCEDURE: Liver length (LL), length of 11^{th} thoracic vertebra (T11), thoracic depth (TD), and thoracic width (TW) were measured on right lateral and ventrodorsal views in all dogs. Liver volume (Lvol) was calculated using the formula; 11.62 + 0.154 (LL X TD X TW), and the ratios including LL/T11 and Lvol per bodyweight were determined.

Results: Lvol per bodyweight of clinically healthy Pekingese (16.73 ± 5.67) was significantly smaller than those of brachycephalic breed dogs (19.54 ± 5.03) and non-brachycephalic breed dogs (18.72 ± 6.52). LL/T11 of clinically healthy Pekingese (4.64 ± 0.65) was significantly lower than those of brachycephalic breed dogs (5.16 ± 0.74) and non-brachycephalic breed dogs (5.40 ± 0.74). Lvol per body weight and LL/T11 of clinically healthy Pekingese were significantly different from those values of Pekingese with liver diseases; 21.19 ± 8.45 and 5.33 ± 0.98, respectively. Reproducibility and repeatability were statistically significant ($p < 0.05$).

Discussion: Liver volume estimated using a formula through abdominal radiograph has significant correlation with real liver volume. Liver length measured on right lateral radiograph can represent for the liver volume. In this study, normal Pekingese has smaller liver volume than other breeds even such as non-brachycephalic breed. We speculated that LL/T11 (4.64 ± 0.65) could be used as a reliable criterion for the liver size in Pekingese. However, it is considered that the clinical significance should be evaluated in large population of Pekingese with liver disease through further study.

OBSERVER VARIABILITY IN RADIOGRAPIC DETECTION OF MEDIAL CORONOID PROCESS DISEASE USING ARTHROSCOPY AS GOLD STANDARD

F.C. Rau, A. Wigger, B. Tellhelm, S. Klumpp, M. Zwick, K. Amort, B. Oltersdorf, M. Kramer. Department of Veterinary Sciences, Justus-Liebig-University Giessen,
Clinic for Small Animals, Surgery, Frankfurter Str. 108, 35392 Giessen, Germany

Introduction

Medial coronoid process disease (MCD) is the most common manifestation of canine elbow dysplasia (ED). Screening for elbow dysplasia (ED) is routinely performed by evaluating radiographs for ED lesions. Presumptive radiographic diagnosis MCD is frequently based on the detection of secondary changes rather than that of primary lesions. In contrast to conventional radiography, the use of CT allows superimposition–free imaging of medial coronoid process and is therefore a more sensitive technique for the detection of MCD. In our experience sensitivity of the presumptive radiographic diagnosis is highly dependent on training and experience level of the observer. Thus, the aim of our study was to investigate the sensitivity of the interpretation of observers with different experience levels in the detection of MCD in radiographs with CT findings using arthroscopy as gold standard.

Methods

Radiographs of 62 elbows of dogs, which all underwent CT and arthroscopy of their elbows, were evaluated for MCD and their secondary changes by 4 observers (student, PhD student, ECVDI 4th year resident, ECVDI diplomate) of different training / experience level. CT images were reviewed for MCD and their secondary changes by an ECVDI resident and arthroscopy findings by an in arthroscopy trained surgeon. Sensitivity of analysis of radiographs and of CT findings was determined by using arthroscopic findings as gold standard.

Results

Sensitivity of the radiographic interpretation for MCD was increasing with higher level of experience and was highest with 98% in the most experienced observer. The sensitivity of the two more-experienced observers with 97-98% was significantly higher than that of the two less-experienced observers ranging between 75-86%. False negatives for MCD showed all heterogeneous radio-opacity of the medial coronoid process and either no or only minimal osteophyte formation. Further, in most of those cases mild subtrochlear sclerosis and minimal radioulnar incongruence with short radius was present. Interobserver agreement was highest with 97% between the two most-experienced and was lowest between the two least-experienced observers with 69%. CT detected MCD with a sensitivity of 100%.

Discussion

The results of this study confirm that training/experience plays an important role in order to reach high sensitivity for the presumptive diagnosis of MCD on radiographs. While the most of the breeder associations require ED evaluation by specialists, there is no recommendation existing for the growing individual canine patient.
Therefore, radiographic screening for MCD is advised to be performed by trained radiologists in order to direct “suspicious” cases to a second diagnostic step before secondary changes occur or progress and prognosis for a life without lameness is decreasing.

EVALUATION OF OCCIPITAL DYSPLASIA IN TOY POODLE AND YORKSHIRE TERRIER. C.O. Baroni, A.M. Hayashi, J.M. Matera, C.M.K. Chamone, A.C.B.C. Fonseca Pinto. School of Veterinary Medicine and Zootecnhy – USP, Av. Prof. Orlando Marques de Paiva, 87, Cidade Universitária, SP, Brasil 05508-270.

Introduction: Occipital dysplasia consists of a dorsal midline extension of the foramen magnum into the occipital bone, which can vary in shape and size. It is the result of the incomplete ossification of the ventromedial part of the supraoccipital bone. Some animals present a membranous tissue on the dorsal enlargement covering the caudal portion of the cerebellum. The supraoccipital bone can be thin on its ventromedial part and if the thickness is decreased, the dorsal extension of the foramen magnum might get overestimated on the radiographic examination. The purpose of this study was to radiographically evaluate the foramen magnum and classify its morphologic and morphometric aspects in two dog breeds.

Methods: Thirty asymptomatic dogs, 15 Toy Poodles and 15 Yorkshire terriers, were selected following individual analysis protocols. Rostrocaudal projection was chosen to observe the foramen magnum. Ventrodorsal projection was made to visualize the odontoid process and lateral projection for the evaluation of the cervical area to exclude other abnormalities. To analyze the morphometry some variables were checked: normal height (h), dorsal extension height (N), total height (H = N+h), width (W), area (A) and width of the dorsal extension (w).

Results: The radiographic evaluation of the cervical spinal cord and the odontoid process of all studied animals was enough to exclude any possible radiographic bone alterations of this region. 40% (6) Toy Poodle dogs were male and 60% (9) were female, with an age group between 9 months and 11 years and weight body from 5,07 lb to 18,29 lb. 47% (7) Yorkshire terrier dogs were male and 53% (8) were female, with an age group between 11 months and 8 years and weight body from 5, 62 lb to 19, 40 lb. 87% (26) of all the animals were radiographically normal and 13% (4) were dysplastics. According to the foramen magnum morphology of the studied animals, it was possible to classify the radiographic shapes into two groups: oval and quadrangular. The average and standard deviation related to the measurements of the foramen magnum were: Toy Poodle: h=13,9 sd=1,5; N=4,6 sd=4,6; H=18,5 sd=4,1; W=17,7 sd=0,9; A=213,8 sd=34,6; w=6,6 sd=4,1; Yorkshire terrier: h=13,0 sd=0,8; N=6,7 sd=3,5; H=19,8 sd=3,1; W=16,5 sd=0,8; A=222,0 sd=40,5; w=8,7 sd=2,5.

Discussion: Asymptomatic animals with oval and quadrangular radiographic shapes of the foramen magnum that present different dorsal enlargements grades and are radiographically classified as dysplastic may simply be representing anatomic variations of the foramen magnum. One of the animals has presented a decreased radiopacity of the supraoccipital bone, one very slender radiopaque line delimitating the foramen magnum and showed a radiographic image of the supraoccipital bone having the same radiolucency observed in dysplastic animals and according to other studies,these can increase the difficulty to make the radiographic diagnosis. Computed tomography and magnetic resonance imaging can help diagnose possible concomitant diseases to the occipital dysplasia, like foramen magnum caudal malformation, also known as occipital hypoplasia or Chiari type I and syringomyelia.

APPLICATION OF THE VERTEBRAL HEART SIZE (VHS) METHOD IN THORACIC RADIOGRAPHS OF POODLES WITH NORMAL AND ENLARGED HEARTS

A.C.B.C. Fonseca Pinto, G.P.R. Banon. School of Veterinary Medicine and Zootechny, University of São Paulo, Av. Prof. Orlando Marques de Paiva, 87, Cidade Universitária, 05508-270, SP, Brazil.

Introduction Thoracic radiography is one of the most important diagnostic tools used in small animal cardiovascular medicine and also one of the most difficult to interpret. Therefore, in order to minimize the subjectivity of the cardiac silhouette evaluation, many methods have been proposed for measuring heart size. Buchanan and Bücheler (1995) proposed VHS method in which the thoracic vertebral bodies have been used as a unit for cardiac dimension. However, to increase the accuracy of the VHS method, it is indispensable to establish an upper limit value for different dog breeds.

Methods In this retrospective study**,** mature, males and females Poodles were allotted to two groups: clinically normal animals and patients with cardiac diseases. Radiographs of twenty-seven sound Poodles, selected in a previous research (Fonseca Pinto and Iwasaki, 2004) by anamnesis, physical examination and electrocardiogram, were reevaluated. The radiographic database at the Diagnostic Imaging Service was reviewed in a lower one-year period (2008) in order to identify dogs with cardiac abnormalities. Forty-six Poodles were selected according to diagnosis of cardiac disease, based on physical examination, electrocardiogram, thoracic radiographs and, in some cases, echocardiogram. All these animals had ventrodorsal, right and left lateral thoracic radiographs done. Among the clinically normal Poodles, first, the empiric analysis was applied. In all animals, the measurement method was performed in right lateral radiographic view, as described bellow: long axis and short axis heart dimensions were transposed onto the vertebral column, starting at the T_4, to transform these distances in vertebral scale (*v*) and afterward, these values were added to express the VHS. The VHS method was performed by an experienced observer and a trainee.Their measurement values were compared using simple linear regression analysis.

Results Among the clinically normal Poodles, the empiric analysis showed some radiographic changes in 9 (33%) dogs. Since the VHS measurements of both observers were not significantly different ($P>0.05$), the interobserver average value was used as final VHS. The obtained VHS values had a normal distribution in both groups. Clinically normal Poodles and dogs suffering from cardiac disease, respectively, had the median VHS 10.11*v* and 11.66*v*, standard deviation 0.50*v* and 1.18*v*, minimum VHS value 9.3*v* and 9.6*v*, and maximum VHS value 11.0*v* and 14.0*v*. 21 (78%) of the clinically normal dogs and 4 (8%) of the diseased dogs have a VHS value equal or smaller than 10.5*v*. Among dogs with cardiac disease, 26 (57%) were diagnosed with mitral regurgitation, 19 (41%) with mitral and tricuspid regurgitation and 1 (2%) with patent ductus arteriosus.

Discussion Empiric approach of cardiac silhouette gave a rough estimate of heart size. If 10.5*v*, proposed by Buchanan and Bücheler for any breeds, was considered the upper limit value for Poodles, the VHS method would give a higher estimate of the heart size. To increase the specificity of this method in Poodles, it would be necessary to consider values over 10.5*v* as normal. The new upper limit of 10.9*v* for Poodles has been found, that leads to a good compromise between specificity (96.3%) and sensibility (71.7%).

RADIOGRAPHIC EVALUATION OF ATLANTOAXIAL JOINT IN HEALTHY TOY POODLES AND YORKSHIRE TERRIERS. C.O. Baroni, G.P.R. Banon, A.M. Hayashi, J.M. Matera, F.A. Sterman, A.C.B.C. Fonseca Pinto. School of Veterinary Medicine and Zootecnhy, University of São Paulo, Av. Prof. Orlando Marques de Paiva, 87, Cidade Universitária, 05508-270, SP, Brazil.

Introduction Several anatomic factors like odontoid process agenesis, hypoplasia, fracture and abnormalities of its ligaments have been reported to predispose atlantoaxial joint instability in small-breed dogs. Diagnoses are based on examination of cervical radiographs and clinical signs. Distances greater than 4 mm from the axis spinous process and dorsal arch of the atlas have been considered abnormal (Seim III, 2005). The aim of this study was to perform a radiographic evaluation of the space between dorsal arch of the atlas and the axis spinous process, and the ratio between odontoid process and axis in healthy Toy Poodles and Yorkshire Terriers.

Methods 27 asymptomatic dogs, 12 Toy Poodles and 15 Yorkshire Terriers, were selected following individual analysis protocols. Ventrodorsal and lateral radiographic views were chosen to observe the odontoid process and its cervical area. A graph was traced as described below: x-axis and y-axis were tangential to the dorsal arch of the atlas and its furthest caudal point, respectively**.** The furthest point on the radiographic curved edge of spinous process of axis was selected as landmark. First, vertical and horizontal axes distances were measured, in order to define its Cartesian coordinates with scale in millimeters; then, the graph area was allotted to four quadrants of the circle and the point position was associated with it. Two variables were checked: odontoid process size (h); axis size (H).

Results According to the Cartesian coordinates, the minimum and maximum x-axis and y-axis values were, respectively: x= -6; x= 3; y= 0 and y= 4. 19% (5), 59% (16) and 22% (6) of obtained coordinates were positioned in quadrants 1, 2 and over the axes, respectively. Relating to odontoid process the obtained values of mean, standard deviation, minimum and maximum value of normally distributed h/H results were, respectively, 0.25, ±0.04, 0.18 and 0.36. The 0.18 to 0.32 h/H interval comprised 92% (25) of these evaluated dogs and 48% (13) of them were included between 0.22 to 0.28 h/H.

Discussion Since the 0.18 to 0.32 h/H interval could include 92% (25) of the dogs; this should suggest that these values are the limits for normal odontoid process size in Toy Poodle and Yorkshire Terrier breeds. In these clinically normal breeds, the furthest point on the radiographic curved edge of spinous process of axis is onto the dorsal arch of the atlas (quadrant 2) or is slightly dislocated to caudal portion (quadrant 1). The displacement of landmark point on y-axis was smaller than on x-axis in clinically normal Toy Poodle and Yorkshire Terrier breeds. The area delimited on quadrant 2 by values at most 4 mm (y-coordinate) and -6 mm (x-coordinate) could be established as a reference pattern position of normal atlantoaxial joint, if the odontoid process agenesis, hypoplasia or fracture was not present. The area delimited on quadrant 1 by values at most 4 mm (y-coordinate) and 3 mm (x-coordinate) could be also defined as an adequate localization between dorsal arch of atlas and axis spinous process, if those abnormalities in odontoid process did not occur.

RADIOGRAPHIC DIAMETER OF THE COLON IN NORMAL, CONSTIPATED AND CATS WITH MEGACOLON

T.J. Trevail, I. Carrera, E.Courcier, M.Sullivan
Division of Companion Animal Sciences, Faculty of Veterinary Medicine, University of Glasgow, Glasgow, Scotland, G61 1QH

Introduction

A quantitative reference range for normal colon diameter specifically in cats has not been established. Differentiation between constipation, obstipation and megacolon in cats based on plain radiography can be challenging and generally requires knowledge of the history. The aims of this study were (1) to establish a radiographic reference range for the diameter of the colon in normal cats and (2) to evaluate the accuracy of radiography for differentiating normal and constipated cats from cats with megacolon.

Methods

Radiographic records were searched for the last fifty abdominal radiographs of skeletally mature cats taken within twenty-four hours of presentation. Cats with a history of gastrointestinal disease or pelvic fracture (>24hours) were excluded. Measurements of the maximal colon diameter (MCD), colon diameter ventral to L5 (CDVL5) and colon diameter at the pelvic inlet (CDPI) were recorded along with measurements of the length of the vertebral body of L2, L5 and L7 and height of the vertebral body of L5 were made by two observers and repeated by one observer after ten days to evaluate intra and inter-observer variability. Clinical and radiographic records were searched for cases of constipation and megacolon with measurements obtained as described for the normal population by one observer. Inter and intra-observer variability was evaluated using Bland-Altman plots and concordance correlation coefficients. Each parameter, along with ratios of the colonic diameter to lumbar vertebral measurements was evaluated using a receiver operator curve to establish accuracy of the measurements.

Results

Thirteen constipated cats and twenty-six cats with megacolon were evaluated and compared to the normal population of fifty cats. There was strong correlation ($r>0.8$) for intra-observer agreement for MCD, CDPI, L5 and L7 length measurements and maximum colon diameter to L5 length (MCD: L5L) and maximum colon diameter to L5 height ratios. Moderately strong inter-observer agreement ($0.6<r<0.8$) was observed for MCD: L5L ratio measurements with moderate agreement ($0.4<r<0.6$) for MCD, L5 length and height and L7 length measurements. 49/50 normal cats had a maximum colonic diameter less than or equal to 27mm. There was a statistically significant difference in MCD, CDPI and CDVL5 between the groups ($p<0.001$). Taking a cut-off of 29.5mm for MCD resulted in a sensitivity of 92% and specificity of 87.3% for differentiating normal from distended colons. Using a cut-off of 1.28 times L5 length for the MCD: L5L ratio gave the most accurate and reproducible results (sensitivity 96.2%, specificity 87.3%). The most accurate measurement to differentiate between constipation and megacolon was again using the MCD: L5L ratio with a cut-off of 1.48 times L5 length (sensitivity 77%, specificity 85%).

Discussion/Conclusions

A ratio of L5 length to maximum diameter of the colon is recommended to evaluate colonic distension. A ratio of less than 1.28 is a strong indicator of a normal colon, while a value greater than 1.48 is a good indicator of megacolon.

UNUNITED MEDIAL EPICONDYLE: DIAGNOSTIC ACCURACY AND PREVALENCE IN A COHORT OF LABRADOR RETRIEVERS

E. R. Paster, D.N. Biery, D.F. Lawler, R.D. Kealy, P. McKelvie, G.K. Smith Department of Clinical Studies, University of Pennsylvania School of Veterinary Medicine, 3900 Delancey Street, Philadelphia, PA 19104-6010

Introduction: Ununited medial epicondyle (UME) is reported as uncommon, is poorly defined and not well documented. UME is more common in Labradors, and is thought to often be bilateral. Radiography is the primary diagnostic method and UME may only be visualized on the craniocaudal (CrCd) projection. Currently, elbow evaluations done by some organizations such as the Orthopedic Foundation for Animals (OFA) only require an extreme flexed medio-lateral radiographic projection. Few cases are reported with radiographic progression in size or recurrence of fragments following excision.

Materials & Methods: Same-sex littermates of 48 Labrador retrievers from 7 litters were paired. One of each pair was free-fed (control group). The restricted group was fed 75% the calories of the control group. Elbows of all dogs were radiographed during 6, 8, 10 and 12 years of age, and at end-of-life.

Results: Seven (15%) were diagnosed by radiography from 5 litters. Right elbows (n=5) were more affected than left (n=3). The control group (n=4) and restricted group (n=3) were almost equally represented. Females (n=5) were affected more than males (n=2). Six (86%) had unilateral lesions. One was bilaterally affected and ultimately euthanized due to lameness. UME was evident on CrCd projections by 6 years in 6 dogs; a bilaterally affected dog was confirmed at 8 years. In only one elbow, UME was detected on the lateral projection; in all others it was not diagnosed using this lateral radiographic projection through end-of-life. UME fragments of 1 dog grew in size. Two dogs had elbow osteoarthritis.

Discussion: UME may be more common than thought. Most cases were unilateral and diet restriction had no effect on onset, severity or progression, although small population size makes significance difficult to determine. Most cases lacked elbow osteoarthritis or fragment growth. The CrCd radiographic projection was critical for accurate diagnosis. The presumed infrequent diagnosis of UME could be attributed to the singular flexed lateral projection. Two radiographic projections are recommended for UME screening and radiographic evaluation should be continued for life particularly in breeding dogs.

Acknowledgement: Research funded by and conducted at Nestle-Purina Petcare

DEXTROCARDIA WITH SITUS SOLITUS IN DOGS:RETROSPECTIVE STUDY OF 18 CASES. Almeida GLG[1,2], Almeida MB[2], Freitas LX[2], Mattos AV[2], Santos ACM[2]
1Serviço de Cardiologia.Hospital Geral da Santa Casa de Misericórdia. Faculty of Medicine-Gama Filho University. 2Centro Veterinário Colina.Rio de Janeiro. Address: Rua Colina 60 lj 26. Ilha do Governador. Rio de Janeiro. CEP 21931-380.

Introduction: dextrocardia is defined as an anatomic positional anomaly in wich the heart is located within the right hemithorax, with the apex pointed toward the right and inferiorly. This peculiar condition can result from the heart being pushed to the right because of other intrathoracic abnormalities such as fluid, mass, fibrosis or air in pleural space (defined as dextroposition in this case).Isolated dextrocardia,with situs solitus (normal visceroatrial arrangement) is a rare condition that is frequently associated with other cardiovascular malformations in humans. However, in dogs,isolated dextrocardia with situs solitus seems to be a very rare abnormality and usually is not associated with other congenital defects, although vascular abnormality can eventually be found. Usually it is a benign asymptomatic condition ,which is most often diagnosed as an incidental finding in routine radiographic examination and in experimental work. We describe characteristics of a series of consecutive cases of isolated dextrocardia observed in a veterinary diagnostic center in Rio de Janeiro.

Methods: we performed a retrospective study from medical records of dogs with isolated dextrocardia identified by radiographic examination (laterolateral and dorsoventral projections) and echocardiography, from January 2003 to September 2008.Data collected and analyzed included breed, gender, age and heart condition.

Results: the investigation had identified dextrocardia with situs solitus in 18 dogs (purebreed 94,4 %), from both genders (male 50%), age 4 to 16-years-old (median 10,5+/-3,4).The anomaly predominated in Poodles (44,4%) but it was also identified in Yorkshire Terrier, Pekingese, Pinscher Miniature, English Cocker Spaniels (two cases each ones), English Bulldog (one case) and in mongrel (one case). Mitral valve disease (endocardiosis) was identified in six dogs (33,3%) and idiopathic dilated cardiomyopathy was diagnosed in one English Bulldog.The other 11 subjects had no cardiac abnormalities except dextrocardia itself.

Discussion: there is no published data on the prevalence of dextrocardia among dogs,although in veterinary literature this abnormality has been considered very rare or exceptional. However, our findings suggest that isolated dextrocardia may not be so rare as it has been said. In the group of dogs with dextrocardia alone this condition was identified later in life probably because they had no symptoms, confirming its usual benignity. The fact that one third of the dogs had endocardiosis is not a surprise, because this disease is highly prevalent among small dogs in Brazil. We speculate that the predominance of dextrocardia we observed in Poodles may be associated with over-representation of this breed in our canine population and/or with genetic predisposition.

MAGNIFICATION RADIOGRAPHY IN LARGE ANIMAL PATIENTS

R. Drees, M. Perrier, S. Brounts, T. Schwarz
University of Wisconsin-Madison, School of Veterinary Medicine, Department of Surgical Sciences, 2015 Linden Drive, Madison, WI 53706, USA

Introduction:

Radiography of thick body parts such as the head, pelvis and hip are a diagnostic challenge in large animals due to strong beam attenuation, scatter and superimposition of various structures. Imaging alternatives are limited in access and diagnostic yield. A radiographic technique to image the temporomandibular joints (TMJ) of horses with contemporary standard radiographic equipment with removable cones was described in 1949 by Alois Pommer, a pioneer in veterinary radiology. Using the principles of magnification radiography, he was able to obtain sharp images of the bony structures of one temporomandibular joint by magnifying and blurring out the contra-lateral joint. Purpose of this study was to reapply this forgotten technique to thick body parts in horses using today's standard radiographic equipment.

Methods:

The anatomical preparation of an equine skeleton and the head, thorax and pelvis of a horse euthanized for unrelated reasons were used in this study. Radiographs of the TMJ, ribs and coxofemoral joints were obtained with latero-lateral horizontal beam orientation without grid with a standard radiographic machine from which the collimator had been removed, and then repeated with standard mounted and portable large animal radiographic equipment. Variable film focal distance (FFD) and source object distance (SOD) were used: 76.2 to 101.6 cm FFD and 0 to 30.7 cm SOD for ribs; 50.8 to 101.6 cm FFD and 8 to 55.8 cm SOD for coxofemoral joints; 25.4 to 101.6 cm FFD and 0 to 73.7 cm SOD for TMJ. The radiographs were evaluated in blinded fashion by a board certified radiologist for visibility and sharpness of the magnified and non-magnified structure and overall diagnostic quality.

Results:

Best image quality was achieved using the following parameters: for ribs 76.2 to 101.6 cm FFD and 0 to 18 cm SOD; for pelvis 50.8 to 101.6cm FFD and 8 to 18 cm; for TMJ 50.8 to 101.6 cm FFD and 0 to 18 cm SOD.

Discussion:

Magnification radiography in large animal patients as described by Alois Pommer in 1949 is reproducible on contemporary radiographic equipment and may be beneficial in diagnosing disease of the ribs, TMJ and coxofemoral joint in the large animal patient.

ANGIOGRAPHY IN RABBITS FOR PATENCY CONTROL OF A NEW VASCULAR PROTHESIS

L.M. Ribas, F. Appolonio, T.F.S. Barros, M.A Farjallat, N.S Dias, S.M.P. Elias, E. Sampaio, T. De Luccia, P. Saldivia, L.F.P. Figueiredo, N. De Luccia. University of São Paulo, Department of Surgery, Av. Dr. Arnaldo, 455 – São Paulo – SP – Brazil
CEP: 01246-903

Introduction: The study was designed to investigate the hypothesis that a fabric reinforced silicon vascular prostheses could work as a small-diameter arterial substitute, and could be assessed by dynamic angiographic fluoroscopy.

Methods: Implant of the essayed vascular tubular prosthesis was done at the infra renal aorta of male rabbits in an end to end interposition. After 30 and 180 days of post operative period animals where submitted to an angiographic control for patency assessment and removal of the specimen for histological examination.
Angiography was done under general anesthesia by intramuscular administration of ketamine (35 mg/kg) and xylazine (10 mg/kg). Advancement of a 3 Fr silastic catheter adapted to an 18G needle, was done after direct dissection of the femoral artery. Injection of contrast media (meglumine diatrizoate) was done under fluoroscopy (OEC Diasonics 9000) with image subtraction road mapping and measurement capabilities. Images were stored and compared with findings of electronic scanning of the suture line of removed grafts.

Results: Procedure was done in 5 animals after 30 and after 180 days of follow up. Overall patency of 90% and 60% for 30 and 180 days groups were observed. Measurement at the suture line showed a lumen reduction of 47 % in average of the second group compared to no reduction of the first ($p<0,005$). Endothelial growth observed on electronic scanning of the suture line could be positively correlated to angiographic findings.

Discussion: Angiography by fluoroscopy is a reliable method of patency assessment of vascular grafts essays in rabbits, and allows correlation with histological findings.

A RETROSPECTIVE STUDY OF RADIOGRAPHIC FINDINGS OF SWANS ADMITTED TO A WILDLIFE HOSPITAL

A.R. Caine, P.K. Curtiss[1], V. Polydoropoulou[2], M.E. Herrtage. University of Cambridge Department of Clinical Veterinary Medicine, Madingley Road, Cambridge CB3 0ES
Current address: 1: Scott Veterinary Clinic, Goldington Road, Bedford, MK41 0DS
2: Institute of Public Health, Forvie Site, Addenbrookes, Cambridge CB2 0SR

Introduction: Swans are frequently radiographed on admission to wildlife hospitals, as a quick non invasive test to look for evidence of trauma and disease, and to assess if metal can be identified in the gizzard which may suggest lead toxicity. Lead poisoning remains a common problem in wild swans, with clinical signs of anorexia, diarrhoea, intestinal ileus and reflux, kinked neck posture and muscle weakness.
The aim of this study was to compare radiographic findings at admission with lead levels and outcome, with the hypothesis that radiographic evidence of trauma and concurrent other disease may be more prevalent in swans with lead poisoning, and also that further evidence of lead poisoning including signs of ileus may be identified on the radiographs at admission.

Methods: The radiographs of all swans admitted to the RSPCA wildlife hospital in Norfolk in one calendar year were reviewed, with the reviewer blinded to outcome, history and lead levels. Radiographic evidence of trauma, concurrent disease (only respiratory concurrent disease was identified), and presence, location and type of any foreign bodies and trauma was identified. The radiological findings were compared to outcome by Pearson's chi-squared and 2 sample independent T-test.

Results: 428 radiographs were reviewed from 202 swans. Information on outcome was available for 122 swans, and lead levels were recorded for 82 swans. 21% swans had lead levels above which clinical toxicosis would be seen.
Many swans had radiographically identifiable foreign bodies: metal fishing hooks were found in the upper gastrointestinal tract in 13.9% of swans, and associated with a good prognosis, and free gas in the cervical region. Airgun pellets were identified in 5.4% of swans, and were associated with a poorer prognosis. Metal was identified in the gizzard of 32.7% of swans, and was not always associated with lead toxicity, and lead toxicity was not always associated with metal in the gizzard.
Evidence of musculoskeletal trauma was identified in 25% swans, and was associated with a poorer outcome; however it was not more prevalent in swans with lead poisoning. Fractures and degenerative joint disease had a poorer prognosis. Similarly, concurrent disease of the respiratory system was identified in 4% swans and had a very poor prognosis, but was not more prevalent in birds with lead poisoning.
Four markers were measured to assess for signs of gastrointestinal ileus, as might be expected to be seen with lead poisoning. None of the markers assessed correlated with lead levels. However one marker, presence of proventricular gas, significantly correlated with a poorer outcome.

Discussion: This study confirms the utility of radiography in the initial assessment of injured and sick swans, and adds some radiographic features that should be assessed to gain maximum benefit from performing this test. The study confirms that radiography alone can not diagnose lead toxicity.

The authors would like to thank the staff at the RSPCA Eastwinch Wildlife Centre, East Winch, King's Lynn, Norfolk, PE32 1NR for their help during this study.

RADIOGRAPHIC STUDY OF MALE BOVINE BEARERS OF DIGITAL DISEASE.

N. C. Borges, I. R. Lima, L. H. Silva, A. P A. Costa, A. M, A. M. Bogoevich. Fonseca. Setor de Diagnóstico por Imagem – Escola de Veterinária – Universidade Federal de Goiás, Campus II - samambaia - Caixa Postal 131 - CEP: 74001- 970 Goiânia - Goiás – Brasil. E-mail: luyzhenryque@hotmail.com.

INTRODUCTION: The digital diseases in cattle are one of the most prevalent and costly affections, causing losses of up to 20% in milk production and 25% in meat. Under these conditions the radiographic examination is essential for diagnosis, delineation of the extent and determination of its nature. The object of this experiment is to identify radiographically the main bone lesions that affect feet of male bovine, adults and bearers of digital illnesses from state of Goiás.

METHODS: Were collected randomly in slaughterhouse 46 distal extremities of adult male bovines with visible external injuries. They were radiographed, including metacarpus or metatarsus-phalanx-phalanx, proximal interphalangeal and distal interphalangeal joints. The foot lesions were radiographic graded from 1 to 4. Grade 1 represented feet without apparent injury, grade 2 mild lesion with damage of up to 20% of the digit, grade 3 moderate lesion representing a damage of 20% to 40% of the digit and grade 4 severe damage, with 50% or more of attacking. The pieces were radiographed in a Tur x-ray machine, model T-350, with antidifusora Potter-Bucky grid. There were used T-MAT Kodak films put on chassis equipped with a pair of intensifier screens. Radiographs were obtained in palmaro/plantaro- dorsal and lateromedial projections.

RESULTS: radiographic lesions and their respective percentages are identified in Table 1.

Table 1. Results of radiographic examination in feet of male bovines in the region of Goiânia-GO

Radiographic lesions	Occurrence frequency (%)
Osteitis	41,3
Osteitis associated with physeal dysplasia	19,3
Isolated fiseal dysplasia	17,4
Increase of soft tissue	10,9
Absence of injuries	6,5
Periostitis	4,6
Total	100

DISCUSSION: In only 6.5% of the members radiographed was not found any type of bone or soft tissue lesions. In the other, 73.5% the highest incidence of lesions was suggestive of osteitis (41.3%) and osteitis associated with aseptic fisitis (19.3%). In the radiographic evaluation mild lesions were predominated (52.2%) followed by moderate (26.1%) and severe (10.9%). Thus, the results reinforce the importance of radiographic evaluation, because in the presence of cattle lesions in pododermathitis should be sought radiographic evidence of lesions involving bone and adjacent soft tissues. The radiographic examination showed to be extremely important in assessing the location, extent and severity of foot lesions in this animal species.

CONTRAST-ENHANCED SONOGRAPHIC EVALUATIONS OF MURINE TUMOR VASCULARITY: A REVIEW.

A.K.W. Wood, [*] R.M. Bunte, [†] T.W. Cary, [‡] C. M. Sehgal [‡]
Department Clinical Studies,* School of Veterinary Medicine, University of Pennsylvania, 3900 Delancey St, Philadelphia, PA 19104, USA; University Laboratory Animal Resources[†] and Department of Radiology, [‡] University of Pennsylvania.

Introduction – In the presence of a circulating ultrasound contrast agent, tumor capillaries that form during angiogenesis appear uniquely sensitive to low-intensity (physiotherapy) ultrasound. This study was aimed at developing contrast-enhanced ultrasound imaging techniques to monitor the post-therapy reduction in tumor perfusion.

Methods – A tumor model was approved by the University's Animal Ethics Committee. Murine melanoma cells (K173522) were injected subcutaneously in the mouse's (C3HV/HeN) flank and imaging (7 to 15 MHz probe; HDI 5000, Philips) was performed on ≥ 9mm tumors (1 to 3 min; 1 to 3 MHz; continuous; I_{SATA}=2W.cm $^{-1}$). Contrast-enhanced (0.02 mL Definity, Bristol-Myers Squibb Medical Imaging) power Doppler observations were made using external gating at 0.5 frames.s^{-1} to minimize contrast bubble destruction, with a mechanical index of 0.8 and the highest dynamic range, to minimize the potential blooming artifact. The perfused area in each neoplasm was measured from digitized images before and after insonation. A software program identified the number of colored pixels (*n*) that demonstrated contrast enhancement. The percent area covered by colored pixels or percentage area of flow (PAF) was calculated as *n.100/N* (*N* is the total number of pixels in the image), representing the area of the tumor perfused with blood containing the contrast agent. Also, delta-projection images of the tumors were constructed by tracking the running maximum of the grayscale difference between a contrast-enhanced B-mode ultrasound image sequence (0.2 mL Definity) and a baseline. Comparisons were made between the area of tumor perfusion in power Doppler images and in delta-projections.

Results – Following insonation, both contrast imaging techniques clearly showed qualitative and quantitative losses of tumor perfusion and PAF was significantly reduced. Delta-projections revealed individual microvessels (≥250 μm diameter) and better resolved the progressive filling of the networks of neovasculature with the contrast agent, and the delta-projection PAF measurements correlated linearly with those from the contrast-enhanced power Doppler images.

Discussion – The agreement between the two ultrasound imaging techniques is evidence that they were assessing the same tissue property: how well a tumor is perfused by the contrast agent. The delta-projection images better resolved the progressive filling of the neovasculature with the contrast agent. The difference may in part be due to the larger sample volume of the ultrasound pulses used in power Doppler images. In conclusion, contrast-enhanced ultrasound is a useful tool for monitoring tumor vascularity and the role of antivascular therapies.

Supported by NIH grant no. CA139657.

CONTRAST-ENHANCED ULTRASOUND (CEUS) IN CATS Leinonen M[1], Raekallio M[1], Vainio O[1], Ruohoniemi M[1], O'Brien RT[2]. Institution:1. Department of Equine and Small Animal Medicine, Faculty of Veterinary Medicine, PO BOX 57, 00014 University of Helsinki, Finland, 2. Department of Veterinary Clinical Medicine, University of Illinois at Urbana-Champaign, 1008 West Hazelwood Dr, Urbana, Illinois 61802, USA

Introduction: CEUS has been previously used to characterize the normal perfusion of the liver, spleen and kidneys in dogs. Our aim was to evaluate perfusion of normal organs in healthy cats with CEUS.

Methods: The liver, spleen, left kidney, pancreas, small intestine and mesenteric lymph nodes) of ten clinically healthy, young, anesthetized male cats were imaged with CEUS (Acuson Sequoia 512, Siemens). Digital imaging series of 30 seconds with a frame rate of 16-22 Hz, was recorded after each injection of contrast media (Definity®). All cats received one to two bolus injections (0.1 ml) for each imaged organ. Mechanical index was maintained at 0.31-0.33 depending on depth of view and adjustable parameters were standardized. Standardized time intensity curves were drawn from selected regions of interest (ROI) in each organ and each recording separately. The perfusion parameters analyzed were; arrival time (At); time to peak intensity from the injection (Tp); baseline intensity (Bi); peak intensity (Pi); time to peak intensity from initial rise (TTP); wash-in rate (Wi); and wash-out rate (Wo). Analysis of variance with repeated measurements (SPSS) was used to compare the parameters of each organ. Statistical significance for analysis was set at $P<0.05$.

Results: The enhancement varied in time and pattern. The spleen had large nonperfused regions during the first 30 seconds. The kidney enhanced in two phases; first the cortex, followed by more gradual enhancement of the medulla. The pancreas, small intestine and mesenteric lymph node all enhanced early, intensely and uniformly. The differences in the perfusion parameters between the kidney cortex and medulla, and the two differently perfused splenic areas were statistically significant.

Discussion: These results indicate that CEUS can be used in cats to estimate organ perfusion correspondingly to other species. The differences in the perfusion parameters observed can be explained mostly with physiological differences.

THE EFFECT OF THE SIZE AND PLACEMENT OF THE ROI'S ON PERFUSION PARAMETERS

Leinonen M[1], Raekallio M[1], Vainio O[1], Ruohoniemi M[1], O'Brien RT[2].
Institution:1. Department of Equine and Small Animal Medicine, Faculty of Veterinary Medicine, PO BOX 57, 00014 University of Helsinki, Finland, 2. Department of Veterinary Clinical Medicine, University of Illinois at Urbana-Champaign, 1008 West Hazelwood Dr, Urbana, Illinois 61802, USA

Introduction: In contrast enhanced ultrasound (CEUS) the perfusion of an organ can be assessed quantitatively from time intensity curves (TIC) in a selected region of interest (ROI). Size and location of the ROI has proven to have an effect on obtained intensity-values in perfusion parameters.

Methods: The left kidney of ten, healthy, anesthetized cats was imaged with CEUS (Acuson Sequoia 512, Siemens). The mechanical index was maintained at 0.32 in the focal zone area and adjustable parameters were standardized. A 1.5-2 minute digital imaging series with a frame rate of 16 Hz was recorded for each contrast injection (0.1ml Definity® intravenously). Three separate sets of ROIs were placed in the kidney cortex, varying in location, size and depth, to evaluate effect of ROI on the perfusion parameters. Standardized TICs were drawn from each ROI. Following perfusion parameters were analyzed; arrival time (At); time to peak intensity from the injection (Tp); baseline intensity (Bi); peak intensity (Pi); and wash-in rate (Wi). Statistical analyses were made with SPSS and Statistix software. Analysis of variance with repeated measurements was used to compare the effect of size and depth of the ROI. Analysis of variance with randomized complete block was used to separate the effect of depth and size of the ROI from the variance between cats and from noise in Pi. Statistical significance was set at $P<0.05$.

Results: A statistically significant difference was found in Pi of the ROIs with varying depth and size. Mean peak intensity decreased with increasing depth and size of the ROI. The variance caused by depth and size of the ROI in Pi was significantly greater than variance caused by noise alone or by individual cats.

Discussion: Placement and size of the ROI both have an effect on peak intensity values. In a patient with focal lesions, when comparing two different ROIs, they should be placed at same depth, and similar in size and shape. Caution must be used when generalizing these results on other organs due to differences in perfusion.

SPATIAL COMPOUND IMAGING RELATED ARTIFACTS. H.G. Heng. Department of Veterinary Clinical Sciences, Purdue University, 625 Harrison Street, West Lafayette IN 47906 USA.

Introduction

Spatial compound imaging is a technology that uses electronic beam steering of a transducer array to rapidly acquire several overlapping scans of an object from different angles. These single-angled acquisitions are averaged to form a multi-angle compound image that is updated in real time with each subsequent scan. Spatial compound imaging claims to reduced speckle, clutter and other acoustic artifacts, and improving image quality compared to conventional ultrasound. Many newer ultrasound machines have incorporated this technology into the transducer. However, they have many different proprietary names including SonoCT (Philips), CrossXBeam (GE), Spatial Compound Imaging (Medison) and SieClear (Siemens). Currently, there are few reports regarding artifacts created by spatial compound imaging. Therefore this study was thus carried out to compare the artifacts created by spatial compound imaging and conventional ultrasound in normal canine abdominal ultrasound.

Methods

Abdominal ultrasound was performed in three healthy dogs to compare the artifacts created by spatial compound imaging and conventional ultrasound. Ultrasound artifacts examined included reverberation, shadowing, edge shadowing and enhancement. All images were obtained using a Phillips iU22 SonoCT system with both 7-12 MHz linear and 5-8 MHz microconvex transducers. The same transducer was used to produce each set of artifacts at different abdominal anatomic locations. Each set of images were obtained in an identical plane without changing the depth and focus. The spatial compound imaging was activated/deactivated by pressing a button on the iU22 system labeled SonoCT. Automatic image optimization was performed on each image.

Results

Spatial compound imaging produces a different appearance of reverberation artifacts compared to conventional imaging. Instead of a single reverberation artifact, there are multiple diverging reverberation artifacts originating from the source of the reverberation. These diverging reverberation artifacts obscure the far field of the ultrasound image. Spatial compound imaging also created a diverging shadowing artifact which increases its width with depth. There is reduction of edge shadowing with the use of spatial compound imaging. The distal acoustic enhancement artifact is unchanged for both imaging techniques.

Discussion

Theoretically, spatial compound imaging should produce a better quality image by reducing the image artifacts. This was not found to always be true as compound imaging also creates a different appearance of artifacts due to the multi-angle beam used to form the image. Spatial compound imaging may be deactivated to investigate certain areas when the reverberation and shadowing artifacts hinder visualization of the far field.

CONTRAST HARMONIC ULTRASOUND IMAGING OF VISCERAL LYMPH NODES IN DOGS. Gaschen,L., Angelette, N., Stout, R.
Louisiana State University School of Veterinary Medicine, Baton Rouge, Louisiana, USA 70803

Purpose: To describe the normal contrast-enhanced harmonic (CEHUS), spectral, color and power Doppler ultrasound examinations of visceral lymph nodes in dogs and compare these with benign and malignant lymphadenopathy by assessing angioarchitecture and perfusion characteristics.

Methods: A CEHUS examination of medial iliac lymph nodes (MILN) was performed on twenty normal dogs after i.v. administered lipoprotein-bound inert gas-filled microbubble contrast media Definity®. These results were compared with four privately-owned dogs with intra-abdominal lymphadenopathy. Pixel intensity time-activity curves were generated for one minute post injection. Quantification of these curves was performed using two software applications. Spectral waveforms were used to calculate resistive indices (RI). Power (PD) and color Doppler (CD) images were made of each node to assess vascular patterns.

Results: Normal lymph nodes exhibited a mean wash-in phase beginning at 6.3s with a mean peak pixel intensity at 14.65s. In one dog diagnosed with lymphoma similar perfusion times occurred (wash-in 6s, peak 15s), yet another dog with perianal adenocarcinoma exhibited a more rapid wash-in phase and peak (5s and 9s respectively). The angioarchitecture was best visualized with CEHUS compared with PD and CD. Normal nodes have a central artery with a centrifugal branching pattern. A dog with perianal adenocarcinoma displayed peripherally located feeding vessels, increased number of aberrant vessels, and a centripetal perfusion pattern. A dog with lymphoma showed angioarchitecture and perfusion pattern similar to normal nodes. Normal nodes had a mean RI of 0.81 (0.61-0.92). Abnormal nodes had a mean RI of 0.73 (0.63-0.89) and were not significantly different.

Discussion:CEHUS is superior for assessing the angioarchitecture of normal visceral lymph nodes as well as in dogs with lymphadenopathy. Color and power Doppler were inadequate for showing small intranodal angioarchitecture. Increased numbers of vessels as well as aberrant lymphangioarchitecture occurs in malignant disease. Other studies have shown a significant difference between the RI of normal and malignant nodes.[1] The lack of significant differences between the RI of normal and abnormal dogs in this study could be due to the small number of abnormal dogs examined or the difference between peripheral vs. visceral lymph nodes. This study suggest that CEHUS is a valuable, non-invasive method of differentiating benign from malignant lymph nodes based on their angioarchitecture.

BLOOD FLOW IN THE MOUSE ABDOMINAL AORTA, RENAL AND FEMORAL ARTERIES: A PRELIMINARY ULTRASONOGRAPHIC PULSED-DOPPLER ANALYSIS

E. Dominguez, J. Ruberte, R. Novellas, Y. Espada. CBATEG. Edifici H. Animal Medicine and Surgery Department, Veterinary Faculty. Edifici V, Universitat Autonoma de Barcelona. Cerdanyola del Valles, Spain, 08193

Introduction

The mouse shows great similarities in development, morphology, physiology and biochemistry to humans. This makes it a key model for research into human disease. It also has a very similar genetic make-up and its genome is susceptible to mutations, allowing to understand the role that the genes play in disease. Non-invasive imaging techniques have been developed for mutant mice phenotyping. B-mode and Doppler ultrasound may characterize cardiovascular system. It is a fast and real-time imaging technique, gives structural, functional and hemodynamic information and it is also useful for longitudinal studies.

The purpose of this study is to describe the normal Doppler wave pattern of the abdominal aorta and femoral and renal arteries in the mouse, and to establish the normal values of their vascular indices and arterial blood flow.

Methods

Nine inbred C57BL6 healthy adult female mice were ultrasound between 9am and 11am. Mice were anesthetized with isoflurane and were scanned in supine position. An ultrasound biomicroscope (Vevo 770, Visualsonics, Toronto, ON, Canada) was used with a 40 MHz transducer. Three localizations of the abdominal aorta (pre-renal, post-renal and pre-iliac bifurcation), left femoral artery and right renal artery were imaged. Systolic area (A) in B-mode, peak systolic velocity (PSV), minimum diastolic velocity (MDV), time average maximum velocity (TAMX) in pulsed Doppler mode were measured. Pulsatility and resistive indices, and mean blood flow were calculated. Mean values were determined averaging a total of three Doppler waveforms. The statistical analysis was performed with the Statistical Analysis System (SAS Institute, Cary, USA) by applying the GLM and LS MEANS procedures.

Results

Abdominal aorta (pre-renal[1], post-renal[2] and pre-iliac bifurcation[3]) has a plug flow profile and a typical high resistance flow pattern, femoral artery[4] and renal artery[5] have a parabolic flow velocity profile and a low resistance flow. Doppler values (mean ± SD) and statistical differences (P<0.05) are shown in table 1.

Table 1.

	Area mm^2	PSV mm/s	MDV mm/s	TAMX mm/s	PI	RI	F mm^3/s
1	0.86 ± 0.19^{a}	660.8 ± 201.6^{a}	51.3 ± 26.6^{ab}	371.4 ± 112.1^{a}	1.62 ± 0.12^{a}	0.93 ± 0.07^{a}	313.9 ± 109.4^{a}
2	0.48 ± 0.09^{b}	500.7 ± 194.5^{a}	74.5 ± 57.5^{ab}	314.4 ± 148.2^{a}	1.5 ± 0.42^{a}	0.86 ± 0.08^{ac}	150.5 ± 68.1^{b}
3	0.43 ± 0.14^{b}	389.4 ± 148.6^{a}	50.1 ± 44.2^{ab}	239.4 ± 77.9^{a}	1.61 ± 0.32^{a}	0.88 ± 0.09^{ac}	99.3 ± 47.4^{bc}
4	0.03 ± 0.01^{c}	101.1 ± 18.5^{b}	42.7 ± 9.3^{a}	72.6 ± 13.8^{b}	0.80 ± 0.07^{b}	0.57 ± 0.04^{b}	2.6 ± 1.24^{c}
5	0.28 ± 0.18^{b}	516.7 ± 222.4^{a}	123 ± 87.7^{b}	310.0 ± 139.1^{a}	1.3 ± 0.36^{a}	0.76 ± 0.13^{c}	79.8 ± 62.0^{c}

Discussion

This preliminary study provides the normal Doppler wave pattern and normal vascular values of the abdominal aorta, femoral and renal arteries in adult female C57BL6 mice by ultrasound biomicroscope. These values may be used as reference for phenotyping mutant mice with cardiovascular alterations.

DOPPLER ULTRASONOGRAPHIC EVALUATION OF THE EXTERNAL ILIAC AND FEMORAL ARTERIES IN DOGS AND CATS. G.B. Jarretta, C.A. Paiva, N.L. Dada, J. Williams. UNIMONTE. Rua São José, 134 Ap.01, Santos – SP, Brazil, CEP 11040-200.

Introduction: Abdominal ultrasound is well established and widely used in small animal veterinary medicine to establish or verify clinical and surgical diagnoses. Dogs and cats can be presented with vascular diseases, and especially cats can be affected by thromboembolism caused by hypertrophic cardiomyopathy. Doppler ultrasound is the accepted method for vascular evaluation in animals; however there is still a void in information regarding hemodynamics of abdominal and peripherical vessels. Normal wavefoms and velocity parameters are not fully established in small animal patients. The goal of the present study is to investigate the statistical differences between the diameter and the peak systolic velocity of external iliac and femoral arteries in dogs and cats and to verify the correlation between the diameter and flow velocities of these arteries.

Methods: Ten adult dogs (5 female and 5 male, weighing 4,9 - 30,0 kg) and 10 adult cats (9 females and 1 male, weighing 3,0 - 4,0 kg) of various breeds were used in the study. The animals had no clinical signs for vascular diseases, and their arterial blood pressure was determined to be within normal limits by oscillometric method (Petmap®). Each animal was positioned in dorsal and then in lateral recumbency to optimize image acquisition of each external iliac artery and each femoral artery; hair was removed from the ventrum of the abdomen and from the medial surface of each proximal rear limb. The diameter of the right and left external iliac and femoral arteries was recorded on B-mode sagittal images. Doppler investigation of these arteries was obtained using a Logic-e GE ultrasound with a linear multifrequency transducer (7-11 MHz), maintaining a Doppler angle less than 60° and a pulse repetition frequency sufficient to prevent aliasing。 Peak systolic velocity (PSV) was recorded for each external iliac and each femoral artery. Statistics evaluation was performed using paired-t test and Pearson correlation test.

Results: The mean diameters of the left and right external iliac and left and right femoral arteries in dogs were 0,4 ± 0,12; 0,37 ± 0,12; 0,32 ± 0,07 and 0,3 ± 0,06 cm, respectively. The mean diameters of the same arteries in cats were 0,23 ± 0,04; 0,18 ± 0,01; 0,19 ± 0,02 and 0,17 ± 0,03 cm, respectively. The mean PSV of the left and right external iliac and left and right femoral arteries in dogs were 110,35 ± 23,57; 100,66 ± 26,48; 101,13 ± 16,39 and 102,27 ± 27,96 cm/s, respectively. The mean PSV of the same arteries in cats were 63,63 ± 22,46; 58,06 ± 14,34; 65,93 ± 30,42 and 59,86 ± 18,67 cm/s, respectively. There was no statistical difference between the PSV of external iliac and femoral arteries in dogs or cats, even though the diameters were statistically different. When comparing dogs and cats, there was a statistical difference between all the parameters. The femoral artery in dogs was the only one which showed a significant correlation between diameter and PSV.

Discussion: External iliac and femoral arteries in small animals have been poorly studied by doppler ultrasound. There is still a great number of studies to be done and the present study demonstrates the importance of further investigations to establish values and better evaluate the similarities and / or differences between vessels and species.

MEASUREMENT OF BLOOD FLOW VELOCITY IN THE AORTA ABDOMINALIS IN THE DOG UNDER THE INFLUENCE OF THE SIGNAL ENHANCERS SONOVUE AND LEVOVIST

Ingmar Kiefer[1], Doreen Succow[1], Antje Hause[1], Gerhard Oechtering[1] ,Michaele Alef[1]
[1]Department of Small Animal Medicine, Veterinary Faculty of the University of Leipzig, Germany, An den Tierkliniken 23, 04103 Leipzig

Introduction

One of the initial indications to use signal enhancers in sonography was the improved representation and assessment of blood vessels which includes the flow pattern but also the measurement of flow velocity. It was investigated if contrast enhancers change this parameter.

Methods

The maximum velocity of the aorta blood flow was measured over a 110 sec time period with 10 second intervals in a group of 11 dogs. A placebo consisting of 0.9% sodium chloride solution with the same concentration as the contrast medium to be applied afterwards was given and the blood flow velocity determined. This was followed by blood flow measurement under native conditions. Immediately afterwards contrast media were injected as intravenous bolus (Levovist at 0.2 ml/kg, SonoVue at 0.01 ml/kg) and the blood flow velocity in the aorta measured over 110 seconds.

Results

Maximum blood flow velocities in the aorta were determined every 10 seconds. Significant differences could neither be found under native conditions nor after placebo application. With contrast enhancers blood flow velocities were clearly increased. SonoVue lead to values between 31 and 140 % of the initial value, in one case the initial velocity of 1.6 m/s was increased to 2.9 m/s. Similarly, Levovist caused relative increases between 28 and 104%, in one typical example the initial value of 0.93 m/s increased to 1.9 m/s. In another patient the values were 0,65 and 0,94, respectively. Neither with placebos nor with contrast media significant changes of heart frequency could be found. Also, there were no correlations between the parameters measured and hematocrit values. Age, gender and body weight did not exert a systematic influence.

Discussion

On the basis of the results reported there is reason to question reported values of blood flow velocities after application of Levovist and SonoVue, both in veterinary as also inhuman medicine. The use of contrast media has to be seen critically especially with stenosis graduation. This is so far not customary but it could be envisaged, e. g. for breeding investigations, if the quality of sonographic images is poor (e.g. because of adipositas, lung fibrosis). The reported increases of blood flow velocity do presumably not reflect a real acceleration as a result of contrast medium application but are due to physical and technical influences. The present study does not yet allow to give a clear answer in this respect.

ULTRASONOGRAPHIC EVALUATION OF RELATIVE GASTROINTESTINAL LAYER CONTRIBUTION TO TOTAL WALL THICKNESS IN CATS WITHOUT CLINICAL EVIDENCE OF GI DISEASE

M.D. Winter, L. Londoño
University of Florida College of Veterinary Medicine
2015 SW 16th Ave
Gainesville, FL 32610 USA

Introduction: Ultrasonographic evaluation of gastrointestinal wall has been used as a diagnostic tool for evaluation of patients with gastrointestinal disease in humans and companion animals. Normal values for overall gastrointestinal wall thickness in cats have been reported. The objective of this study was to establish the normal relative contribution of each gastrointestinal layer to overall wall thickness in the different segments of the clinically normal, non-distended feline gastrointestinal tract.

Methods: Subjects of the study included all feline patients seen at the University of Florida Veterinary Medical Center with no history of gastrointestinal disease and who obtained a complete abdominal ultrasonographic examination. Patients included in the study had normal serum biochemical analysis, complete blood counts and urinalysis. Three measurements of overall intestinal wall thickness, mucosal thickness, submucosal thickness, muscularis thickness, and serosal thickness were made in each gastrointestinal sub-segment (stomach, duodenum, jejunum and ileum). The gastric measurement was made at the inter-rugal regions. Measurements were averaged and the results used to generate the average percentage of the contribution of individual layer thickness to overall wall thickness in each intestinal sub-segment.

Results: A total of 20 ultrasonographic studies of feline patients with no clinical signs or history of GI disease and with normal serum biochemical analysis, complete blood counts and urinalysis were reviewed. The overall mural thickness of the stomach, duodenum, jejunum and ileum was measured and correlated well with previous studies. The contribution of the mucosal layer to overall thickness was found to be 32% in the stomach, 49% in the duodenum, 43% in the jejunum and 37% in the ileum. The submucosal layer contribution was 24% in the stomach, 19% in the duodenum, 16% in the jejunum and 22% in the ileum. The muscularis layer contribution was 24% in the stomach, 17% in the duodenum, 22% in the jejunum and 25% in the ileum. Finally, the serosal layer contributed 18% in the stomach, 16% in the duodenum, 17% in the jejunum and 17% in the ileum to overall wall thickness.

Conclusions: The mucosal layer makes the greatest contribution to overall gastrointestinal wall thickness in all segments of the gastrointestinal tract while the serosal layer contributes the least. Submucosal and muscularis contributions are similar in most GI segments. This normative data may assist the clinician in a more quantitative diagnosis of muscularis layer hypertrophy in cats.

ULTRASONOGRAPHY OF PANCREATIC DISEASE IN CATS

K.M. Hittmair, E. Gamperl, I. Schwendenwein, M. Reifinger. Clinic for Diagnostic Imaging, Department for Companion Animals and Horses, University of Veterinary Medicine, Vienna, Veterinaerplatz 1, 1210 Vienna, Austria

Introduction:

Pancreatic disease in cats is more common than previously acknowledged. Diagnosis is usually difficult due to unclear clinical symptoms and inefficient laboratory results. The purpose of this study was to use ultrasonography as a means to detect pancreatic disease in cats and to characterize the lesions.

Methods:

17 cats (mean age 11 years; 5 female, 12 male) with ultrasonographic lesions of the pancreas were included in the study (Group 1). These cats had variable clinical signs and were patients at our clinic. Only those patients were included, where fine needle aspirates, biopsies or histopathology of the pancreas were performed. The pancreas was evaluated for size, echogenicity, and parenchymal lesions. Additionally, in 50 randomly chosen, euthanized cats (mean age 9 years, 18 females, 32 males), the pancreas was examined ultrasonographically, either before or after it was removed from the cat (Group 2). Again, size, echogenicity, and parenchymal lesions were noted. A fine needle aspirate was taken, followed by histopathology.

Results:

The results of the ultrasonographic examination in the 17 cats (Group 1) showed 10/17 with pancreatitis, 4/17 with pancreatic edema, 4/17 with pancreatic necrosis, 4/17 with pancreatic cysts, 2/17 with pancreatic abscess, 6/17 with pancreatic neoplasia, 1/17 with pancreatic fibrosis, and 5/17 with focal peritonitis (some cats with more than 1 finding). These findings were confirmed either by cytology or histology. In the 50 cats of Group 2, 24/50 (48%) were sonographically without findings. Cytology revealed pancreatitis in 2/24, while histology showed nodular hyperplasia in 11/24, inflammation in 3/24 and lymphocytic infiltrates in 3/24. Other ultrasonographic results included nodular hyperplasia (14/50, 28%), which was confirmed histologically. Pancreatitis was ultrasonographically evident in 6/50 cats (12%), pancreatic cysts in 5/50 (10%), mineralization of the pancreatic ducts in 5/50 (10%), neoplasia in 2/50 (4%), and fibrosis in 3/50 (6%). Cytology and histology showed similar findings, except for pancreatic fibrosis, which was diagnosed as amyloidosis.

Conclusions:

The results show that ultrasonography is a good tool to diagnose pancreatic disease in cats, even without clinical signs. And yet, in the 24 pancreases without ultrasonographic findings in Group 2, histology revealed nodular hyperplasia in almost half of them, while 6/24 showed either inflammation or infiltration. Diagnosis of pancreatic fibrosis was incorrect and was determined as amyloidosis. Awareness of these findings may help to improve ultrasonographic diagnosis of pancreatic disease in the cat.

ULTRASONOGRAPHIC DIAGNOSIS OF HYPOECHOIC FOCAL LESIONS IN THE LIVER OF YORKSHIRE TERRIERS

K.M. Hittmair, M. Christan, I. Schwendenwein. Clinic for Diagnostic Imaging, Department for Companion Animals and Horses, University of Veterinary Medicine, Vienna, Veterinaerplatz 1, 1210 Vienna, Austria

Introduction:

Hypoechoic focal lesions in the liver are often seen in small breed dogs, especially the Yorkshire Terrier. These focal lesions may be solitary or disseminated in a hyperechoic and heterogeneous parenchyma. They are commonly seen in dogs with gastrointestinal disease, but also in healthy dogs. The purpose of this study was to determine the cause of these lesions by comparing them to the patient's history and laboratory blood work.

Methods:

117 pure breed Yorkshire Terriers (mean age 9.9 years, 58 females, 59 males) underwent abdominal ultrasonography. Besides the ultrasonographic evaluation of all abdominal organs, especially of the liver, all clinical records were reviewed. The dogs were put into 6 categories: without clinical symptoms, gastrointestinal disease, hyperadrenocorticism, neoplasia, cardiac disease, and other diseases such as endocrinopathies, trauma, and medications. Blood work included liver enzymes ALT, ALP, and GLDH.

Results:

89/117 dogs (76%) showed ultrasonographic abnormalities of the liver, 47 of these (52%) had characteristic hypoechoic focal lesions. 4/47 Yorkshire Terriers (8%) showed no signs of disease besides the hepatic lesions, 16/47 dogs (34%) had symptoms of gastrointestinal disease. In the remaining 27 dogs (57%) other diseases affecting the liver were diagnosed (e.g. hyperadrenocorticism, tumours, cardiac insufficiency). 3 fine needle aspirates of the liver showed fatty and/or non-fatty degeneration of the liver parenchyma. Compared to the liver enzymes in the remaining 70 dogs, Yorkshire Terriers with hypoechoic hepatic foci showed the highest enzyme activity of ALT, ALP, and GLDH.

Conclusions:

Hypoechoic focal lesions of the liver in dogs are rarely neoplastic. The more common occurrence of these lesions in Yorkshire Terriers may be due to the hypoglycemia-fatty liver syndrome in puppies of this breed and other small breeds. The correlation of fat content and liver echo intensities may explain these lesions, as the size of fat droplets determines the echogenicity.

THREE-DIMENSIONAL POWER DOPPLER ULTRASONOGRAPHY OF ACUTE PYELONEPHRITIS VASCULARIZATION IN DOG. M. Molazem, A. Vajhi, M. Masoudifard, S. Soroori, N. Sayah. Faculty of Veterinary Medicine, University of Tehran, Azadi st., Tehran, Iran, PC: 14155-6453.

Introduction: Recently new technique in Power Doppler(PD) angiography using three-dimensional(3D) ultrasonography(US) has been developed . We investigated the role of 3D PD US in the diagnosis of pyelonephritis in dogs.

Methods: The examinations of 15 patients with findings of pyelonephritis and 15 normal kidneys were reviewed. The patterns of blood vessels were extracted by 3D PD US data to facilitate the capturing of vascular morphological changes. Features including Vascularization Index (VI), Flow Index (FI), Vascularization-Flow Index (VFI), number of vascular trees, and number of branching, were extracted from the thinning results.

Results: The results, obtained from both inflamed and healthy cases, were compared together using a paired T-Test; showing that VI, VFI, and FI indexes were significantly increased during inflammation ($p<0.05$). However, number of vessel trees and branches were not changed significantly. Acute pyelonephritis had been diagnosed in involved patients using ultrasound guide biopsy.

Discussion: This study revealed that 3D PD US may permit confirmation of the diagnosis of acute pyelonephritis in dogs which can be helpful in planning of treatment and avoiding invasive diagnostic procedures.

ULTRASOUND DOPPLER RENAL CIRCULATION XYLAZINE EFFECT EVALUATION IN HEALTHY DOGS.

Saez, D., Thompson, C., Crossley,R

Introduction: Xylazine is a sedative drug frequently used in short time procedures in dogs like radiographic and ultrasonographic exams. Its α2-adrenergic action, reversible by use of yohimbine, produces dose dependent sedation or analgesia with a great relaxation and analgesia. Its side effects include vomits, bradycardia and hypotension. Its peripheric hypotensor effects are well recognized but its consequences over renal circulation in dogs have not been described. The purpose of this study was to evaluate the effect of xylazine sedative doses on renal circulation by Doppler ultrasound in healthy dogs.

Materials and Methods: 12 healthy dogs evaluated by cardiac frequency, systolic pressure and urinalysis. All dogs were mixed breed dogs between 2 and 7 years old and 10 and 30 kilograms weight. Systolic pressure (SP), cardiac frequency (CF), arcuate artery resistive index (AARI), renal artery resistive index (RARI) and renal artery blood flow volume (RABFV) were measured before and 5 minutes after a single 5 mg/kg xylazine chlorhydrate given intravenously. All Doppler ultrasound measures were done on the left kidney.

Results: The mean SP before and after administration was 125.8 ± 6.904 mmHg and 108.3 ± 10.94 mmHg with a significant difference ($p>0.05$). Mean CF before and after administration was 117.7 ± 22.59 (bpm) and 65.17 ± 8.462 (bpm) with a significant difference ($p>0.05$). Mean RABFV before and after administration was 31.49 ± 7.506 ml/min/mm² and 26.33 ± 9.610 ml/min/mm² with a significant difference ($p>0.05$). Mean RAIR before and after xilazine administration was 0.738 ± 0,101 and 0.686 ± 0.078 (cm/seg) and it had no significant differences ($p>0.05$). Mean AAIR before and after xilazine administration was 0.597 ± 0.040 (cm/seg) and 0.604 ± 0.051(cm/seg) and it had no significant differences ($p>0.05$).

Discussion: In the present study, administration of a sedative dose of xylazine produced a significant decrease in systemic hemodynamic parameters and renal artery blood flow without changes in both RARI and AARI. This means that mild decreases in systolic pressure and cardiac frequency do not alter the continuous kidney flow. This could be explained by the intrinsic defense and autoregulation mechanisms of the kidney. Decreased renal artery blood flow volume could be explained because of the decrease in cardiac frequency situation that could be resolved by the use of a positive chronotropic drug like atropine.

Conclusion: The administration of a sedative dose of xylazine in healthy dogs produces a mild decrease in hemodynamics parameters without changes in resistive index of the renal artery system.

ULTRASOUND EVALUATION OF CANINE MENISCUS: *EX VIVO* AND EMBEDDED IN GELATIN. P.M. Souza, M.J. Mamprim, I.F.C.Santos . Faculdade de Medicina Veterinária e Zootecnia, Universidade Estadual Paulista. Distrito de Rubião Júnior, s/n, Botucatu – São Paulo – Brasil. 18618-000.

Introduction

In Veterinary Medicine, ultrasonography is a diagnostic method that provides information on the normal sonographic aspects, as well as on the main disorders affecting the joint system of animals. However, there are few reports on the use of ultrasound examination to visualize and diagnose canine meniscus alterations. The present work aimed to establish normal ultrasound images of menisci *ex vivo* and embedded in gelatin, as well as to detect possible alterations, making macroscopy a gold standard.

Methods

Thirty pelvic limbs were used, accounting for 60 menisci of dogs presenting radiographic evaluation of the possible joint diseases and ultrasound examination for meniscus standardization. The pieces were from the Zoonosis Center of Botucatu City Hall, São Paulo State, Brazil. For ultrasound examination, pieces were subjected to extensive shaving of the joint region and acoustic gel application. Positioning included: dorsal with the limb flexed, ventral extended, lateral extended, flexed and semi-flexed. They were analyzed through transversal and longitudinal sections, both in the medial, lateral, cranial, caudal and infrapatellar regions at 20° angulation. Then, pieces were dissected to remove menisci, which were macroscopically classified according to the lesion and embedded in gelatin, obtaining the same sections as those for the pieces; however, a dorsal section was added to visualize the whole surface. The ultrasound equipment used in the experiment was LOGIC 3 model, GE, in mode B, with multi-frequency micro-linear transducer of 7.5 to 10MHz.

Results

Menisci were best visualized in 93.33% joints from dogs weighed more than 20 kg; 6.67% belonged to dogs weighed less than 17 kg and could be visualized. In cranial and caudal longitudinal sections, menisci had a homogeneous structure with average echogenicity of triangular format; in cranial and caudal transversal sections, a thick linear structure was hyperechogenic dorsal to the tibia lateral condyle, both compatible with the image obtained in gelatin. In longitudinal and transversal sections, there was a hypoechogenic line compatible with the total rupture of the medial meniscus, classified as complex transversal.

Discussion

Studies on the use of ultrasound for visualization and diagnosis of menisci in dogs are scarce in literature. In the present research, an ultrasound pattern was established for the visualization of menisci and the association of radiographic and ultrasound techniques, allowing the greatest amount of information and an efficient alternative to evaluate the knee joint structures.

CONTRAST ENHANCED ULTRASONOGRAPHY OF OCULAR AND RETROBULBAR DISEASES IN DOGS AND CATS. J. Labruyère, C. Hartley, A. Holloway. Animal Health Trust, Lanwades park, Newmarket, CB87UU, Suffolk, UK.

Introduction

Contrast-enhanced ultrasonography (CEU) using stabilized microbubbles contrast agents has been reported in the localisation and characterization of hepatic and splenic nodular and mass lesions. The hypothesis of this study is that CEU would be more sensitive than colour Doppler techniques to detect persistent vascularization in a detached retina (RD) allowing differentiation from benign vitreous membranes, and allows better subjective assessment of the vascularization of orbital neoplasia.

Methods

In this prospective study, three categories of diseases were studied: retinal detachments, intra-ocular masses and retrobulbar masses. For each animal, both eyes were systematically assessed using conventional B-mode ultrasonography including colour and power Doppler examination. For unilateral diseases, the normal eye was used as a control. A bolus intravenous injection of 1 to 2mls of Sonovue® was injected after placement of a peripheral i.v. catheter. The examination was performed using array transducers and the built-in harmonic settings.

Results

The group of retinal detachments was composed of 13 dogs. CEU demonstrated the presence of vascularization in the detached retina of 12 eyes, 2 of which were partial retinal detachments. No vascularization was visible in 10 eyes affected with vitreous membranes of a different origin. The group of intra-ocular masses was composed of 3 dogs and 2 cats. CEU demonstrated a marked microvascular enhancement pattern in 2 cats diagnosed with intra-ocular neoplasia, and confirmed the presence of a non-vascularized blood clot in one dog. Contrast uptake was demonstrated in 2 dogs with confirmed extra-ocular neoplasia. Examination using Doppler techniques was not possible in most of eyes due to the artefacts caused by eye movement.

Discussion

CEU is useful to differentiate retinal detachments (complete or partial) from other benign vitreous membranes, and more sensitive than colour/power Doppler. It allows differentiation of orbital neoplasia from non-vascularised pathology such as a blood clot.

TWIN PREGNANCY IN THE SAME PLACENTA DETECTED BY ULTRASOUND EXAME IN SIAMESE QUEEN. M.P. Castro. Cevet (Av. Rui Barbosa, 29, lj 108, Sao Francisco, Niteroi, Brasil, Rio de Janeiro, CEP 24360-440)

Introduction

During a ultrasound exam for detecting pregnancy in a Siamese queen with about 30 days, it was detect a twin fetus pregnancy in the same placenta. The litter was the number of 5 fetus total.

Methods

The queen was positioned, dorsal ventral, and the acoustic gel applied. The ultrasound exam realized with logic book GE equipment using a linear multi frequencies transducer (6 MHZ to 10 MHZ).

Results

The ultrasound exam was very helpful to the success of this litter, with the result of the ultrasound exam, detecting twin fetus in the same placenta, the veterinarians ware able to plain the surgery, at the right moment.

Discussion

The ultrasound exam for detection of pregnancy in queens, it’s a safe, non invasive and no painful exam that could help any pregnancy and especially at the unusual pregnancy. When we can plan and work for the success of the litter.

CT AND MRI FINDINGS IN INTRACRANIAL FUNGAL DISEASE IN DOGS AND CATS

S. Hecht, W.H. Adams, J.R. Smith, W.B. Thomas. Department of Small Animal Clinical Sciences, University of Tennessee College of Veterinary Medicine, 2407 River Drive, Knoxville, TN 37996, USA.

Introduction/Purpose: Fungal infections affecting the central nervous system in dogs and cats are rare and may provide a diagnostic challenge. With few exceptions descriptions of imaging findings are limited to individual case reports. The purpose of this study was to evaluate imaging findings in small animals with intracranial fungal infection.

Methods: The radiology case log was searched retrospectively for patients with a diagnosis of intracranial fungal disease. Imaging studies and medical records were reviewed.

Results: Five dogs and 3 cats were identified. Neurological signs were variable. Nasal discharge was the major presenting complaint in 3 dogs, 2 of which had no neurologic abnormalities. CT (n = 6) and MRI (n = 2) revealed a single contrast enhancing intraaxial mass (n = 4), a nasal mass disrupting the cribriform plate (n = 3), and multiple punctate contrast enhancing foci (n = 1). Diagnosis was established by means of necropsy (n = 2), surgical biopsy (n = 2), rhinoscopic biopsy (n = 2), serum and CSF cryptococcus antigen test (n = 1) and urine blastomycosis antigen test (n = 1). Fungal organisms identified were *Blastomyces dermatiditis* (n = 5), *Histoplasma capsulatum* (n = 1), *Cladophialophora bantiana* (n = 1) and *Cryptococcus neoformans* (n = 1).

Discussion: Imaging findings in intracranial fungal disease in small animals are variable and may mimic nasal/intracranial neoplasia.

THE BETTER MOUSETRAP™ : A DEVICE FOR COMPUTED TOMOGRAPHY IMAGING OF CATS WITHOUT GENERAL ANESTHESIA

C.R. Oliveira, G.J. Pijanowski, S. Hartman, M.A. O'Brien, M. McMichael, R.T. O'Brien
University of Illinois at Urbana-Champaign, 1008 W. Hazelwood Dr., Urbana, IL, 61802

Introduction: Thoracic computed tomography (CT) in cats has been historically performed using general anesthesia. This produces a nonphysiological state associated with varying degrees of atelectasis and is contraindicated in most patients with dyspnea. The purposes of this study were to 1) design a low attenuating device that provided oxygen and venous catheter access, minimized movement of the patient without being restrictive and to 2) create protocols for a 16 detector CT for optimal high resolution lung imaging of awake cats with no respiratory motion.

Methods: A cylindrical acrylic device was designed specifically for cats and other small animal patients. Consideration of the clinical requirements for imaging of dypneic cats included the need for oxygen therapy, fluid administration, ability to constantly observe the patient, ease of removal of the patient from the device in emergency situations and security of the closure without metallic components. Varying lengths and diameters of materials were tested for CT attenuation and artifact production. Supplemental foam wedges were occasionally added to passively align the cats more symmetrically with the device, promoting routine planar imaging perpendicular to the long axis of the body. All CT scans were performed using a 16 multi-detector-row helical CT unit (GE Medical Systems Light speed). Six CT protocols were tested by imaging normal nonsedated, nonanesthetized cats using 100, 120 kVp, and 100, 120 and 160 mA. Tube rotation time (0.8 seconds), pitch (1.375), field of view (20 cm) and algorithm (standard) were kept constant for all exams. All images were acquired in 5 mm and reconstructed in 3.75 and 0.625 mm slice thickness, in bone and lung algorithm in the three standard imaging planes. Subsequent evaluation of the preferred protocol was performed on clinical dypneic patients.

Results: The final design of the device was 24 cm diameter acrylic tube with wall thickness of 5 mm. The construction allows for secure closure without additional metallic or plastic components. Patients can be visually monitored throughout the imaging and quickly removed, as necessary. Patients were easily administered oxygen. Normal and dyspneic cats were imaged awake without detectable motion artifact or atelectasis. No beam hardening or angular artifacts were seen. All images were considered of excellent diagnostic quality. A protocol of 120 kVp, 160 mAs was considered the optimal for high-resolution image of the lungs of cats.

Discussion: The acrylic device ("The Better Mousetrap™") and imaging protocol met the imaging and clinical needs of normal and dyspneic cats. The device has been incorporated into the emergency service for oxygen delivery of dyspneic cats upon initial presentation. Images are of very high quality with little to no motion artifact and had no artifactual alveolar pattern due to anesthesia- or sedation-induced atelectasis. The device and CT protocols described herein appear to improve upon routine care and imaging in a clinical setting.

INCOMPLETE OSSIFICATION OF THE ATLAS IN 5 DOGS WITH CERVICAL SIGNS

C.M.R. Warren-Smith[1], S. Kneissl[2], L. Benigni[1], P. Kenny[1] and C.R. Lamb[1]. [1]The Royal Veterinary College, University of London, Hawkshead Lane, North Mymms, Herts AL9 7TA, United Kingdom and [2]University of Veterinary Medicine of Vienna, Veterinarplatz 1, 1210 Vienna, Austria.

Introduction: Most reported congenital conditions affecting the atlas in dogs are combined occipito-atlantoaxial malformations rather than abnormalities affecting the atlas alone. Incomplete ossification of the atlas has been reported only once in a dog with neurological signs. Incomplete ossification of the atlas in humans is a well-recognised condition that is usually asymptomatic unless exacerbated by cervical trauma. Computed tomography (CT) is considered the optimal imaging modality for the atlas in humans. Here we report a series of 5 dogs with cervical signs associated with incomplete ossification of the atlas.

Methods: Review of medical records of dogs that had evidence of incomplete ossification of the atlas in either CT or magnetic resonance images in the period 2002-2008.

Results: Records were found of 5 dogs of different breeds, aged 4 months - 4 years. Blunt trauma was observed in 1 dog and suspected in another. Four dogs had neurological deficits and 2 had signs of cervical pain. Defects in the atlas compatible with incomplete ossification corresponded to the normal positions of sutures between the halves of the neural arch and the intercentrum. Defects in the atlas were variable in width, but alignment between the portions of the atlas appeared normal in 4 dogs. Displacement compatible with unstable fracture was evident in 1 dog. Concurrent atlantoaxial subluxation, with dorsal displacement of the axis relative to the atlas, was evident in 4 dogs. Three dogs were treated surgically and 2 dogs were treated conservatively.

Discussion/Conclusions: Incomplete ossification of the atlas occurs in a variety of canine breeds and can be associated with cervical signs. This condition is a differential diagnosis for dogs with cranial cervical pain or neurological deficits. CT clearly depicts these defects and should be considered in dogs with clinical signs referable to this area. Incomplete ossification of the atlas may predispose to atlantoaxial subluxation. The choice of management for incomplete ossification will depend on the degree of atlantoaxial instability and the severity of neurological signs.

COMPUTED TOMOGRAPHY OF CERVICAL MASSES IN DOGS

L. Benigni, E.H. Lavender. The Royal Veterinary College, Hawkshead Lane, North Mymms, Hatfield, Hertfordshire, AL9 7TA, United Kigdom.

Introduction / Purpose: Cervical mass is a common clinical presentation in dogs that encompasses a heterogeneous group of conditions affecting salivary glands, thyroid gland, the retropharyngeal or submandibular lymph nodes, larynx, oesophagus, muscles and/or vasculature. Determining which structure is involved in a mass is necessary for diagnosis, prognosis and planning treatment, particularly surgical resection. The aim of this study was to describe the computed tomographic (CT) features of cervical masses in a series of dogs.

Methods: Retrospective review of dogs with cervical masses that had CT imaging and a definitive diagnosis by either histopathology or cytopathology in the period of 2004-2008. Images were reviewed with respect to mass location, margins, signs of local invasion, multifocal spread and attenuation pre- and post-contrast administration.

Results: Twenty-four dogs had the following diagnoses: abscess (6 dogs, 2 with foreign body), thyroid carcinoma (3), squamous cell carcinoma (3), salivary adenocarcinoma (2) and metastatic malignant melanoma, pharyngeal myxosarcoma, lymphoma, undifferentiated carcinoma, hyperplastic lymph node, botryomycosis, glossitis, sinus tract, fat necrosis and salivary gland necrosis (1 each)**.** In all dogs CT enabled identification of the submandibular and retropharyngeal lymph nodes, and the salivary and thyroid glands. All thyroid carcinomas were correctly identified as thyroid masses on CT; all had clearly demarcated circular margins and two out of three had a large central cavity. Foreign body within an abscess was visualised in one of two affected dogs. Pre- and post-contrast images were obtained in all but one (foreign body) of the dogs. All but one abscess showed distinct margins and all but one had cavities within the mass; these features were better visualised in post contrast images. Bone lysis was seen in one dog with metastatic thyroid carcinoma and one dog with locally invasive squamous cell carcinoma.

Discussion/Conclusion: CT enabled localisation of cervical masses, visualisation of adjacent critical structures, guided biopsy and surgical planning. Use of contrast consistently enabled clearer visualisation of lesion features and is recommended for CT of cervical masses. Some CT features were common to different diseases, hence definite diagnosis cannot be based on the CT findings alone. For example, neoplastic and inflammatory conditions affecting lymph nodes appeared similar. Some disease processes, for example thyroid carcinomas, showed some characteristic CT features but a larger series of cases will be necessary to better define associations between CT features and diagnosis.

MRI DIAGNOSIS IN DOGS SPINE INJURIES: A RETROSPECTIVE STUDY OF 56 CASES. F.E. Grosu[1], N. Tudor[1], I. Oancea[2], C. Vlagioiu[1], [1]Faculty of Veterinary Medicine, Splaiul Independentei 105, Bucharest, Romania, 050097, [2]Phoenix Diagnostic Clinic, Calistrat Grozovici 1, Bucharest, Romania, 021105

Introduction

Spine pathology has variable aspects in dogs as they are conditioned by the cause, age, well being, breed, genetic structure etc. Clinical signs are expressed differently depending on the type of the injury, grade of evolution and goes from an easy sensibility/pain of the affected region through monoparesis/paraparesis/paraplegia/ paralysis. Very often the clinical exam and the simple Rx exposure can not establish a sure diagnosis therefore a high fidelity technique is needed. MRI represents a technique relative new that permits high resolution, soft tissue characterization, multiplanar capabilities. This study proposes spinal column abnormalities diagnosis, characterization and spinal pathology prevalence through MRI in dogs.

Methods

There were 57 dogs examined from 23 breeds, 25 females and 32 males, between 5 months and 13 years old, examined between April and November 2008. All MR examination was done after clinical evaluation and X-ray examination using a one point five (1.5) Tesla machine using dedicated coils according to the region of interest. There were 10 cervical MR examinations, 3 thoracic, 22 lumbar, 21 thoraco-lumbar and 1 cervico-thoraco-lumbar. The dogs were in sterno-abdominal recumbency after a classic anesthesia with Acepromasine and Ketamine. The MR protocol consisted in T1 TSE (Turbo Spin Echo) and T2 TSE sequences in all three perpendicular imaging planes, sagital, coronal, axial. In some cases we used T1 fat suppressed sequences after gadolinium administration.

Results

All investigations of the dogs revealed: 61.40% (35/57) cases of disc herniation, 12.28% (7/57) spinal column tumors, 8.77% (5/57) demielinization injuries, 7.02% (4/57) spondylosis with compression of the nerve root, 3.51% (2/57) with intramedullar inflammatory changes, 1.75% (1/57) discospondylitis and 1.75% (1/57) with butterfly vertebra. 3.51% (2/57) cases didn't reveal any spinal column changes.

Discussion/Conclusions

Disc herniation occurred by protrusion or extrusion being accompanied, in some of the subjects, by disc degeneration and in some others without any adjacent changes, possible traumatic etiology. In some cases disc extrusion caused sequestration of the migrated fragments that determine medullar compression and dilation of the central canal (hydromyelia). At dogs with demielinization injuries we concluded the dilatation of the spinal cord. Vertebral tumors occurred on consequence of metastasis, or local invasion or as a primary process. MR diagnosis of the spinal column showed intervertebral disc diseases predominance. Our results suggest that MRI is a valuable, noninvasive method for spinal column examination in dogs and gives an opportunity to identify some hidden injuries for the conventional radiographic exam.

MULTIPHASIC CONTRAST-ENCANCED MULTIDETECTOR ROW CT: CORRELATION OF THE PEAK ATTENUATION IN THE AORTA ABDOMINALIS AND PORTAL VEIN WITH EASY DETECTABLE CLINICAL PARAMETERS

B. Bosch, I. Kiefer, E. Ludewig, A. Hause, G. Oechtering
Department of Small Animal Medicine, Veterinary Faculty of the University of Leipzig,
An den Tierkliniken 23, 04103 Leipzig, Germany

Introduction

The aim of this study was to explore significant correlations between easily detectable clinical parameters such as body weight, heart rate, and age with the peak attenuation time in the aorta (pETA) and portal vein (pETP) in contrast enhanced CT. Further we want to proof the data recorded could be used to establish a standard protocol.

Methods

Contrast dynamic CT was performed in 39 dogs of different body weight (mean 29 kg ± 12.3), age (mean 80.6 month ± 56.6) and breed. The dogs were sedated intravenously with one of the following anaesthesia protocols: 1.) Diazepam, Ketamin, Xylazin and Atropin (9 dogs; 23.1%), 2.) Diazepam and Levomethadon (6 dogs; 15.4%), 3.) Diazepam, Levomethadon, Ketamin and Xylazin (18 dogs; 46.2%) or 4.) Levomethadon and Medetomidin (6 dogs; 15.4%) Anaesthesia was maintained with Isoflurane in oxygen via intratracheal tube to achieve an adequate anaesthetic depth. During the dynamic CT the dogs were in apnoea. The heart rate at the beginning of the injection was measured and documented.
The contrast agent Imeron 300® Bracco was injected with 3 ml/s and 2 ml/kg body weight in the right or left vena cephalica antebrachii through a 20 gauge catheter. The dynamic CT with a Perfusion Protocol (CT Philips Brilliance 190) was started manually at the same time and lasted for 60-80 seconds.
Using the Time Injection Program the peak enhancement time in a ROI in the aorta (pETA) and portal vein (pETP) were measured.
The normal distribution of the data was checked by the Kolmogorov-Smirnov test. The different anesthesia protocols were compared with ANOVA and Bonferroni correction.

Results

All data were normally distributed. There are no statistically significant differences between the different anesthesia protocols and the peak time attenuations.
The median pETA was 24.5 ± 8.6 seconds. The forward regression model includes as variables the body weight and the heart rate with a coefficient of correlation $r=0.92$ ($r^2=0.81$). The regression equation is pETA = 12.23 + 0.61 body weight + 0.07 heart rate.
The median pETP is 43.6 ± 13.4 seconds. The forward regression model includes as variables the body weight and the age with a coefficient of correlation $r=0.66$ ($r^2=0.43$). The regression equation is pETP = 17.5 + 0.71 body weight + 0.07 age in months.

Discussion

There is a strong correlation between the pETA and the body weight in combination with the heart rate and a moderate correlation between body weight and age and pETP. Outliers, however, present a problem because they cannot be selected before the examination which limits the straightforward applicability of the regression equation.

IMPROVEMENT OF STIR SEQUENCES USING TI TUNING: APPLICATION TO MR EXAMINATION OF THE EQUINE DISTAL LIMB

F. Audigié, D. Didierlaurent, S. de la Farge J.-M. Denoix.
CIRALE - National Veterinary School of Alfort, 14430 Goustranville, FRANCE.

Introduction: short inversion time (TI) inversion recovery (STIR) sequence is one of the most useful techniques to diagnose with low field MR system bone injuries. Nevertheless, high quality fat suppression is difficult to achieve in some patients. Thus, the purposes of this study were to determine whether individual differences exist in the TI values at a given field strength and to develop a protocol usable in clinical patients improving fat suppression on STIR sequences.

Methods: A method was developed to determine the TI value providing of the best fat suppression of second phalanx. This optimal TI was calculated using several sagittal STIR sequences performed with different values of the TI parameter ("TI tuning") on a low field MR system (0.2T). Three conditions were then evaluated. 1. Cadaveric limbs: optimal TI values were determined on 3 digits (1 hind- and both forelimbs) of 8 horses (mean age: 8.6 ±4.3 y.o.) to evaluate intra- and inter-individual differences. 2. In vivo versus post-mortem: optimal TI values were measured on both forelimbs of 2 horses in vivo and during the 30h following their euthanasia. 3. Equine patients: optimal TI values were obtained as previously described in 23 horses (mean age: 8.3 ±3.3 y.o.) undergoing a foot MR examination and also using a fast protocol made of 3 short STIR sequences with an acquisition time of 30s each. Statistical differences were evaluated with either Student t-tests or one-way analysis of variance and multiple-comparison tests ($p<0.05$).

Results: Optimal TI values of cadaveric limbs (TI = 81.6 ±7.4 ms) were significantly lower than those of equine patients (TI = 108.4 ±8.3 ms). In contrast no statistical difference was found between the 3 limbs of euthanized horses. Optimal TI measured on 2 horses in vivo and following euthanasia showed a fast decrease of the TI values in the 2 hours post-euthanasia. A slower decrease of the TI was then observed until approximately 24h post-mortem. The 24-30h post mortem period was characterized by a slight increase in the TI values. Optimal TI of equine patients ranged from 88 to 120 ms (mean: 108.4 ±8.3 ms). No statistical difference was observed between TI calculated with the complete protocol and with the fast one, the mean difference in optimal TI between both protocols being 1ms ± 3.6 ms.

Discussion: Considering large differences of TI values observed in this study (reaching 32 ms in our group of equine patients) and the fact that the TI can be accurately assessed in less than 2 minutes using a fast dedicated protocol, it may be recommended to perform this test protocol to determine the optimal TI before acquiring the clinical STIR sequence. Improvement of fat suppression obtained using this TI tuning may allow the detection of slight signal abnormalities and a better delineation of the extent of pathologic processes. Because TI reflects the T1 value of the tissue (TI=0.69T1), several hypotheses may explain individual TI differences observed on normal cancellous bone such as changes in fat composition due to breed, age, activities and feeding differences or variations in blood flow or limb temperature. Nevertheless, further investigations are necessary to improve the understanding of individual TI differences.

TOMOGRAPHIC EVALUATION OF BONE MINERAL DENSITY IN LUMBAR SPINE OF DOGS SUBMITTED TO PREDNISONE THERAPY. L.A. Vescovi, J.R.P. Júnior, B.F. Lopes, M.J.L. Cardoso, F.S. Costa. Universidade Federal do Espírito Santo, Centro de Ciências Agrárias, Departamento de Medicina Veterinária. Alto Universitário s/n^{o}, Alegre – ES, Brazil. Postal Code: 29500-000.

Introduction: Glycocorticoids are widely used in veterinary medicine to treat a variety of clinical signs and infirmities due to their anti-inflammatory and immunosuppressive action. However series of collateral effects develop in patients using these medicines, mainly in long time therapies. Although the physiopathology of the process is poor elucidated, the bone metabolism can be affected in patients submitted to corticotherapy, occurring loss of bone mass and elevation of pathological fractures risk due to an inhibition in osteoblastic activity. This study aimed at evaluating possible variations of bone mineral density in the lumbar spine of dogs treated with prednisolone, by computed tomography.

Methods: This study has the approval of the *Comitê de Ética em Experimentação Animal* of the *Universidade Federal do Espírito Santo* – Brazil. Eight healthy dogs with no race or sex distinction, and with none clinical or laboratorial alterations were studied. All animals received oral tablets of prednisone (2 mg/kg body weight) during 30 days. Bone mineral density evaluation was realized by computed tomography of the second lumbar vertebrae. It was used a helical tomograph with volumetric acquisition of 2 mm. Three regions of interest (ROI) were selected in the vertebral body, and a mean value was obtained from them in each experimental moment. All the variables were measured immediately before and by the end of the administration of the medicine. The statistic analysis of the variables was made with Student's t parametric test ($P < 0,05$).

Results: It was characterized a significant decreasing of second vertebrae's vertebral body X-rays attenuation by the end of the experimental protocol. In the initial moment, the experimental group mean value for the bone density was 437,55 ± 80,05 Hounsfield unities. While in the final moment, the mean bone density was 365,16 ± 59,18 Hounsfield unities, what demonstrates a bone mass loss of approximately 17%. None of the animals presented pathologic fracture by the end of the experiment.

Discussion: The dosage of prednisone employed in this study is frequently indicated to treat immunomediated diseases, in order to obtain immunosuppression, in dogs. Diverging from some reports, the present study proves that the alterations in bone metabolism can occur in a short time period after the beginning of corticotherapy. For that reason it's important to follow up patients submitted to a therapy with high doses of prednisone, even in short time periods, allowing preventive pharmacological intervention against bone demineralization and minimizing pathological fractures risk in these patients.

TOMOGRAPHIC EVALUATION OF HEPATIC DENSITY IN DOGS SUBMITTED TO PREDNISONE THERAPY. L.A. Vescovi, J.R.P. Júnior, B.F. Lopes, V. Colombi-Silva, A.B. Lanis, F.S. Costa. Universidade Federal do Espírito Santo, Centro de Ciências Agrárias, Departamento de Medicina Veterinária. Alto Universitário s/n°, Alegre – ES, Brazil. Postal Code: 29500-000.

Introduction: Glycocorticoids are widely used in veterinary medicine to treat a variety of clinical signs and infirmities due to their anti-inflammatory and immunosuppressive action. In the liver, the corticoids are capable of promoting hepatomegaly and hepatocyte vacuolar degeneration, with lipids or glycogen accumulation. The degree of X-ray attenuation provided by computed tomography (CT) is important for the diagnosis and follow-up of patients with diseases that modify hepatic parenchyma density. This study aimed at evaluating possible X-ray attenuation variations in the hepatic parenchyma of dogs treated with prednisone.

Methods: This study has the approval of the *Comitê de Ética em Experimentação Animal* of the *Universidade Federal do Espírito Santo* – Brazil. Eight healthy dogs with no race or sex distinction, and with none clinical alterations were studied. All animals were previously submitted to abdominal ultrasonography and serum dosage of albumin, urea, ALT, AST, ALP and GGT. After these trial exams, only healthy dogs were selected. The animals received oral tablets of prednisone (2 mg/kg body weight) during 30 days. An anesthetic protocol with intravenous diazepam and propofol was used, in order to allow the realization of computed tomography exam. It was used a helical tomograph with volumetric acquisition of 2 mm. After tomographic images digitalization, the liver's degree of X-ray attenuation, expressed in Hounsfield units, was determined through a mean value of three selected regions of interest (ROI) in hepatic parenchyma. All the variables were measured immediately before and by the end of the administration of the medicine. The statistic analysis of the variables was made with Student's t parametric test ($P < 0,05$).

Results: It was characterized a statistically significant increase in X-ray attenuation between the initial moment (59,57 ± 4,73 Hounsfield unities) and the final moment of the experiment (66,29 ± 3,33 Hounsfield unities). The hepatic density, obtained by the computed tomography, increased in all the evaluated animals.

Discussion: Computed tomography examination is a technique with great sensibility to evaluate variations in hepatic parenchyma density, helping in the diagnosis of several hepatic diseases. The corticosteroids use must be done with caution due to its collateral effects, which includes the possibility of hepatic accumulation of glycogen or lipids. According to literature, the processes that promote glycogenosis unchain an increase of radiographic attenuation, while hepatic steatosis promotes a considerable decrease. The results suggest that the corticotherapy promoted hepatic alterations compatible with glycogen accumulation in the hepatocytes of the experimental group animals. For that reason it's important to follow up patients submitted to a therapy with high doses of prednisone, even in short time periods, once hepatic alterations are quickly promoted.

THREE DIMENSIONAL COMPUTED TOMOGRAPHIC RENDERING IMAGING AS A TEACHING TOOL FOR VETERINARY STUDENTS. J. KIM, J. KO, H. LEE, M KIM, N. KIM, K. LEE[1]. College of Veterinary Medicine, Chonbuk National University, 664-14, 1 ga, DuckJin-dong, Jeonju 561-756, Republic of Korea.

Introduction; Three dimensional computed tomography (3D CT) imaging was provided as a new teaching tool to ensure that no veterinary student is left behind in an aspect of radiographic anatomy. Veterinary radiology, one of the important curriculums for veterinary students has been well recognized for an initial diagnostic imaging method in small animal field. Meanwhile, most of the students confronted with the difficulty of comprehension of the 2-dimensional X-ray film image depicting 3 dimensional organs, though the knowledge of anatomy has been achieved previously.

Methods; The new teaching tool was delivered to 113 students at veterinary medical school who passed the basic curriculum such as anatomy, pathology, and physiology and so on.

Results; In the first radiology classes, plain radiographs of thorax and abdomen of a dog with heavy heartworm infection were presented and score analysis showed that only 13% and 20% of them understand entirely in thoracic part and in abdomen region, respectively. Meanwhile, after learning from the 3D CT images from the same dog, more than 94% of them figured out why the radiographic alterations happened on X-ray films completely and significantly ($p<0.001$).

Discussion; This result suggests that 3-D CT imaging is an effective tool for teaching radiographic interpretation and radiographic anatomy to veterinary medical students.

Key words: 3-D CT, veterinary medical students, radiography, dog, teaching tool.

THE CORRELATION OF MAGNETIC RESONANCE IMAGING FINDINGS OF PARANASAL SINUSES AND NASAL PASSAGES IN HORSES WITH FINDINGS DURING SURGERY

C. Tessier, A. Bruehschwein, J. Lang, P. Kircher. Department for clinical veterinary medicine, Vetsuisse Faculty of Bern, Länggassstrasse 128, Postfach 8466, 3001 Bern, Switzerland.

Introduction: Sinonasal diseases in horses have been well described. They include primary and secondary sinusitis, sinus cysts, progressive ethmoid hematoma, trauma, nasal polyps, nasal septum deviation and neoplasias. Clinical examination, endoscopy, sinoscopy, radiography, nuclear scintigraphy, computed tomography (CT) have been used in the diagnosis of these diseases. Lesions involving the sinuses and nasal passages can be a diagnostic challenge because of the complex anatomy of the equine head and limitations of current diagnostic modalities. Magnetic resonance (MR) imaging has been shown to provide excellent anatomical details and and has superior soft tissue resolution compared to CT. The aims of this study were to describe MR features of diverse sinonasal disorders in horses and describe a protocol for imaging the sinuses and nasal passages in anesthetized horses using a low field 0.3 Tesla magnet.

Methods: 13 horses presented for MR evaluation of sinonasal disorders were included in this study. All horses underwent also surgical exploration or post-mortem examination of the sinonasal lesions. A low field magnet 0.3 T (Hitachi Airis II-2) was used to image all horses. The horses were placed under general anesthesia and moved on a nonmetallic constructed support table. All examinations were performed with the horse in right lateral recumbency. Sequences used were FSE T2 sagittal and transverse, SE T1 transverse, STIR (fat suppression) dorsal, FE 3D T1 high resolutionMPR dorsal (native and with contrast enhancement), SE T1 fatsep (with contrast enhancement). 40mL of contrast medium (gadobenate dimeglumine) were administered intravenously to obtain contrast enhanced sequences.

Results: Lesions identified were nasal neoplasia (2 cases), nasal septum deviation (1), paranasal sinus cyst (1), primary sinusitis (2), secondary sinusitis (2), progressive ethmoid hematoma (2) and trauma (3). The most useful sequences were FSE T2 transverse and sagittal, STIR dorsal and FE 3D T1 (plain and with constrast). Fluid accumulation, mucosal thickening, presence of encapsulated contents, bone deformation and thickening were common findings observed in MR imaging. In most cases, MR imaging diagnosis correlated very well with intra-operative or post-mortem findings. Lesions of the tooth roots were difficult to evaluate in some cases of sinusitis because of the high sensitivity of MR to inflammatory changes, with a risk to overead and suggest false positive localisation. (oder false positive..)

Discussion: MR imaging showed not only excellent soft tissue resolution but was also an accurate method to detect bony deformation and tumors within the paranasal sinuses and nasal passages. Magnetic resonance imaging is a useful tool in diagnosing lesions of the paranasal sinuses and nasal passages in horses. However, experienced analysts are required to make accurate interpretation of the findings.

COMPUTED TOMOGRAPHY OF THE THORAX AND ABDOMEN IN THE NORMAL COMMON MARMOSET (*CALLITHRIX JACCHUS*). W. M. Wagner, H. Groenewald. Departments of Companion Animal Clinical Studies & Anatomy and Physiology, Onderstepoort Veterinary Academic Hospital, University of Pretoria, Private Bag X04, Onderstepoort 0110, Republic of South Africa (wencke.wagner@up.ac.za)

Introduction: The common marmoset (*Callithrix jacchus*) is a popular pet in the Republic of South Africa and is a common patient of our Diagnostic Imaging Section. Even though some publications exist on the ultrasonographic and radiographic anatomy of the common marmoset, there are no publications on the normal computed tomographic anatomy of the common marmoset or associated species to the best of the researchers' knowledge. The object of this paper was to develop a standard computed tomographic procedure, and to provide a description and reference values for the computed tomographic anatomy of thoracic and abdominal organs in the normal common marmoset.

Materials and methods: Five clinically healthy, anaesthetised mature common marmosets were examined using computed tomography (CT). They were positioned in dorsal recumbency. A helical scanner (Emotion Duo Helical Scanner with moving gantry, Siemens, Forchheim, Germany) was used. Images were acquired in a high frequency algorithm with edge enhancement ("inner ear" algorithm) with 1 mm collimation and a pitch of 1.5 pre-contrast as well as post-contrast after i.v. administration of 1 ml/kg + 0.05 ml of Omnipaque (300 mg I/ml). Images were reconstructed using different window and kernel settings with a minimized field of view. All CT images were evaluated by one author (WMW) and results entered on a custom-made form.

Results: Considering the size of the patient, the image quality was good. Motion artefacts did however occur and influenced the quality of some of the images. In the thoracic cavity most of the thoracic organs could be nicely identified, except for lymph nodes. In the abdominal cavity the lymph nodes could once again not be visualised, contrary for example to the adrenals. I.v. contrast enhanced anatomic detail of the thoracic and abdominal organs markedly, and blood vessels could be used as landmarks for organ identification.

Discussion: This study once again emphasised that significant species-specific differences exist in the computed tomographic anatomy. Simply applying canine or feline computed tomographic interpretation principles to the common marmoset will result in misdiagnosis, however similar examination principles should be used. The results of this study will need to be compared to previously published data of other diagnostic imaging modalities. Volumetric measurements, particularly of the kidney and liver, should be considered, since they might provide additional important information for liver and kidney disease which commonly occur in the marmoset. Further studies are anticipated in order to establish the significance of this study for clinical cases.

Acknowledgement:
The authors thank the World Primate Sanctuary for supplying the marmosets for this study, the Exotic Animal Clinic and Dr. Leon Venter for helping with the anaesthesia, and the radiology sisters of the Onderstepoort Veterinary Academic Hospital for technical assistance for the computed tomography procedures.

COMPUTED TOMOGRAPHY (CT) FEATURES OF 14 ADRENAL MASSES IN 12 DOGS. R.F. Giglio, M.D. Winter, D.J. Reese, C.R. Berry. University of Florida College of Veterinary Medicine, 2015 SW 16th Avenue, Gainesville, FL 32610

Introduction: In humans, computed tomography (CT) is the imaging modality of choice for evaluating adrenal masses. In people, adrenal tumors with Hounsfield Units (HU) units lower than 10 are likely to represent adrenal adenomas, rather than malignant lesions. In veterinary medicine, case reports of adrenal masses evaluated using CT have been reported. Reported adrenal tumors include pheochromocytomas (PH), adenocarcinomas (ADCA), adenomas (AD) and nodular hyperplasia (NH). A series of cases evaluating the CT features of adrenal tumors has not been described. The objectives of this retrospective study were to 1) characterize the features of benign and malignant adrenal tumors and 2) determine the possibility of differentiating these tumor types based their CT features.

Methods: Twelve dogs (2 dogs had bilateral tumors) with histopathologically confirmed adrenal tumors were evaluated using a multi-slice with the exception of one case which was evaluated using single-slice CT. All CT studies were reviewed in transverse, sagittal and dorsal plane 5 mm thick data sets pre and post intravenous contrast medium, with the exception of the single slice CT study, which was only reviewed in axial 5 mm thick data sets. Criteria evaluated included morphologic appearance, HU of the mass and contralateral adrenal gland (if the lesion was not bilateral), presence of tumor necrosis, venous invasion, tumor mineralization, pulmonary nodules and HU of the liver, aorta, caudal vena cava and portal vein. Where applicable, HU were compared between the different tumor types and the pre and post contrast enhancement from the same tumor using a one-tail, paired student's t test. Chi-square analysis was used to determine if any of the parameters evaluated were predictive of malignancy. A p value of < 0.05 was considered significant.

Results: In the 12 dogs, there were 5 dogs with PH (1 had bilateral PH), 3 dogs with ADCA (1 had bilateral ADCA), 2 dogs with AD and 2 dogs with NH. All tumors had heterogeneous contrast enhancement except for the NH ($p < 0.05$). There were no significant differences noted in the HU of the liver, or the morphology of the tumor between the tumor types. Mineralization was present in all groups except the NH group. There was no trend as to a predilection for a specific tumor to a specific location (right vs. left). Five of the six PH had vascular invasion (phrenicoabdominal vein and caudal vena cava), whereas none of the other tumors had CT evidence of vascular invasion. There was no correlation between the tumor volume and the presence of vascular invasion.

Discussion: In summary, CT appears to be a logical approach to evaluating adrenal masses; however, this preliminary data suggests that specific CT characteristics do not appear to help delineate tumor type in this sample of patients. Due to the small numbers of dogs and tumors of each type, further investigation into the role of CT in distinguishing adrenal tumor type is warranted.

COMPUTED TOMOGRAPHIC EVALUATION OF ABDOMINAL FAT IN MINIPIGS

Jinhwa Chang, Joohyun Jung, Hyeyeon Lee, Mieun Kim, Junghee Yoon, Mincheol Choi, Department of Medical Imaging, College of Veterinary medicine, Seoul National University, Gwanak_599 Gwanak-ro, Gwanak-gu, Seoul 151-742, South Korea

Introduction;

This study was performed to determine the Hounsfield unit (HU) value distribution of abdominal fat, and to measure the volume and cross-sectional area of the abdominal visceral and subcutaneous fat in minipigs. To analyze their relationship, we compared the CT-based volume and area, and anthropometric data including sagittal abdominal diameter (SAD), and waist circumference (WC) in normal healthy minipigs. In addition, we compared the volumes calculated at the vertebral location T11, T13, L3, and L5 level by defining them as landmarks to measure the total abdominal fat distribution and to verify the critical level.

Methods;

Six 6-month-old male minipigs, weighing 23-25 kg, were used. Minipigs had a helical CT scanning using a single-detector CT, beginning at the upper edge of the liver and continuing until the L5 level under general anesthesia. The SAD and WC were calculated after the CT scanning. Three readers assessed the HU value of visceral and subcutaneous abdominal fat by manually drawing the constant region of interests (ROIs) upon every single T11, T13, L1, L3, and L5 levels. After doing this, we determined the range of abdominal fat and evaluated the reliability and validity of the measurements. We evaluated the volume of visceral (V), subcutaneous (S), total abdominal fat, as well as the volume and cross-sectional area at the vertebral location T11, T13, L3, and L5 plane.

Results;

The mean HU of visceral fat at the T11, T13, L1, L3, and L5 level (mean ± SD) were -112.77 ± 11.61, -113.40 ± 11.59, -118.57 ± 6.1, -119.41 ± 6.9, and -115.27 ± 8.61, respectively. The mean HU of subcutaneous fat at the T11, T13, L1, L3, and L5 level (mean±SD) were -110.98 ± 9.51, -112.67 ± 8.88, -112.26 ± 8.63, -111.77 ± 8.56 and -108.8 ± 5.77, respectively. The HU value of visceral fat was significantly lower than that of subcutaneous fat at the L1 ($P < 0.01$), L3 ($P < 0.01$), and L5 ($P < 0.05$) level. There was high agreement of abdominal fat HU value among three measurers (intra-class coefficient = 0.9). The total abdominal fat volume was highly correlated with area of abdominal fat at the T13 level ($r = 0.97$, $P < 0.0001$).

Discussion;

Computed tomography (CT) is an accurate, reliable method which is convenient to measure body fat, and has an advantage in that distinguishing between visceral and subcutaneous fat is possible. Therefore, using CT was helpful in determining of volume of visceral and subcutaneous fat on its own in this study. The T13 plane was a better landmark to measure the total volume distribution of abdominal fat in normal healthy minipigs.

MRI T_1 MAPPING OF THE EQUINE DISTAL LIMB FOR OPTIMISED FAT SUPPRESSION IMAGING - RESEARCH ON A HALLMARQ STANDING MRI SYSTEM

A. Adrian[1,2], M. Koene[2], S. Roberts[3], P. Doughty[3], W. Brehm[1], K.Gerlach[1]
[1]Large Animal Surgery, Veterinary Faculty of the University of Leipzig, An den Tierkliniken 21, 04103 Leipzig, Germany; [2] Veterinary Hospital for Horses, Luesche, Essener Str. 39a, 49456 Lüsche, Germany; [3] Hallmarq Veterinary Imaging LTD, Unit 5, Bridge Park, Guildford, Surrey, GU4 7BF, England

Introduction: Fat suppressed imaging sequences are of great clinical importance and are one of the main scans within magnetic resonance imaging (MRI) protocols. Short T_1 inversion recovery scans (STIR) are commonly used to suppress MRI signals from fatty tissue. To help optimise the contrast of STIR scans, factors which influence the level of fat suppression should be investigated. The aim of this study has therefore been to find out if the age of the horse and/or the temperature of the hoof have an influence on the T_1 of fat within the hoof. With this information it should be possible to adjust the settings within the STIR scan to help optimise the level of fat suppression.

Methods: MRI was conducted on the fore limbs of 30 standing horses (″Limbs in Vivo Study″(VS)) as well as of 20 euthanised horses (″Cadaver limb Study″ (CS)), using a Hallmarq EQ2 Scanner (0.27T). The horse ages varied between 4 weeks and 19 years (median 9 years). The hoof temperature was measured using a ″testo 925" thermal camera at the lateral side of the coronary band. The temperature range has been 30 (+/- 1.8°C) in the VS and 19.1 (+/- 3.8°C) in the CS. A special STIR scan has been developed with four images per slice, each with a different inversion time (TI) (40, 80, 120, and 150ms). This STIR scan has been used to measure the T_1 of fat at six different points along the distal limb: (1) distal P1, (2) proximal P2, (3) distal P2, (4) proximal P1, (5) distal P1 and (6) Navicular Bone. The resultant data have been used to estimate the T_1 of fat using the ″Golden Section Search“ computer algorithm technique.

Results: Looking at the influence of the hoof temperature on the T_1 of fat, a significant correlation between them could be proven for the CS (Adj. R-Square 0.6607) as well as the VS (Adj. R-Square 0.3067). The effect can be described as $\Delta T_1/\Delta T = 1.8\text{ms}/°\text{C}$. In contrast to this, the age seems to correlate with the T_1 of fat in the CS, but not in the VS. While in the CS the T_1 of fat decreases by 1.9ms per year of age, the VS showed no significant difference.
Further on a slight difference between the positions (1-6) could be discerned. While the effects have been less at positions 1-3, they have been slightly more at point 4-6.

Discussion: The study documents a correlation between age and hoof temperature and the T_1 of fat. A greater effect of the temperature is shown in the CS compared to the VS, because the temperature in the VS is <27 °C. Age related effects were only found in the CS and not, for some unknown reasons, in the VS.
These results can be used to help develop a more optimised STIR scan. By changing the parameters according to the age and the hoof temperature, optimised image contrast can be achieved.

COMPARISON OF COMPUTED TOMOGRAPHY AND RADIOGRAPHY FOR EVALUATION OF MAXILLARY TUMOURS IN DOGS

C.O. Ghirelli, L.A. Villamizar, A.C.B.C.F. Pinto. Faculdade de Medicina Veterinária e Zootecnia da Universidade de São Paulo, São Paulo, Brasil, 05508-270.

Introduction/Purpose Oral cancers represent the fourth most common cancer in dogs. Imaging of oral tumors is important to determine the tumor extension and the affected local tissues, contributing to choose the most appropriated treatment. In veterinary medicine, convencional radiographs still have been used to evaluate the head, however computed tomography (CT) enables the observation of anatomic structures without superimposition, for that reason CT is presented as an important method to study the complex structure of the head. The aim of this study was to perform a comparative analysis between tomography and radiography of animal's head with oral mass.

Material and Methods Tweenty-two dogs presented with maxillary mass were submitted to simple radiography and simple and contrasted CT exams.

Results Melanoma was the most frequent histopathological type. Survey radiographs showed bony changes in 77.3% of the patients, of these cases osteolysis corresponded for 88,2%, exclusively. The possibility of adjacent tissues invasion was noticed in 6 cases (27,3%), demonstrating by increased opacity in nasal cavity (five) and frontal sinus (one). In the other hand, CT showed bony involvement in 91% of cases, and 90% were characterized exclusively by osteolysis. Considering local invasion, it was observed in 86,4% of the cases, demonstrated by the involvement of orbit, nasal cavities, frontal and sphenoidal sinuses, nasopharynx and maxillary recess.

Discussion/Conclusions Comparing the tomographic and radiographic findings was possible to verify that CT detected bony involvement in a great number of cases, besides its presents an important difference in detection of tumoral extension. In this way, the better resolution, anatomic detail and great sensibility of density differences of CT and the absence of overlapping, makes CT an essential instrument for the pre surgery evaluation of animals with maxillary tumours.

CONTRIBUTION OF NEGATIVE CONTRAST IN COMPUTED TOMOGRAPHY ARTHROGRAPHY OF THE NORMAL CANINE STIFLE. M.F. Almeida, M.J. Mamprim, L.C. Vulcano, S.C. Rahal, I.F.C Santos. Faculdade de Medicina Veterinária e Zootecnia, Universidade Estadual Paulista. Distrito de Rubião Júnior, s/n, Botucatu – São Paulo – Brasil. 18618-000.

Introduction – In Human Medicine, magnetic resonance imaging is the test of choice for knee alterations. As this test is not always available, mainly in Veterinary Medicine, there are several studies directed to establish computed tomography as an alternative in stifle evaluation. The present work aimed to evaluate the contribution of negative contrast in computed tomography arthrography of the normal stifle of dogs for the visualization of intra-joint structures such as cranial and caudal cruciate ligament, patellar ligament, menisci, and fat pad, standardizing the use of such contrast in the stifle joint.

Methods – Twenty-four pelvic limbs from dogs of varied breeds were included in the study. They were selected base on their history of absence of previous stifle joint disease and normal radiographic and ultrasonographic tests. Experimental design consisted of two groups: Group A, animals weighed up to 20 kg, and Group B, animals weighed more than 20 kg. The studied limbs were from the Pathology Sector of the School of Veterinary Medicine and Animal Science-FMVZ, São Paulo State University-UNESP, Botucatu, São Paulo State, Brazil. For the tomographic test, the limbs were kept in dorsal decubitus and the pelvic limb was flexed for introduction of the negative contrast (air); the injected dose was chosen according to the quantity needed to cause distension in the joint capsule. After the contrast injection, the limb was flexed and extended to allow air diffusion through the joint. Tomographic sections were done with the limb flexed and extended. The computed tomography equipment used in the present experiment was SCT-7800TC model, Schimadzu. Sections were helicoid, 1mm thick per 1 mm increment (1x1), at 160mA and 120 Kv, with bone hardening filter RF5, PF9. Images were reconstructed using MPR (multiplanar reformation) with sagittal and coronal sections in bone window (WW3800, WL600). After tomographic tests, joints were dissected for macroscopic evaluation of their structures.

Results – The tomographic image allowed the visualization in all joints of the following structures: cranial and caudal cruciate ligament, medial and lateral menisci, patellar ligament, medial and lateral collateral ligament, joint capsule and fat pad. The air quantity used for the joint capsule distension could be standardized as follows: animals weighed up to 20 kg, from 40 to 60 ml; animals weighed more than 20 kg, from 80 to 100 ml. A compression bandage was used on the distal portion of the stifle to reduce air escaping through the long digital extensor tendon, which has intra-joint communication. In four limbs, compression was not enough and a great air quantity escaped through this tendon.

Discussion and conclusion – Previous studies had already shown that computed tomography arthrography allows the evaluation of the knee intra-joint structures using double contrast in humans and only positive contrast in dogs. The structures isolated in this experiment were the same as those identified by Samii & Dyce (2004) in the evaluation of normal canine joints using positive contrast. Thus, the negative contrast (air) showed to be an effective alternative in the evaluation of the stifle anatomical structures by using tomography arthrography safely and at a low cost.

FAPESP and Cnpq support

RADIATION HAZARDS TO PATIENTS IN DIAGNOSTIC RADIOLOGY: CONSIDERATIONS ON COMPUTED TOMOGRAPHY IN DOGS AND CATS.

Juergen Kiefer[3], Ingmar Kiefer[1], Eberhard Ludewig[1], Dieter Gosch[2], Gerhard Oechtering[1]

[1]Department of Small Animal Medicine, Faculty of Veterinary Medicine, University of Leipzig, Germany, An den Tierkliniken 23, 04103 Leipzig

[2]Klinik und Poliklinik für Diagnostische und Interventionelle Radiologie, Universitätsklinikum Leipzig, Germany

[3]Justus-Liebig-University Giessen, Am Dornacker 4, Wettenberg, Germany

Introduction

Radiation protection of patients has recently gained considerable attention in human medicine. In veterinary medicine it is often tacitly assumed that the shorter lifespan of small animals is not sufficient for the development of clinical symptoms. One has to take into account, however, that the increasing use of computed tomography may lead to comparatively high exposures of critical organs. We show here by phantom computations that with protocols which are now typical standard in dogs doses to the eye may reach values which are so high that the risk of cataract formation cannot be excluded.

Methods

Three different helical CT-scans of the head, the nose and the whole respiratory tract of dogs were taken for the assessment of head malformations and for the planning of LATE-operations. The investigations were performed under anaesthesia (inhalation anaesthesia with apnoephase, if necessary) using a Philips Mx8000 IDT/Brilliance 6. The parameters were : head: 120 KV, 150mAs/slice, Pitch 0,6, Collimation 6* 0,75 mm, Slice thickness 1,00 mm; nose: 140 KV, 214 mAs/slice, Pitch 0,6, Collimation 2* 0,6 mm, Slice Thickness 0,6 mm; respiratory tract: 120 KV, 250 mAs/slice, Pitch 0,9, Collimation 6*1,5 mm, Slice Thickness 2.00 mm. Organ doses were computed with the aid of the programme CT-Expo V1.6 which is based on conversions factors for different human phantoms (“Adam”, “Eva”, “child” and “baby”) with no special adjustments for dogs.

Results

The skeleton, the eye lens, the brain and the thyroid were found to be the most exposed organs. The computed doses depended on the phantoms used with “baby” giving the highest values. Considering the size of typical patients in small animal practice the use of this programme appears to be the most realistic approach. The total doses after the complete investigation with three scans were: skeleton 305 mGy, lens 218 mGy, brain 188 mGy and thyroid 80 mGy. Although these values cannot be generalised they may be considered as typical for a clinical situation. They are not low as far as a possible radiation hazard is taken into account.

Discussion

It is clear from these model computations that radiation hazards to patients in small animal veterinary cannot be neglected. The formation of eye cataracts cannot be excluded. There are only few data with dogs but recent investigations in human indicate that threshold doses (if they exist at all) are well below 500 mGy. They may be exceeded in the case of multiple examinations. It should, therefore, be considered if the scan geometry should be modified in such a way (e. g. by tilting the gantry) that the eye lens is not directly exposed to the primary beam. Dose reduction may also be achieved by changing the scan parameters but this leads to a deterioration of the image quality and thus also to a loss of diagnostic precision.

ROLE OF MULTI-MODALITY IMAGING TO GUIDE PROCEDURES OF TRANSVENOUS COIL EMBOLISATION FOR THE TREATMENT OF CANINE INTRAHEPATIC PORTO-SYSTEMIC SHUNT

F. Rossi °, O. Domenech *, R. Bussadori *, C. Bussadori *
° Clinica Veterinaria dell'Orologio, Via Gramsci ¼ - 40037 Sasso Marconi (Bologna) – Italy
* Clinica Veterinaria Gran Sasso – Via Donatello 26 - 20124 Milano - Italy

INTRODUCTION

Transvenous coil embolisation is a recently described interventional radiology technique for the treatment of intra- and extrahepatic porto-systemic shunts (PSS) in dogs. Under fluoroscopic guidance, a stent and a variable number of coils are placed in the caudal vena cava and in the PSS with the aim of progressively embolise the anomalous vessel without development of portal hypertension. The aim of this study was to combine information obtained from helical Computed Tomography (CT), trans-esophageal endoscopic ultrasound (EU) and fluoroscopy (F) imaging to better understand the exact anatomy of the vascular anomaly and to guide the operator during the procedure. Advantages and disadvantages of the different imaging modality were highlighted.

METHODS

Thee dogs (one 5 months old female Labrador, one 6 months old male mixed breed and one 1 year old male Dachshund) affected by left intra-hepatic PSS underwent trasnvenous coil embolisation. Diagnosis was made by trans-abdominal ultrasonography and confirmed by helical dual phase CT scan of the abdomen using a single-slice unit (GE Pro-Speed). Transverse and reconstructed CT images were used to measure vessels diameters and select the proper size of the stents and coils. During the interventional procedure, CT images were available and oriented to match with the fluoroscopic images. Moreover, trans-esophageal EU (Esaote, My Lab 30Vet) and F (Villa Genius) were used to visualize the vessels and to follow the position of the catheters and devices in real time. Measurements of the vessels were repeated by ultrasound and compared with the CT results. The exact position of the catheters was confirmed by EU and F, injecting shaked saline solution or iodinated contrast medium to fill the PSS, respectively.

RESULTS

CT images gave the best global representation of the vascular anatomy of the abdomen and were extremely useful to help the operator to guide the catheters in the correct position and angulation to enter the PSS during F. Matching the CT transversal images with the CT scout images enabled to correlate CT and F during the procedure. Trans-esophageal EU was able to show the caudal vena cava and the stent in this vessel, the portal vein, the origin of the PSS and the coils in all three cases. The tortuous PSS could be followed cranially however it was difficult to clearly visualize its entering point in the caudal vena cava, because of artefacts due to the caudal lung during respiration. Injection of saline was useful to confirm the exact position of the catheters before placing the coils. Combining CT and EU information, the use of F and iodinated contrast medium was reduced, with an advantage for the patient and the operators. There was a total agreement between CT and EU measurements.

DISCUSSION/CONCLUSIONS

Multi-modality imaging combining CT, EU and F is useful during procedures of transvenous coils embolisation by adding anatomical information and helping the quick correct placement of the stent and the coils.

A COMPARISON OF CT AND MRI FOR THE IDENTIFICATION OF INTRACRANIAL LESIONS IN DOGS AND CATS.

K. Kromhout[1], P. Gavin[2], L. Van Ham[3], H. van Bree[1], I. Gielen[1].
[1]Department of Medical Imaging & Small Animal Orthopaedics, Veterinary Faculty, Ghent University, Salisburylaan 133, 9820 Merelbeke, Belgium.
[2] Radiology, Washington State University, Pullman, Washington, USA.
[3]Department of Small Animal Medicine, Veterinary Faculty, Ghent University, Salisburylaan 133, 9820 Merelbeke, Belgium.

Introduction

Magnetic Resonance Imaging (MRI) and Computed Tomography (CT) are the techniques commonly used for evaluating intracranial diseases. The choice between these techniques is mostly based on availability, economics and the neurological anamnesis. Previous studies have proved that MRI has a more superior soft tissue contrast resolution as CT is more sensitive for bone abnormalities. Lesions in the brainstem and cerebellum are frequently missed on CT due to beam hardening. The purpose of this study is to compare characteristics associated with lesions on MR and CT images of the brain.

Methods

Over a period of 2 years, 61 patients underwent both MRI and CT studies. MR images were obtained on a 0, 2 Tesla unit (Airis Mate, Hitachi Medical Corporation, Japan). The animals were positioned in dorsal recumbency under general anaesthesia with their head placed into a human head or wrist coil and submitted to transverse and sagittal slices in T1 and T2 spin-echo sequences. Additional dorsal FLAIR and transverse post-gandolinium T1-weighted sequences were applied. CT transverse pre- and postcontrast images were obtained with a 3rd generation helical CT scanner (GE ProSpeed, General Electric Co., Milwaukee, WI). The CT and MR images were blinded and evaluated independently. Evaluated parameters included: presence of lesions, occurrence, lesion localisation, pre- and post contrast intensity, size of the lesions, regularity/pattern, shape, margins, mass effect, peri-tumoural oedema, presence of hydrocephalus, calcification, cystic lesions, haemorrhage, herniation, and eventual involvement of calvarium.

Results

By use of CT in 34 and by use of MRI in 37 out of the 61 patients, lesions were detected. On CT in 32 cases and on MRI in 24 cases a mass effect was seen. Concerning the localisation of the lesions, on CT 22 were localised in the cerebrum, 7 in the cerebellum and 5 in the brain stem. On MRI 19 were localised in the cerebrum, 7 in the cerebellum and 8 in the brain stem. On CT 2 lesions were localised within the ventricles whereas on MRI 7 were found within the ventricles. On CT 30 solitary and 4 multiple lesions were detected and on MRI 29 solitary and 8 multiple lesions were found. On CT 16 lesions and on MRI 25 lesions were localised intra-axial.

Conclusions

By the use of CT most lesions could be detected especially when producing a mass effect. With MRI more lesions within the brain stem and within the ventricles could be seen and more multiple lesions were detected. The difference in identification of intra-cranial lesions between CT and MRI was not very spectacular. The advantages of CT are the lower cost of the equipment and the shorter duration of the examination time.

DIAGNOSTIC VALUE OF CT AND MRI IN DIAGNOSIS OF CORONOID PATHOLOGIES IN THE DOG

Stephan Klumpp, Martin Kramer

Introduction and methods

In the study we compared the results of different diagnostic imaging modalities in dogs, suffering from medial coronoid process pathology. In clinically and radiographically suspicious dogs for cornoid process pathology computertomograpy (CT) and magnetic reconance imaging (MRI) was performed. The lack of superimpositioning with both techniques allows a good evaluation of the medial coronoid process (pcm) for the following criterias:

a) fissure at the level of the pcm
b) fragments at the level of the pcm
c) deformation at the level of the pcm
d) increased opacity at the level of the base of the pcm
e) heterogenous opacity at the apex of the pcm

Results

Altogether 44 elbow joints of 12 different breeds were examined. Labrador Retriever (38,6%), mixed breed (22,7%) and Golden Retrievers were the three most common breeds. 68% (n=30) were male and 32% (n=14) were female. The age of the dogs ranged from 6 to 117 month. The body weigth was between 19 and 57 kg.

Within the following points CT and MRI were compared:

a) fissure at the level of the pcm
b) fragments at the level of the pcm
c) deformation at the level of the pcm

Within these three points no significant difference between CT and MRI was seen.

d) increased opacity at the level of the base of the pcm
e) heterogenous opacity at the apex of the pcm

Discussion

Therefore both diagnostic imaging modalities are appropriate for evaluating a coronoid process pathology in the dog.

The two points:

d) increased opacity at the level of the base of the pcm
e) heterogenous opacity at the apex of the pcm

are only evaluable on CT images. From our point of view at that time these two points can be of crucially importance for diagnosing a coronoid pathology in the dog. Further studies are necessary to evaluate the anatomically normal CT picture to secure these findings and their importance for the diagnosis of coronoid pathology in the dog. The shorter examination time in CT compared to MRI and the ability to evaluate both elbow joints with one examination are great advantages of CT. Therefore at this time CT is prior to MRI in clinical patients with suspicion of coronoid process pathology.

Stephan Klumpp (Stephan.Klumpp@gmx.net)
Klinikum Veterniärmedizin der Justus-Liebig-Universität Giessen
Klinik für Kleintiere, Radiologie, Frankfurter Str. 108, 35392 Giessen, Germany

CARDIAC MAGNETIC RESONANCE ANGIOGRAPHY AND CARDIAC MRI – TECHNIQUE AND APPLICATION IN TWO DOGS WITH INVASIVE HEART BASE TUMORS

Mai W. Section of Radiology, University of Pennsylvania School of Veterinary Medicine, Philadelphia, PA 19104.

Introduction/Purpose:
The excellent soft tissue contrast of MRI is routinely exploited in human cardiology where the development of hardware and software has allowed excellent imaging of the moving heart. Even though cardiac MRI (CMRI) has become the optimal technique for morphological assessment and quantification of ventricular function in people, it has only been reported in a few preliminary studies in veterinary medicine, and is primarily used in clinical research. This presentation describes the method and feasibility of gated CMRI in dogs. CMRI and cardiac magnetic resonance angiography (CMRA) were then applied to imaging of two dogs with invasive heart base tumors.

Methods:
Three clinically normal dogs and five colony dogs affected by a genetic disease involving various muscles were imaged using gated CMRI. Six animals received repeated examinations separated by a few weeks and a total of 21 CMRIs were performed using a similar protocol. Then two dogs with a known heart base tumor and right sided heart failure were imaged with CMRA (using a previously reported method for portal MRA), as well as gated CMRI to assess the location and extension of the neoplasia in planning for minimally invasive stenting. CMRI was performed using both black blood imaging (Oblique Fast Spin Echo [SE] Double Inversion Recovery) and bright blood Cine imaging (gradient echo Cine stack). Data acquisition was gated to the cardiac cycle using the ECG signal and obtained during apnea, to prevent motion induced artifacts.

Results:
CMRI consistently yielded good quality images. SE sequences yielded excellent contrast between blood and myocardium while Cine imaging allowed dynamic assessment of contractility. Depending on the heart rate, 4-5 cuts (8 mm thick) could be obtained using black blood CMRI in 1 to 1.5 min, and 2 cuts using Cine-CMRI in approximately 2 min (sampling 30 data points within the R-R interval). 3D cardiac MRA with 4 phases was obtained in less than 2 min. In the 2 dogs with a heart base tumor, excellent imaging of the tumor and its relationship to the cardiac structures, caudal vena cava and pulmonary veins was obtained.

Discussion/Conclusions:
To the author's knowledge, this is the first report of the use of MRI to assess heart base tumors in dogs. The method is simple, effective and subjectively better than other cross-sectional imaging techniques such as echocardiography and contrast-enhanced CT in assessing the anatomic relationships of the neoplasm to surrounding structures. The preliminary study in the colony dogs showed that CMRI was consistently feasible and reproducible in dogs under anesthesia with short acquisition times. It is anticipated that CMRI and CMRA will develop as an effective method to image the heart in veterinary patients with complex cardiac conditions (congenital diseases or neoplasia), especially as minimally invasive procedures to treat these patients are being developed.

DETERMINATION OF THE MANDIBULAR CANAL COURSE BY MEANS OF COMPUTERIZED TOMOGRAPHY IN MANDIBLES OF BRACHYCEPHALIC AND MESATICEPHALIC *CANIS FAMILIARIS*. ABSTRACT Martinez

For some surgical procedures in dentistry, as the exodontia, the orthognathic surgery, orthopedic surgery, oral neoplasm resection, and the dental implants placement, it is important to know the accurate localization of the mandibular canal (MC), which contains the vascular and nerve package. The aim of this research was to determine the course of the mandibular canal through the mandible with relation to the structures that surround it (lingual surface, vestibular surface and ventral surface), alveolar crest and dental roots in two kinds of dog skulls by means of computerized tomography (CT). For that, 10 skulls of mesaticephalic dogs and 10 skulls of brachycephalic dogs were evaluated in the Image Diagnosis Service of the Veterinary Hospital of the Veterinary and Zootechny School of the São Paulo University. In order to determine the localization of the canal passage in the mandible, measures were taken, in relation with: lingual surface, vestibular surface, ventral mandible surface and alveolar crest with CT help. The measurements were submitted to statistical analysis and showed that the mandibular canal course was similar in brachycephalic and mesaticephalic dogs, the measurements indicated that the mandibular canal descends slightly from the mandibular foramen to the molar area, slightly closer to the lingual surface than the vestibular surface until the molar region. The MC continues rostrally occupying the ventral region of the mandible body, reaching its maximum depth in relation with the alveolar crest border at the level of the 1st molar and 4th premolar teeth area. In the 4th and 3rd premolar region the MC maintains a similar distance between the vestibular and lingual border. At the level of the 3rd premolar the MC originates the mental caudal mental foramen before increases the distance in relation with the lingual and ventral border just before its termination at the medial mental foramen on the vestibular surface, ventral to the 2nd premolar roots.

Key Words: Mandibular canal. Computed tomography. Veterinary dentistry. Mesaticephalic dogs. Brachycephalic dogs

RELATIONSHIP BETWEEN CANINE STIFLE STRUCTURAL DAMAGES AND FUNCTIONAL IMPAIRMENT IN EXPERIMENTAL OSTEOARTHRITIS: PEDOBAROMETRIC GAIT ANALYSIS COUPLED WITH 1.5T MRI.

L. Blond,[1] M. Moreau,[1,2] M.-A. D'Anjou,[1] J.R.E. del Castillo,[2] C. Boileau,[3] J. Martel-Pelletier,[3] F. Abram,[4] J.-P. Raynauld,[3] J.-P. Pelletier,[3] and E. Troncy, [2]

[1]The Companion Animal Research Group, [2]GREPAQ, Faculty of veterinary medicine, Université de Montréal, P.O. box 5000, St-Hyacinthe (QC), J2S 7C6 Canada;
[3]Osteoarthritis Research Unit, University of Montreal Hospital Centre, Notre-Dame Hospital, [4]ArthroVision Inc., Montreal, Quebec, Canada

Introduction

Lameness is a cardinal feature of osteoarthritis (OA) and reflects painful functional impairment. The impact of OA joint structural damages on the dog's gait has been poorly documented. Therefore, this study explored the relationship between structural damages induced in the dog model of OA, as assessed on high-field (1.5T) magnetic resonance imaging (MRI), and limb function over a 26-week period.

Methods

In a prospective experimental study, OA was surgically induced by transection of the right cranial cruciate ligament in 5 anesthetised dogs. Peak vertical force (PVF) was acquired at baseline (before), as well as 4, 8, and 26 weeks post-surgery in parallel to MRI scan of the dog's right stifle. Osteophytosis, joint effusion and meniscal tears and degenerative changes were scored (0-3, each). Cartilage defect (0-4) and subchondral bone marrow lesions (BML) (0-3) were scored while loss of cartilage volume (mm^3) was computed. $P<0.05$ was considered significant using correlation tests and analysis of variance.

Results

Significant limb impairment (lower PVF) and OA joint damages perceived upon MRI were induced in this model. Initially (over the first 2 months), PVF is negatively correlated to BML, and subsequently to cartilage defect and BML. The evolution of PVF is not influenced by cartilage volume loss, and minimally by osteophytosis score or joint effusion. At W26, higher PVF significantly correlated with more severe meniscal tears, showing a trend ($P<0.10$) toward cartilage volume loss. Inline with these findings, extend of meniscal tears correlated significantly with less osteophytosis and joint effusion.

Discussion

This study originally highlights the role of structural defects such as evaluated by MRI on OA-induced functional disability as explored with PVF. If PVF is mainly affected by BML and cartilage defects, meniscal integrity looks more affected by functional joint activity.

CANINE STIFLE MR IMAGING – CORRELATION TO ARTHROSCOPIC FINDINGS

S.P. Holmes[1], R.L. Tucker[2], P.R. Gavin, S. Martinez[2], J. Lincoln[2]
([1] – Illumipet, LLC. 542 Turkey Creek, Alachua, FL 32615; [2] – Washington State University, 100 Grimes Way, Pullman, WA, USA 99164)

Introduction

Cranial cruciate ligament (CCL) injury is considered the most common surgical orthopedic disease of canines. Currently, the diagnosis of CCL injury is based on patient history, physical examination findings, and stifle radiography. In human medicine, magnetic resonance imaging (MRI) is the gold standard for the assessment of knee pathology because it allows better pre-surgical planning and distinguishes surgical and non-surgical diseases. MRI has had limited implementation into veterinary stifle orthopedics. This study was undertaken to evaluate the clinical application of stifle MR in patients undergoing stifle arthrography prior to surgical intervention.

Methods

A prospective, randomized study of twenty dogs, with body weights greater than 15kg, was conducted. The patients were randomly selected from all patients presented for stifle lameness, presumed cranial cruciate ligament (CCL) injury and those scheduled to undergo corrective stifle surgery. The exams were performed on Phillips Gyroscan 1.0T MRI unit. The imaging protocols, adapted from routine human knee exams, were used on all patients, with no manipulation of the imaging parameters. The MR exams were reviewed by 3 board certified radiologists who were blinded to the patient's clinical data (history, physical exam findings, and stifle radiographs). The MR images were evaluated for the integrity of the cruciate ligaments, menisci, collateral ligaments, articular cartilage and for the presence of joint effusion, synovitis, bone hyperintensity and extra-articular irregularities.

Results

Stifle MR correctly distinguished partial (n=17) and complete (n=13) cruciate ligament rupture in all cases. The amount of tearing in patients with mild partial cruciate tears was underestimated compared to arthroscopy, which was attributed to partial volume artifact. The Outerbridge score (articular cartilage assessment) for approximately 50% of the patients was greater than 3 and for 20% patients was 1-2. Definitive visualization of cartilage erosion was not reported by any radiologist reviewer. Reviewers were suspicious of cartilage lesions in areas of subchondral bone hyperintensity on fat-suppressed images. When these lesions were included as presumed cartilage erosions, the lesions detected by MR still underestimated the number and extent of cartilage damage detected with arthroscopy.

Discussion

MRI distinction of partial versus complete caudal cruciate ligament tears is not surprising since superior soft tissue contrast resolution is a primary strength of MRI. The marked difference in the detection of cartilage abnormalities is most likely due to the thinness of canine stifle cartilage (reported 0.6–1.3 mm for dogs). Accurate detection of canine cartilage lesions is challenging; similar experiences are reported in human knee imaging.

RADIOGRAPHIC, CT AND MRI FEATURES OF COMPRESSIVE CERVICAL MYELOPATHY IN YOUNG TEXEL AND BELTEX SHEEP. R. Hagen*, K. Mc Lean[Ø], C.N. Hahn[¥], C. Penny[¥]. *Section of Diagnostic Imaging and Radio-Oncology, Vetsuisse Faculty, University of Zürich, Switzerland; [Ø] Sustainable Livestock Systems Group, Scottish Agricultural College, Edinburgh, Scotland; [¥] Department of Veterinary Clinical Sciences, Royal (Dick) School of Veterinary Studies, University of Edinburgh, Scotland.

Introduction: Cervical compressive myelopathy has been well studied in horses and dogs but only few case reports of lesions and anatomical variation in sheep are published. Causes for compression of the cervical spinal cord are vertebral malformations, malarticulations, intervertebral disc degeneration, enlargement of the synovial joints, hypertrophy of the ligaments, trauma and space occupying lesions in the vertebral canal. In young Texel and Beltex Sheep, small masses of fat tissue that prolapse from dorsal into the vertebral canal, thus causing spinal cord compression have recently been described. These lesions were diagnosed by myelography and CT myelography and post-mortem and histopathological examination confirmed the lesions consisted of fatty tissue. MRI also clearly demonstrated the lesions.

Methods: 14 Texel and Beltex sheep, aged 9-26months, 11 males and 3 females, presented with various degrees of neurological deficits compatible with cervical spinal cord compression. These underwent plain radiography and conventional myelography (4) and (2)/ or CT myelography (8) of the cervicothoracic region. Radiographs were performed in live sheep under sedation and in 7 cases on post mortem specimens. Myelography and CT myelography were performed under general anaesthesia after injection of 0.15 ml/kg Iohexol (Omnipaque 300mg/ml, Amersham Health, Princetown NJ) into the atlanto- occipital cistern. Radiography was performed with an Agfa CR system (Agfa Healthcare, UK), CT myelography using a helical CT scanner (Somatom Esprit, Siemens, Germany) to examine the cervical and cervico-thoracic regions. Images were acquired contiguously and reconstructed using soft tissue and bone algorithms. Two post-mortem specimens of the cervico-thoracic vertebral column were examined by MRI. MR images were obtained as T1, T2* and STIR sequences in transverse, dorsal and sagittal planes, using a low field (0.27 Tesla) MR unit (Hallmarq Veterinary Imaging, Guildford, UK) with an equine carpus or fetlock coil, depending on the size of the specimen.

Results: No significant abnormalities were identified on plain radiographs. Myelography showed extradural compression at the level of C6-7. Pre-contrast CT scans demonstrated in cases with large masses a hypoattenuating (isoattenuating to fatty tissue) region that corresponded to the extradural lesions found in CT myelography. At post-mortem examination these regions were diagnosed as consisting of lipomatous masses, and the underlying spinal cord showed typical pathological changes associated with chronic compressive lesions. All but one lesion were at a single site, localised at C6-7, and most lesions were bilateral (7/9). In one case lesions were present at C5-6 and C6-7. On MRI, compared to the spinal cord, the fatty masses were hyperattenuating in T1 weighted images, slightly hypo-attenuating in T2* weighted images and clearly hypoattenuating in the STIR sequence.

Discussion: The recently described novel type of ovine compressive cervical myelopathy manifests distinct imaging features that are best identified using cross sectional imaging. Radiographic myelography demonstrated these lesions, but in addition, both CT an MRI allowed exact localisation and assessment of tissue composition.

This study was part funded by the British Texel Society.

EVALUATION OF RADIOGRAPHIC AND ULTRASONOGRAPHIC CHANGES OF THE PATELLAR LIGAMENT FOLLOWING TIBIAL TUBEROSITY ADVANCEMENT

K. Kühn[1], M. Makara[1], S. Ohlerth[1], M. Hässig[2], T. Guerrero[3]

[1]Section of Diagnostic Imaging, [2]Department for Farm Animals, [3]Clinic for Small Animal Surgery, Vetsuisse-Faculty, University of Zurich, Winterthurerstrasse 260, CH-8057 Zurich, Switzerland

Introduction – Tibial tuberosity advancement (TTA) and tibial plateau levelling osteotomy (TPLO) are two common dynamic techniques for treatment of cranial cruciate ligament (CrCL) disease. Patellar tendinitis has been described after TPLO. The suggested cause is an increased stress on the patellar ligament due to a decreased lever arm length of the patellar ligament. By performing TTA, the distance between the femorotibial contact area and the new positioned insertion of the tibial tuberosity is increased, and therefore the lever arm is larger. This results in lower forces required to extend the stifle and less stress on the patellar ligament. So far, clinically relevant patellar tendinitis after TTA has not been described. The aims of this prospective clinical study were to radiographically and ultrasonographically evaluate the patellar ligament subsequent to TTA.

Methods – Examination of the patellar ligament was performed preoperatively, at approximately 6-8 weeks and 4 months post-TTA. Total length and thickness were radiographically measured 1 cm distal to its origin and 1 cm proximal to the level of its insertion. Thickness and transverse area were ultrasonographically evaluated in the same locations and also midway of the ligament. The ultrasonographic appearance of the patellar ligament was also scored subjectively (0: normal, 1: ligament thickening only, 2 and 3: ligament thickening and moderate or severe signs of tendinitis).

Results – Preoperatively, 14 dogs were examined, 12 dogs were scored normal and 2 dogs had score 1. Thirteen dogs underwent postoperative follow-up examination after 6-8 weeks and mean radiographic and ultrasonographic ligament size increased (P = 0.0000 – 0.007; paired t-test) and subjective ultrasound score worsened (P = 0.002; Wilcoxon signed-rank-test). Seven dogs underwent the second follow-up examination after 16 weeks. Most ultrasonographic ligament size measurements and subjective score at this time differed significantly from the preoperative measurements (P = 0.003 – 0.057); radiographically, measurements did not differ. Between the two follow-up examinations, measurements did not differ statistically. However, 2 dogs improved their sonographic score at the second follow-up.

Discussion – Although after TTA there is less biomechanical stress on the patellar ligament, tendinitis was diagnosed in the present study. Other causes such as surgical trauma, arthrotomy, perfusion injury, complete versus partial CrCL rupture, excessive advancement, excessive postoperative activity or altered insertion angle of the patellar ligament at the tuberositas tibiae should be also considered. More cases and further studies are needed to elucidate the causes of patellar tendinitis observed in our study.

INTEGRATION OF 3-D IMAGING TECHNOLOGY INTO GROSS ANATOMY INSTRUCTION FOR THE ENHANCEMENT OF VETERINARY EDUCATION.

R. L. Tucker[1], V. M. V. Machado[2] & L. K. Sprunger[1], [1]College of Veterinary Medicine, WSU, Pullman WA, USA 99164-6610, [2]Medicina Veterinaria e Reproducao Animal, FMVZ-UNESP, Botucatu, Sao Paulo, Brasil CEP 18609-040

Introduction: Conventional instruction of veterinary gross and applied anatomy fails to achieve the goals of long-term retention and appreciation of many important anatomic relationships, especially 3-D relationships of relevant anatomy. There is inadequate student comprehension of modern cross-sectional anatomic imaging methods, including ultrasound, computed tomography and magnetic resonance imaging. Integration between basic anatomy knowledge and application of the information during clinical rotations is compromised by the delay between introduction of anatomy early in traditional veterinary curriculums and integrated use later during clinical years. Veterinary schools have not kept pace with increasing applications of cross-sectional imaging techniques in veterinary patients and expectations of animal owners, or with researchers and industries involved in animal studies demanding high resolution imaging of advanced anatomic relationships, pathophysiology, interventional procedures and other treatment protocols.

Methods: An integrated teaching module using canine pelvic limb anatomy was developed with a computer-based auto-tutorial of the 3-D anatomy of the canine pelvic limb using digital radiography (DR), computed tomography (CT), and magnetic resonance imaging (MRI) to demonstrate cross-sectional anatomic relationships. Interactive instructional programs were created outlining relevant anatomy, cross-referencing all imaging modalities and photography of gross preparations. Freeze-dried cross-sectional gross anatomic preparations were generated oriented in the exact image planes as the transverse cross-sectional imaging modalities. A cursory lecture to freshman veterinary students introduced conventional radiography and 3-D imaging technologies and illustrated application of DICOM viewing software used in the integrated project. Voluntary self-evalaution quizzes were provided for students to test their knowledge on DR, CR and MRI images of the limb.

Results: Veterinary freshman students achieved better appreciation of relevant anatomy by integrating 3-D imaging technologies with gross anatomy instruction and cross-sectional preparations of the canine pelvic limb.

Discussion: The clinical relevance and application of basic anatomic knowledge into clinical training can be partially addressed by creating anatomy teaching modules, incorporating the latest imaging modalities and viewing programs, coupled with gross anatomy dissection and cross-sectional anatomic preparations to better illustrate the 3-D anatomic relationships essential to clinical and research applications. Future analysis will be required to access the impact on longer term knowledge retention and integrated anatomic applications.

COMPLICATED ATLANTOAXIAL SUBLUXATION IN A POMERANIAN REQUIRING MULTI-MODALITY IMAGING FOR A DIAGNOSIS. D. Rodriguez, K. Clapp, L. Gaschen, N. Rademacher.
Department of Veterinary Clinical Sciences LSU School of Veterinary Medicine. Skip Bertman Drive · Baton Rouge, LA 70803. USA

Introduction

This report describes a 7-year-old MC Pomeranian diagnosed with atlanto-axial subluxation which was complicated by cervical vertebral malformation and occipital dysplasia, Chiari malformation and spinal cord disease that required a multi-modality approach to make an accurate diagnosis.

Methods

A 7-year-old male castrated Pomeranian presented to the Veterinary Teaching Hospital and Clinics of the Louisiana State University School of Veterinary Medicine with a history of syncope of unknown origin and a previous single seizure episode at 1 year of age. Cardiac disease was ruled out. A right-sided head tilt, lateral right-sided strabismus, CP deficits in forelimbs with absent propioception in the hind limbs, extensor rigidity, horizontal nystagmus, ataxia in all four limbs, and depressed mentation were revealed upon neurologic examination. Neuro-imaging was planned.

Results

Spinal radiographs, computed tomography (CT) and magnetic resonance imaging (MRI) were performed. Survey radiographs of the cervical spine showed atlanto-axial subluxation. CT findings: 1) Cerebellar crowding with a reduced caudal fossa and enlarged foramen magnum, 2) caudal occipital malformation with condylar hypoplasia, 3) C1-C2 malalignment with dorsal deviation of the dens, 4) mild hydrocephalus. MRI findings: 1) cerebellar crowding with mild cerebellar herniation, 2) mild hydrocephalus, 3) medullary kinking, 4) C1-C2 dorsal compressive lesion with secondary mild syringohydromyelia, 5) dorsal deviation of the dens and 6) chronic intervertebral disc disease at C5-C6 and C6-C7. A final diagnosis of Chiari-like malformation with secondary mild syringohydromyelia, concurrent cervico-medullary junction instability due to atlanto-axial subluxation, dorsal displacement of the dens, occipital dysplasia and suspected dysplasia of the occipital condyles was made.

Discussion

Neurologic signs in dogs with Chiari-like malformation are similar to those present in dogs with high cervical compressive lesions and neuro-localization is challenging.
CT volume rendering and MRI is necessary to determine skeletal (occipital, C1 and C2 malformations) and CNS involvement present with Chiari-like malformations such as medullary kinking and secondary syringohydromyelia. The presence of syringohydromyelia may be equivocal although severity seems to correlate with severity of clinical signs. Recently cervico-medullary junction anomalies were considered common in a group of 64 Cavalier King Charles (20%). This finding adds complexity to the understanding of the pathophysiology involved in the generation of symptomatic patients. No information regarding atlanto-axial subluxation as part of the Chiari-like malformation syndrome has been described until now. Diagnosing atlantoaxial subluxation in patients with Chiari is important for therapeutic planning and determining prognosis.

RADIOGRAPHIC DETECTION OF THE AIRWAY OBSTRUCTIVE SYNDROME IN A TECKEL DOG – CASE REPORT. M.A.R. Feliciano, C.A.L. Leite, T. Silveira, A.C. Nepomuceno, W.R.R. Vicente. Universidade Estadual Paulista (UNESP), Campus Jaboticabal, Departamento de Reprodução Animal, Via de Acesso Prof. Paulo Donato Castellane, s/n°, Jaboticabal, São Paulo, Brazil, 14884-900.

Introduction: In humans, in the field of Otolaryngology, there are several causes of the airway obstructive syndrome, also called sleep obstructive apnea syndrome. The large increase of the soft palate generates reduction of the nasopharynx and increase the contact between the soft palate and the tongue, contributing to the collapse in this region. In canines and felines, the main and the most common hard palate diseases are defects, cracks, swellings, erosions and trauma secondary to malocclusion. In relation to the soft palate there are the mucosa erosions and ventral depression by nasopharyngeal mass. Airway obstructive syndrome is often found in the breeds of brachiocephalicus dogs. The disease, also called airway obstructive brachiocephalicus syndrome, develops as a consequence of hereditary anatomical characteristics of the brachiocephalicus skull. As a result, the oropharynx presents shortened and twisted, with a relatively long soft palate (found in 100% of the brachiocephalicus), an inadequate length of the nostrils (stenosis, found in 50% of the affected animals) and larynx diseases (larynx collapse in 30% of the cases). The disorder contributes to exercise intolerance and stress intolerance and, in more advanced cases, collapse and cyanosis. The purpose of this study is to report a case of extension of the palate in a Teckel dog (not brachiocephalicus), not yet described in the veterinary literature.

Methods: An animal of the canine species, male, Teckel breed, nine years old, weighing 9.6 kilograms, had a history of whitish nasal secretion, when it lie down, for three years. The owner reported sneezing without cough, fatigue or dyspnea. He also reported that antibiotics had been performed, observing clinical improvement, but with recurrence. The animal lived indoors, in an environment with the presence of mattress, carpets and duvet. Vaccination was updated. They were made general and specific physical examination of the respiratory system and additional examination (radiography).

Results: At general physical examination, parameters such as heart rate, pulse, rectal temperature, capillary reperfusion time, respiratory rate, hydration, mucous membranes and lymph nodes were unchanged. The animal was obese. On examination of the respiratory system, was heard a laryngeal tracheal sound more noisy, without pulmonary crackles. Cough reflex was normal. Through radiographic examination was possible to complete the diagnosis of the airway obstructive syndrome, showing the extension and the increase of radiopacity of the soft palate.

Discussion: The sounding of this finding confirms the snoring as the main clinical sign of this disease. The main affected dog breeds are the brachiocephalicus, Pinscher and Chow Chow. In this present study, it was verified the disorder in a dog of the Teckel breed, not yet cited in the veterinary literature. Associating the clinical data with the radiographic findings is possible to conclude that the animal of the Teckel breed presented change in the morphology of the soft palate, characterized by the extension of this structure, concluding the diagnosis of airway obstructive syndrome. To establish this diagnosis, it is noteworthy the novelty of this change in animals of this breed and the radiographic characterization of this change.

RADIOGRAPHIC ASPECTS OF FELINE CHONDRODYSTROPHY – A CASE REPORT. M.A.R. Feliciano, C.A.L. Leite, T. Silveira, A.C. Nepomuceno, W.R.R. Vicente. Universidade Estadual Paulista (UNESP), Campus Jaboticabal, Departamento de Reprodução Animal, Via de Acesso Prof. Paulo Donato Castellane, s/n°, Jaboticabal, São Paulo, Brazil, 14884-900.

Introduction: Congenital, hereditary and development osteoarticular diseases are common in clinical and radiological routine in dogs, however, they are considered uncommon in cats. The majority of the conformational anomalies is derived from of dominant autosomal genetic interactions, with highly variable expressivity. Chondrodystrophy is characterized by osteoarticular angular deformities and may also occur shortening of the limb due to bone hypoplasia. This bone disease predisposes to degenerative joint disease. In dogs, it is common in breeds such as Basset Hound, Pequinês, Pug and Teckel, and highly undesirable in the Alaskan Malamute and German Shepherd. How is uncommon in cats, there are no reports of the prevalence in the races. The only obvious clinical sign is persistent or intermittent lameness. The diagnosis of this disease is important for the control of the crossings, avoiding that the anomaly could occur in the future generations. This alteration usually is incidental radiographic findings or deformities and anomalies without clinical consequences for the animal. The purpose of this study is to report the radiographic aspects of a case of feline chondrodystrophy, since there are no published studies in veterinary medicine, in respect of this disease in felines.

Methods: A female cat, mixed breed, presented tortuous limbs. They were performed physical and radiographic examination of the animal. After physical containment of the patient, thoracic and pelvine limbs were radiographed in craniocaudal and mediolateral projections, using X-ray generator equipment Medtronix, model BR200®.

Results: At physical examination was verified that the animal presented deformity in all limbs, but was not noticed any clinical symptoms that compromise the general health of the animal. Radiographic examinations allowed the visualization of change in bone angulation of humerus, radius, ulna, carpus, metacarpus, femur, tibia, fibula, tarsus and metatarsus. It was also visualized an enlargement of the joints related to bone structures of the limbs.

Discussion: Radiographic signs that characterize the chondrodystrophy are angular deformities of the joints, in their various presentations. It is also possible to observe smaller and malformed bones, in relation to the contralateral limb. Thus, in analogy to the canine species, was possible to observe alterations consistent with chondrodystrophy, suggesting the occurrence of this disease in felines. Although uncommon in cats, chondrodystrophy can be suspected at radiographic examination of felines and is of great relevance to the strategy of conservative treatment and reproductive management of the patient.

RADIOGRAPHIC SURVEY OF 430 DOGS WITH TRANSITIONAL VERTEBRAE.
Cavaletti F. C. & Urtado S. L. R. 2009. Institute Veterinary of Image, R. Agissê, 128, V. Madalena, São Paulo, SP, 05439-010, e-mail: fercavaletti@yahoo.com.br

Introduction: Transitional vertebrae is a congenital anomaly characterized by abnormal development of the vertebral body, with anatomical characteristics of the region adjacent (Owens & Biery 1998). Can be found with radiographic finding or foster instability and degeneration of the vertebral body. Affects dogs of various breeds, large or small size and both sexes, however, German Shepherd, Lhasa apso and Shih-tzu show has a high frequency (Thrall 2002).
Materials and Methods: All animals were radiographed in the Institute Veterinary of Image with a Techno-design analog, 500mA, high frequency, floating table, Porter-bucky Techno-design, chassis and film Kodak with sizes proportional to the dogs. The protocol of the institute for study of the column is to radiographic projections látero-lateral, and if there is a need to supplement with the projection ventro-dorsal, but the regions have been requested by colleagues to refer their patients for the exam. We conducted a survey of the radiographic reports of 430 dogs with transitional vertebrae, aiming to contribute to the study of the disease and show the regions most affected and prone to develop a degenerative process.
Results: Noticed that most of the transitional vertebrae is in the lumbosacral region and thoracolumbar with 65.5% (282 animals) and 28.1% (121 animals). In 70.9% (200 animals) cases of transitional vertebrae in the lumbosacral region are signs of instability and degeneration associated and thoracolumbar region, 47.1% (57 animals). Sacralization of L7 was the most frequent that lombarização of S1 with 68.4% and (193 animals) 31.5% (89 animals) respectively. In thoracolumbar region did not reveal significant difference between the lombarização of T13 and L1 thoracolization with 56.1% (68 animals) and 43.8% (53 animals). The region sacrococcygeal also showed high incidence, with 20.7% (89 animals). In 42.6% (38 animals) of these cases, had a transitional vertebrae in another region of the spine. The cervicothoracic region not presented importance radiographic with only 15 cases. In 77 animals (17.9%) were found over a region affected by the transitional vertebrae and 15% (65) of the dogs had scoliosis, kyphosis or lordosis. In sacralization of L7, the fusion of left transverse process (55.4%) occur more frequently than the right (38.3%) and in few cases the merger was bilateral (6.2%). In lumbarization of T13, the bilateral aplasia of the ribs is more frequent (57.3%), followed by aplasia left (26.4%) and right (16.1%).
Discussion and Conclusions: The lumbosacral and thoracolumbar region were represented in higher radiographic and clinical importance, as shown a high incidence, degenerative signs frequent and often associated with intervertebral disc disease or caudal equina syndrome (Flãckiger et al 2006). In the lumbosacral region, the sacralization of L7 is more frequent that lombarização. Most animals with transitional vertebrae sacrococcygeal show other regions affected by disease, though the merger between Cco1 with S3 is seen only as a radiographic finding. The cervicothoracic region showed no significant importance. Difficulty in diagnosis may occur when more than one region is affected by the transitional vertebrae, impossible to count the vertebrae without X-ray the entire length of the spine. Know that the transitional vertebrae favors the instability of the vertebral body, but in the lumbo-sacral noted that this process occurred with greater frequency and severity. Another important factor we should consider and that has not been much studied is the influence of the transitional vertebrae lumbosacral with the development of hip-dysplasia which can encourage the process of osteoarthritis.
References: Owens J. M. & Biery D. N. 1998. Radiographic Interpretation for the Small Animal Clinician, 2:133-134, Willians and Wilkins. - Thrall D. E. 2002. Textbook of Veterinary Diagnostic Radiology, 4:99-100, Saunders. - Flãckiger M. A., Damur-Djuric N., Hãssig M., Morgan J. P. & Steffen F. 2006. A lumbosacral transitional vertebra in the dog predisposes to cauda equina syndrome. Veterinary radiology & ultrasound, 47: 39-44.

Index terms: Spine, transitional vertebrae, dogs.

WHAT IS YOUR DIAGNOSIS? EMPHYSEMATOUS PYOMETRA IN A DOG. J.P.A. Santos, F. Medina, P.J.R. Frazão. Spécialité – Diagnóstico Veterinário. Av. João Paulo Ablas, 465, Cotia/SP, Brazil, CEP 06711-250.

Introduction: Emphysematous pyometra is a necrotizing, gas-producing infection of the uterine tissue. In this report, we will present radiographic, ultrasonographic and laparotomy correlation encountered in one dog with emphysematous pyometra appearance.

Case Report: An 8-years-old, 36 Kg body weight, female, German Shepherd Dog presenting serosangenous vaginal secretion, few days of inappetence, polydipsia and lethargy was submitted to ultrasound and radiographic examination. The ultrasound and abdominal x-ray revealed a tubular structure approximately 6 cm in diameter and with gaseous content but the imaging exams could not know the difference between uterus and intestine. An ultrasonographic examination was difficult in this patient in light of the large amount of air in the structure to be evaluated. During exploratory laparotomy, it was found the uterus was enlarged and full-filled with gaseous and exudate content. The ovariohysterectomy was then performed.

Discussion: This patient was unusual because of the gas-producing organism and consequently the gas distension of the uterus. Emphysematous pyometra is a necrotising, gas-producing infection of the uterine tissue and must be treated as both a surgical and a medical emergency if the patient is to recover. Radiographic and ultrasound differential diagnosis in this case included emphysematous pyometra and less likely large or small intestinal dilation.

Figure 1 - Lateral abdominal plain radiograph. There is a dilated gaseous tubular structure suggestive of either intestine distension or gaseous pyometra.

QUANTITATIVE RADIOGRAPHIC MEASUREMENT OF THORAX AND HEART IN CATS WITH INDUCED THYROTOXICOSIS. D.C. Oliveira, D.C. Borlini, W.G. Santos; J.N.M. Monteiro; L.A. Vescovi; L.F.A. Marques; M.J.L. Cardoso, F.S. Costa. Universidade Federal do Espírito Santo, Centro de Ciências Agrárias, Departamento de Medicina Veterinária. Alto Universitário s/n°, Alegre – ES, Brazil. Postal Code: 29500-000.

Introduction: Hyperthyroidism is a common endocrinopathy in cats, and it's caused by excessive serum concentrations of thyroid hormones. Hyperthyroid cats can present cardiovascular alterations such as arrhythmias, dilatation and hypertrophy of the cardiac chambers, cardiogenic pulmonary edema and pleural effusion. The aim of this study was to evaluate the presence of cardiac alterations in cats submitted to a thyrotoxicosis protocol, by the obtainment of quantitative radiographic measures.

Methods: Nine healthy cats with no race or sex distinction, and with none clinical alterations were studied. The thyrotoxicosis was achieved by the administration of sodium levothyroxin oral tablets (150μg/kg body weight) once a day, during 60 days. The exams were realized immediately before the induction and by the end of the experimental protocol. Right lateral decumbent and ventrodorsal decumbent radiographs were obtained. Then they were digitalized with a professional digital camera, in order to allow the measurement of the relation between cardiac area and thoracic area (CA:TA) and vertebral heart size values (VHS) using Adobe Photoshop CS4® software. The statistic analysis of the variables was made with Student's t parametric test ($P < 0,01$). This study was realized under the approval of the *Comitê de Ética e Bem Estar Animal* of the *Universidade Estadual Paulista*, Botucatu Campus - Brazil.

Results: VHS values proved that the cats were radiographically normal in the beginning of the experiment. A significant elevation in lateral cardiac long axis promoted an increase of VHS by the end of the experimental protocol. In the ventrodorsal radiographs, both long and short axis increased, promoting an elevation of VHS mean values. The relation between cardiac area and thoracic area suffered a statistically significant elevation in both radiographic views, proving an enlargement of cardiac silhouette due to excessive serum concentrations of thyroid hormones. None of the experimental group animals presented radiographic signs of pulmonary edema or pleural effusion by the end of the experiment.

Discussion: According to other studies that used the same experimental protocol, it's possible to affirm that the cats of this experiment presented a serum elevation of thyroid hormones and developed a hypermetabolic state similar to that observed in the endogen hyperthyroidism. The radiographic findings proved that a short time period of thyrotoxicosis promoted cardiac alterations in the experimental group animals. There are no papers in literature that uses the cardiac area, and its relation with the thoracic area, to evaluate the feline cardiovascular system. These measures are a new alternative for an accurate radiographic investigation, and for the serial follow-up of patients with cardiac disease. It's detached the early diagnosis of feline hyperthyroidism, for preventing the aggravation of cardiovascular alterations secondary to thyrotoxicosis.

NEW TECHNIQUE FOR CARDIOVASCULAR QUANTITATIVE RADIOGRAPHIC EVALUATION IN CATS. D.C. Borlini, D.C. Oliveira, W.G. Santos; J.N.M. Monteiro; L.A. Vescovi; F.S. Costa. Universidade Federal do Espírito Santo, Centro de Ciências Agrárias, Departamento de Medicina Veterinária. Alto Universitário s/nº, Alegre – ES, Brazil. Postal Code: 29500-000.

Introduction: Several measurement methods have been suggested to evaluate the cardiac silhouette in radiographs, in order to reduce the subjectivity of empiric evaluation. VHS (vertebral heart size), which compares cardiac dimensions with thoracic vertebras lengths, has been widely used in veterinary medicine. However, a new technique, which measures cardiac area in radiographs using computer programs, was described recently for cardiac silhouette quantitative evaluation. Only a few studies use this technique to evaluate animal's cardiovascular system, and there are no papers in literature using this technique in cats. The aim of this study was to provide a diagnostic method with higher precision than the radiograph visual analysis, and also establish normal ranges for radiographic cardiac size in cats.

Methods: Nine healthy cats with no race or sex distinction, and with none clinical, radiographic or echocardiographic alterations were studied. Right lateral decumbent and ventrodorsal decumbent radiographs were obtained during inspiratory peak, in order to improve the contrast and ease cardiac silhouette visualization. The radiographs were previously analyzed and then they were digitalized with a professional digital camera. After that, the radiographic images were processed using Adobe Photoshop CS4® software, and the radiographic measures of vertebral heart size, cardiac area and thoracic area were obtained. Then the cardiac area:thoracic area relation was calculated for each animal. The results were tabled and analyzed as mean ± standard deviation.

Results: Table 1 – Radiographic measures of cardiac short axis (CSA), cardiac long axis (CLA), vertebral heart size (VHS), cardiac area (CA), thoracic area (TA) and cardiac area:thoracic area relation (CA:TA) in normal cats. Values expressed as mean ± standard deviation.

	Lateral View	**Ventrodorsal View**
CSA	3,2 ± 0,2 v	3,5 ± 0,2 v
CLA	4,3 ± 0,3 v	4,8 ± 0,4 v
VHS	7,5 ± 0,4 v	8,2 ± 0,6 v
CA	9,3 ± 0,9 cm²	11,1 ± 1,9 cm²
TA	57,1 ± 7,3 cm²	52,9 ± 7,7 cm²
CA:TA	16,5 ± 2,0 %	21,1 ± 3,5 %

Discussion: There are no papers in literature that uses the cardiac area, and its relation with the thoracic area, to evaluate the feline cardiovascular system. The results obtained in this study standardize normal ranges for cats' cardiac area, allowing the use of these values in clinical practice or in similar studies. These measures are a new alternative for an accurate radiographic investigation, and for the serial follow-up of patients with cardiac disease.

HEPATIC QUANTITATIVE RADIOGRAPHIC MEASURES IN CATS TREATED WITH PREDNISOLONE. D.C. Borlini, D.C. Oliveira, W.G. Santos; J.N.M. Monteiro; L.A. Vescovi; L.F.A. Marques; F.S. Costa. Universidade Federal do Espírito Santo, Centro de Ciências Agrárias, Departamento de Medicina Veterinária. Alto Universitário s/n°, Alegre – ES, Brazil. Postal Code: 29500-000.

Introduction: The use of corticosteroids can unchain series of adverse effects in dogs and cats. Hepatic effects include alterations such as hepatomegaly and vacuolar hepatocyte degeneration, with glycogen and/or lipid accumulation. Radiography is an important exam to the evaluation of the hepatic size, because it allows the visualization and measurement of its silhouette, reducing the subjectivity of the radiographic evaluation. This study aimed at evaluating the liver of cats submitted to corticotherapy with prednisolone, by the obtainment of quantitative radiographic measures.

Methods: Nine healthy cats with no race or sex distinction, and with none clinical or laboratorial alterations were studied. All animals received oral tablets of prednisolone (6 mg/kg body weight) during 14 days. The radiographic examinations were made immediately before and by the end of the experimental protocol. First of all, right lateral recumbent radiographs were obtained. Then they were digitalized with a professional digital camera, in order to allow the measurement of the liver and falciform ligament using Adobe Photoshop CS4® software. The values obtained from hepatic size (maximum hepatic craniocaudal length) and falciform ligament (minimum distance from dorsocaudal edge of the xyphoid process to the liver) were converted into vertebral values for better comparison, excluding interference from animals' weight and size. The statistic analysis of the variables was made with Student's t parametric test ($P < 0,01$). This study was realized under the approval of the *Comitê de Ética em Experimentação Animal* of the *Universidade Federal do Espírito Santo* – Brazil.

Results: Table 1 – Hepatic quantitative radiographic measures in cats treated with prednisolone: falciform ligament and liver mean vertebral values obtained in right lateral recumbent radiographs.

FALCIFORM LIGAMENT		**LIVER**	
M0	**M1**	**M0**	**M1**
1,1v	1,3v *	3,3v	3,8v *

M0, initial moment; M1, final moment.
* $P < 0,01$.

Discussion: The quantitative radiographic evaluation allows more precision and reduces de subjectivity of the visual analysis. Only a few studies describe quantitative measures for radiographic hepatic size. The methodology developed in this research proved to be efficient, allowing the characterization of hepatic size variations in the experimental group. It was radiographically verified that prednisolone in the used dosage quickly promoted hepatomegaly and also increased the falciform fat. The corticotherapy, even in a short time period, induces adverse effects in the cat's liver, for this reason, some prudence is needed when using this drug in cats.

ADAPTATION OF THE PARALLEL AND BISECTING-ANGLE DENTAL RADIOGRAPHIC TECHNIC USING HAN SHIN POSITIONER IN FELINES. A.C. Nepomuceno, J.C. Canola, C.A.L. Leite, T. Silveira, M.O. Salán, L.R. Mesquita, D.G. Melo, A.L.C.M. Fernandes. P.M.S. Silva. A.J. Boreli. Universidade Estadual Paulista (UNESP), Campus Jaboticabal, Departamento de Cirurgia Veterinária, Setor de Diagnóstico por Imagem, Via de Acesso Prof. Paulo Donato Castellane, s/n°, Jaboticabal, São Paulo, Brazil, 14884-900.

Introduction: Oral radiographic examination of cats is required as part of the treatment and prophylaxis of the periodontal disease. However, this type of alternative examination is still incipient in veterinary practice, since the available techniques correlate with conventional or extraoral exposures, making difficult the radiological interpretation by structures overlap and giving results not very reliable. The proposal of this research was to evaluate the hemiarcade from superior right maxillae through parallel and bisecting-angle dental radiographic techniques, similar to that used in humans, using intraoral films associated to Han Shin positioner. The purpose was to establish advantages and disadvantages as practicality, sharpness and ease to detect possible dental and periodontal diseases.

Methods: It was evaluated 15 cats, mixed breed, males and females, with 1 year-old. Intraoral films used were Kodak Insight®, zero size, and Han Shin positioner Cone Indicator®, infant size. X-ray dental apparatus was Gnatus Model Timex 70®, with 70kVp and 7mA. Exposure time was adjusted to 0.4s. The positioner was coupled in the distal region of the cylinder of the X-ray apparatus head, allowing correct angulation for the exposure. With the animals under general anesthesia and left lateral position, was introduced Han Shin positioner into their mouth, so that incisor, canine, premolar/molar teeth of the hemiarcade from superior right maxillae was radiographed for each film individually. For incisors and canines, the film was positioned with its major axis in the vertical and for premolars and molars, the film was positioned with its major axis in the horizontal. Subsequently, the radiographic films were processed into a portable dental revelation box.

Results: The technique used provided a wide view of all dental structure and adjacent bone region, and can emphasize the enamel, the dentin, the alveolar crest, the hard layer, the pulp chamber and the foramen. Some changes could be observed as fractures, thickening of the pulp chamber, irregularity of roots, reabsorption and dental calculus.

Discussion: The dental radiographic technique using Han Shin positioners, in felines, showed great value in the observation of teeth and anatomic structures. This technique provided great details in the assessment of incisor and canine, without any interference of overlap or difficulties of positioning. The feline oral anatomy, whose zygomatic arch is located near to premolar and molar roots and its hard palate has low depth, is related to the difficulty of positioning and with the presence of overlaps of the zygomatic arch on the dental roots in some cats of small size. However, this was not seen in cats of large size, which the technique was very effective for the evaluation of premolar and molar teeth.

Support: Fundação de Amparo à Pesquisa do Estado de São Paulo (FAPESP)

OCCIPITAL DYSPLASIA ASSOCIATED TO ATLANTOOCCIPITAL SUBLUXATION IN DOG. CASE REPORT. C.A.B. Lorigados, L.A. Guiffrida, H.M.G. Reis. Guarulhos University, Av. Anton Philips, n°1, Guarulhos, São Paulo, Brazil.07192-140.

Introduction

The occipital dysplasia is characterized as a foramen magnum malformation**,** which presents an abnormal dorsal extension, due to incomplete ossification of the ventromedial supraoccipital bone. It is frequently described in small breed dogs, though there are reports in medium breed dogs, like Beagle and Cocker Spaniel. It can also be associated to others abnormalities, with the atlas dorsal arch shortening, odontoid agenesis or hipoplasy and affections that involves the central nervous system, as syringohydromyelia, cerebral herniation or hydrocephalus. The atlantooccipital subluxation has been mentioned in literature as traumatic, either for occipital condyles or atlas fractures, resulting in an articular instability. In men, atlantooccipital joint subluxation is characterized in Down's syndrome patients, resulted by ligaments lassitude in this region of the patients. It wasn't found reports of the association between occipital dysplasia and atlantooccipital subluxation in dogs.

Methods

This report describes a three months old female Poodle breed dog presenting cervical hyperestesia, tetraparesy, thoracic and pelvic limbs proprioceptive loss of 1 month' duration, with progressive worsening. There was no traumatic historic. A radiograph in rostrodorsal-caudoventral view of the skull presented a foramen magnum malformation and according to the foramen dorsal extension measure compared to its total height was classified as a second degree occipital dysplasia (moderated). In lateral view of the cervical spine was observed an atlas ventral dislocation compared to occipital condyles (subluxation). There were no C1 vertebral body and occipital condyles fractures. It was prescribed oral prednisone and cervical collar. The animal came to death within two days after the consultation and the owner did not allow the necropsy.

Discussion/Conclusion

Lots of dogs that present occipital dysplasia are asymptomatic, what suggests that the foramen magnum morphological alteration alone is not the cause of neurologic dysfunctions. Atlantooccipital articular instability can cause spinal cord compression and respiratory arrest due to rostral segment of medulla and bulb infarction, by vertebral artery compression and occlusion, what might explain the patient's death. Although there is no trauma historic and the simple radiograph couldn't evidenciate any bone fracture involving an atlantooccipital joint, many authors claim the need to a computed tomography to detect traumatic alterations of this region that is not possible to be detected in conventional radiographic examination. The magnetic resonance examination can also evaluate ligament structures and other central nervous system alterations that can be associated.

COMPARISON OF ULTRASONOGRAPHIC, MRI AND TENOSCOPICAL FINDINGS IN CHRONIC TENOSYNOVITIS OF THE DIGITAL FLEXOR TENDON SHEATH – AN *EX-VIVO* STUDY.

A. Thomas[1], D. Verwilghen[1], C. Sagerman[1], O. Simon[2], F. Audigie[3], J-M. Denoix[3], V. Busoni[1]

[1]Faculté de Médecine Vétérinaire, Bd de Colonster 20, Sart-Tilman, 4000, Liège, Belgium (Busoni - Diagnostic Imaging B41, Thomas, Verwilghen - Equine Clinic B42, Sagerman - Epidemiology B42)

[2]Equine Veterinary Clinic "De Morette", Edingsesteenweg 237, 1730 Asse, Belgium

[3]CIRALE (Centre d'Imagerie et de Recherche sur les Affections Locomotrices Equines) Rte Départementale 675, 14430 Dozulé, France

Introduction: Chronic tenosynovitis of the digital flexor tendon sheath is a common pathological condition of equine fore and hind limbs in which synovial structures, ligaments and enclosed flexor tendons may be affected. A precise diagnosis of the lesions is essential to accurately predict prognosis for athletic horses as well as to establish the most relevant curative strategy. The aim of the present study was to evaluate and compare diagnostic capacities of ultrasonography (US), tenoscopy and magnetic resonance imaging (MRI) according to type and localisation of the lesions in limbs affected by chronic tenosynovitis of the digital flexor tendon sheath.

Methods: Nine cadaver limbs with chronic tenosynovitis underwent consecutively US, tenoscopy, MRI and macroscopic dissection. Examinations were carried out blindly by 3 experienced operators. Nine anatomical structures *per limb* were assessed and the severity of each lesion was quantified using a four point scoring system. Spearman's rank correlation (called r_s in the text) was used to assess the comparison between examinations ($P < 0,05$).

Results: 122 lesions were detected using the 4 techniques: 27 lesions were identified by US, 33 by tenoscopy, 44 by MRI, and 18 by at macroscopic inspection after dissection. None of the tendon lacerations detected by tenoscopy and confirmed by the macroscopic examination was identified by US or MRI. There was a positive significant correlation between US and macroscopic examination results (r_s = 0,778), and between US and MRI results (r_s = 0,827). When only synovial structures and ligaments were considered, a positive significant correlation was also found between MRI and macroscopic examination (r_s = 0,758). When only tendonous structures were considered a positive significant correlation was only found between US and macroscopic examination (r_s = 0,805).

Discussion: The results of the present study suggest that, in patients with chronic digital tenosynovitis, US and MRI are the 2 best techniques for detection of synovial and ligament injuries. Results also suggest that US is superior to assess tendon lesions in general, whereas tenoscopy is the only accurate technique to establish the diagnosis of tendon laceration. Because it is easily available and does not require general anesthesia, US is therefore the first choice examination in clinical cases. However, this *ex-vivo* study shows the importance of combining imaging techniques for complete assessment of digital chronic tenosynovitis, especially when lacerations of the flexors tendons are suspected.

PNEUMOPERICARDIUM RADIOGRAPHIC DIAGNOSIS IN DOG

Cardoso L.A., Teixeira M.A., Witz M.I., Fischer C.D., Garrafielo C.S., Universidade Luterana do Brasil – ULBRA Faculdade de Medicina Veterinária, Canoas, RS, Brasil CEP 92425-900

Introduction

Pneumopericardium is a rare disease in veterinary medicine. It consists in the presence of air in the pericardium sac, which may be asymptomatic, it may be identified radiographically as a radioluscent area around the heart in the pericardial sac. The aim of this paper is to report the radiographic monitoring of a dog´s penumopericardium during 46 days.

Method

A five month female Boxer with clinical signs of cough, mild dyspnea and cardiac tamponade sounds. Chest radiographs were obtained in ventrodorsal and left lateral decubitus, every week for 46 days.

Results

In the first examination it was found increased radiopacity of the lung fields predominantly an alveolar pattern consistent with pneumonia and an image radioluscent around the cardiac silhouette surrounded by a thin radiopaque line, compatible with pneumopericardium. The animal received antibiotic treatment and after 7 days the pulmonary alveolar pattern was no longer observed, but the penumopericardium persisted showing a slight increase. In this moment the dog was active, with no cough or other clinical signs. During the 4 week control examinations the animal remained stable, the pneumopericardium did not involute, but the radiopaque line of the pericardial sac was more irregular indicating that the air retained was not causing too much tension. After 46 days, the pneumopericardium image was no longer observed and the animal was released.

Conclusion/Discussion

This case of pneumopericardium probably occurred as a consequence of pneumonia and cough initially found in the dog exam. Pneumonia and cough are reported as causes of pneumopericardium in humans, beyond, poisoning, spontaneous and idiopathic etiology. The clinical evaluation associated with radiographic control were essential to the conduction of the case. The patient remains stable during this period and that was the reason why the air was not drained from the pericardial sac after the diagnosis. In this report the pneumopericardium involuted naturally after 46 days.

EVALUATION OF LUNG PATTERNS AND TECHNICAL QUALITY IN THORACIC FILMS OF DOGS. R.F. Dornas, M.C.F.N.S. Hage, S.T. Pires. Departamento de Veterinária, Universidade Federal de Viçosa, Av. P.H. Rolfs, sem número, Viçosa, Minas Gerais, Brasil, 36.570-000.

Introduction:
The interpretation of thoracic films in veterinary medicine has been aided by recognition of lung radiographic patterns. These patterns are based on differences in radiographic appearance when specific anatomic structures of the lung are affected. Good technical quality is also important for the correct interpretation. In order to verify the radiographic quality, the distribution according to breed, age and sex, and the frequencies of lung radiographic patterns, thoracic films of 43 dogs suspected of lung diseases attended at the Veterinary Teaching Hospital in the Department of Veterinay Medicine – Viçosa Federal University, Brazil, in the first semester of 2008 were analysed.

Methods:
The films were analysed according the technical quality that consists of views produced, position and exposition quality. The lung patterns were classified in interstitial, alveolar, bronchial, vascular or mixed according the anatomic structures affected.

Results:
Regarding the breed, mongrel dogs (27,90%) and Poodles (20,93%) were the most frequent breeds suspected of lung diseases. The females (76,75%) as well as dogs over ten years old (41,88%) were the most studied. It were produced 127 films of the 43 dogs, in 95,36% of the cases the dogs were studied in ventrodorsal and right and left views. The inadequacy of the positions were observed in 88,20% of the films because of rotation of the thorax. Adequate exposition was obtained in 60,67% of the films, but 24,40% were overexposed. The bronchial pattern was the most frequent, occurring in 46,56% of the cases. Mixed pattern was found in 16,35% of the studies, followed by 9,30% of alveolar pattern and 2,32% of vascular pattern. There was no case of isolate intersticial pattern and 16,62% of the studies showed no radiographic found.

Discussion:
The high frequency of mongrel dogs could be related with their high local population and because they are less confined than other dogs of pure breed, being more exposed to climatic changes and contagious diseases. Poodles are also a very commum breed in our casuistic. The most frequent isolate lung pattern was bronchial pattern, mainly because of calcification of bronchial walls and can be related with aged dogs. The expressive number of females can be related with the high incidence of lung metastases search in cases of mammary cancer. The results of this study showed that the films had technical fails, mainly with concern the positioning, that must be improved to avoid erroneous interpretation. Thanks Fellowship FUNARBIC – Viçosa Federal University.

SLIDING ESOPHAGEAL HIATAL HERNIA IN MANED WOLF (CHRYSOCYON BRACHYURUS, ILLIGER, 1815). J.V. Peixoto, M.C.F.N.S. Hage, T.A.R. Paula, F.M. Alvarenga, M. Carretta Júnior, P.R.S. Costa, F.T. Carneiro, L.C. Silva. Departamento de Veterinária, Universidade Federal de Viçosa, Av. P.H. Rolfs, sem número, Viçosa, Minas Gerais, Brasil, 36.570-000.

Introduction:
The maned wolf is the biggest dog of the South America and is listed in the appendice II of the Convention on International Trade in Endangered Species of Wild Fauna and Flora. Despite the anatomic and physiological similarity with *Canis familiaris* there are few reports of congenital diseases in these animals. The aim of this abstract is to report a case of sliding esophageal hiatal hernia in a maned wolf. According to our researches this is the first related case of this disease in *Chrysocyon brachyurus*.

Methods:
A case of a six-month-old male maned wolf (*Chrysocyon brachyurus*) born at the Centro de Triagem de Animais Silvestres da Universidade Federal de Viçosa (Wild Animal Trial Center of the Viçosa Federal University), presenting intermittent signs of reflux esophagitis like anorexia, regurgitation of thick white saliva and retching with progressive weight loss is described. The animal was treated with dimeticona without improvement of the clinical condition. It was indicated a radiographic study of the esophagus for search of foreign bodies or megaesophagus.

Results:
On survey radiographs there was a small collection of gas contained by a water radiopac wall overlying the diaphragmatic crus at the level of the esophageal hiatus. There was gas distention of the stomach and some intestinal loops. An esophagram was performed and showed thoracic esophagus with moderate dilatation, detection of the gastroesophageal sphincter displaced cranially to the diaphragmatic crus and contrast outlinning rugal folds allowing the recognition of the stomach passing through the esophageal hiatus, what was confirmed by another exposition with compression of the abdomen. The radiographic diagnosis was sliding esophageal hiatal hernia.

Discussion:
The hiatal hernia is a protrusion of the stomach through the esophageal hiatus into the thorax. Two types of hiatal hernia have been recognized in the dog and cat: sliding hiatal hernia and paraesophageal hiatal hernia. Vulcano et al. described a case of paraesophageal hiatal hernia in maned wolf in 2000. In the sliding esophageal hiatal hernia, the abdominal esophagus and part of the stomach are displaced cranially through the esophageal hiatus so that the caudal esophageal sphincter is located within the thoracic cavity. This malpositioning and the loss of support of this sphincter lead to reduced sphincter pressure and secondary gastroesophageal reflux. In this case the scenery that contribuited with the radiographic diagnosis was the intermittent symptoms of esophagitis and the fact that sliding esophageal hiatal hernia be, in small animals, usually congenital and observed in young animals. The animal is been treated with conservative management that includes: ranitidine, metoclopramide, domperidone and fractionated diet with the animal in bipedal positioning. If there is no improvement with this management it will be indicated cirurgical correction.

ELECTRONIC ATLAS OF BOVINE RADIOLOGY

U. Geissbühler, A. Siegrist, V. Delley, L. Mock, M.H. Stoffel, M. Wegmüller, A. Steiner
Dept. Of Clin. Vet. Med., Clin. Radiology, PO Box, Länggassstr. 124, CH-3001 Berne

Introduction

Literature of bovine radiographic evaluation is rare and limited - with the exception of one book dating from 1989 - on publications about selected anatomic regions and clinical cases. Bovine radiographic knowledge however is desired in regions and breeds, where individual bovine medical care is practiced. Furthermore, the comprehension of comparative radiographic findings in different species and the acquisition of bovine radiographic anatomy is of significant value for student's and resident's education.

Methods

Normal and abnormal bovine digital radiographs of the appendicular skeleton, the head, the vertebral column, the pelvis, the thorax and the reticulum were chosen and collected from our electronic image archive. Abnormal radiographs originate all from clinical cases. As much as possible, normal radiographs from calves and adult cows were also collected from clinical cases (for example comparative radiographs of the contralateral limb of a cow with lameness). All the missing normal radiographs were performed either on a fresh dead born calf or on an adult cow determined for slaughterhouse. The images of this cow were performed under the supervision and with permission of the national animal protection committee.

Image quality optimizing, correct image orientation and image labelling were performed with the aid of graphic software. Radiographic anatomic structures were labelled and named under the supervision of an anatomist (MHS) and a board certified radiologist (UG).Then the images were uploaded as jped-files on an in house programmed, Microsoft Windows® based image viewing software.

Normal images were completed with schemes to illustrate image acquisition technique and with information about exposure and positioning data and used auxiliary radiographic equipment.

The radiographs of the clinical cases were completed with labels pointing on the radiographic findings, with a clinical case report and with a radiographic report.

The electronic atlas was completed by text chapters about software instructions (handbook), applied radiation protection, radiographic interpretation guideline and systemic skeletal diseases.

RADIOGRAPHIC RETROSPECTIVE STUDY OF WILD ANIMALS ATTENDED ON DIAGNOSTIC IMAGING DEPARTMENT OF LAVRAS FEDERAL UNIVERSITY/MG. M.O. Salán, A.C. Nepomuceno, J. De Bortoli, A.L.C.M. Fernandes, C.A.L. Leite. Universidade Federal de Lavras (UFLA), Campus Universitário, Departamento de Medicina Veterinária, Serviço de Diagnóstico por Imagem, Lavras, Minas Gerais, Brazil, 37200-000.

Introduction. Radiographic exposure is extremely important and widely used in clinical evaluation of wildlife animals. The radiographic examination of the whole body is desirable, including to better understand the anatomy and detect others changes, that may not be the main cause for which the animal was sent. The objective of this study was to describe a retrospective study of X-rays exams in wild animals attended in the Diagnostic Imaging Department of Lavras Federal University.

Methods. Were analyzed 71 wild animals, males and females of different ages, classified into genus and species (when possible). Animals are obtained from the south region of Minas Gerais state and brought by the Forest Police, IBAMA and owners/creators. Animals were divided into three groups: birds, mammals and reptiles. The X-rays were examined and classified by type of radiographic lesion within groups.

Results. Of the 71 animals, 46.48% were birds, 29.58% were mammals and 23.94% were reptiles. Analyzing each group, it was obtained, in bird group, 24.24% parakeets (*Pionus* sp.), 12.11% parrots (*Amazona* sp.) and 63.65% of other 15 species; in mammal group, 42.87% black-ear-tuffed marmosets (*Callithrix penicillata*), 28.57% rabbits and 28.56% of 4 different species; and in reptile group, 76.48% tortoises (58.83 *Geochelone carbonaria* and 17.65% *G. denticulata*) and 23.52% terrapins. The major radiographic alterations in birds were fracture in members (50.00%). Approximately 30% of the birds show no radiographic changes. Among mammals, it was detected 69.20% of fractures (in decreasing order of involvement: members, spine and skull). Normal exams were visualized on 38.10% of these animals. The reptile group obtained 96.30% of animals attended, showing widespread decalcification as the major alteration (42.30%).

Discussion. In birds, the higher prevalence of parakeets, possibly, is to the higher occurrence of this species in region near to towns, and several people believe is not illegal to catch them, which end up being considered as pets. The prevalence of fractures, probably, is to attempt to capture these birds to breeding and proximity to these towns, leading to various injuries. Among the mammals, the highest occurrence of marmosets is because the region is inserted in its habitat, with areas of environmental preservation and ecological corridors nearby. The large number of rabbits seen is due to the presence of breeding by the University of Lavras. In general, the high frequency of fractures (72.73%) is related to the human invasion of these animal habitats, increasing the proximity and the occurrence of injuries by several factors. In regard to the reptiles, the tortoises are in larger number because they are kept in captivity for more time, especially because to cultural factors and illegal black market. *G. carbonaria*, with occurs in all national territory, has higher prevalence in this study. It was observed in most animals of this group, lack of information about the management and absence of early signs of alterations, being sent to the veterinary already with serious abnormalities. The inadequate nutrition, probably, is the main responsible for most of the changes diagnosed on this species.

RADIOGRAPHIC PELVIMETRY IN THREE DIFERENT BREEDS OF FEMALE DOGS

V. PÁFARO, J. C. CANOLA, R. ZANATTA, T. C. F. CINTRA.
UNIVERSIDADE ESTADUAL PAULISTA "JÚLIO DE MESQUITA FILHO" -UNESP – *CAMPUS* JABOTICABAL, Rodovia Dr. Prof. Paulo Donato Castelane s/n Jaboticabal, SP, Brasil, 14884-900

Introduction

The distocy in female dogs is commum in veterinary routine. The frequency in the dog population is smaller than 5%, however, in some breeds it can reach values between 50-100%. The radiographic pelvimetry basically consists in the metric determination of the pelvic dimensions e its utilization is directly related to the reproduction, basing a prophylactic method to prevent complications in birth caused by deformation, bad formation or sequel of affections in pelvis.

Methods

X-rays in ventrodorsal projection had been selected of pelve of 30 adult canine females of the Pinscher race, 50 of the Poodle race and 30 of the Teckel race, exempt of topologic problems. The measurements of pelvis was carried through in accordance with the pelvimetric methodology that approaches the following aspects:

Pelvis diameter (DC): horizontal distance between the two-tuber ilium.
Transverse diameter (DT): horizontal distance between the bodies of the ilium in distal face.
Acetabulum diameter (DA): horizontal distance between the internal face of the two-acetabulum bodies (under the aciform line, in the height of the semilunar face).
Lateral ischiadicum diameter (DIL): horizontal distance between the two lateral tuber ischiadicum.

Results

The results of pelvimetry, referring to the measures achieved in radiographs, were presented in arithmetic mean and standard deviation, respectively: Pinscher DC=2,91cm±0,109, DT=3,403cm±0,10, DA=4,273cm±0,23 e DIL=5,876cm±0,263; Poodle DC=3,486cm±0,475, DT=3,902cm±0,645, DA=4,636cm±0,701 e DIL=6,718cm±1,086; Teckel DC=3,896cm±0,285, DT=4,630cm±0,431, DA=5,670cm±0,450 e DIL=7,866cm±0,

Discussion

Studies about radiographic pelvimetry in domestic animals are relatively scarce in literature. In the described methodology, the variations of the pelvic diameters allow classify the animals in accordance with the type of pelvis in dolicopelvic, as well as in the evaluation of the pelvis of neotropical primates. Satistatory obstetric results were obtained in the evaluation of pelvis in female dogs of Boston Terrier and French Bulldog, reducing the index of distocic births (4% to 2,7% and 2,5%, respectively). These results emphasize the importance of this study, since the mensuration of pelvic diameter, beyond the congenital abnormalities and acquired deformities, also evaluated the pelvic canal, preventing or reducing the cases of obstetric distocy significantly.

RADIOGRAPHIC RETROSPECTIVE STUDY (2006-2009) OF FRACTURES IN A FREE-RANGING GIANT ANTEATER (*Myrmecophaga tridactyla*)

Lacreta Jr ACC, Cruvinel TMA, Cruvinel CAT, Regonato E, Monteiro FOB. Universidade Federal Rural da Amazônia, Brasil, Belém-PA, CEP: 66.077-530

Introduction/Purpose

The giant anteater belongs to the order Xenarthra and the family Myrmecophagidae. In Brazil, the species occurs in all biomes. It is the largest representative of its order, with total length reaching 2 meters and weighing 18 to 40kg in the wild. The number of injured individuals of this species, mainly run over by cars, is increasing. This observation has direct relation to the socio-economic development and increased production of sugar cane in northwestern São Paulo, Brazil.

.

Methods

This study refers to 21 giant anteaters examined between 2006 and 2009, with history of trauma, admitted for medical care at the "Dr. Halim Atique" Veterinary Hospital, UNIRP, São José do Rio Preto, São Paulo, Brazil.. All animals had physical examination findings of motor deficit with orthopedic fractures and were sent to the diagnostic imaging department, where radiographic examinations evidenced different fracture types.

Results

A total of 61 fractures was diagnosed. As for the anatomical region, 49 fractures were diagnosed in the appendicular skeleton (80.32%), where 32 occurred in the pelvic limb (65.31%) and 17 thoracic limbs (34.69%). Other 12 fractures were diagnosed in the axial skeleton (19.68%), where seven occurred in the spine (58.33%) and five in the skull (41.67%). As for the anatomical structures affected, there were 20 fractures of pelvis (32.78%), seven of the spine (11.47%), seven of radio (11.47%), five of ulna (8.19%), five of skull (8.19%), four of femur (6.55%), four of tibia (6.55%), four of fibula (6.55%), two of humerus (3.27%), two of scapula (3.27%) and one carpus (1.63%). Regarding the classification of the fractures, 57 were complete (93.44%) and four were incomplete (6.56%). Among the complete fractures, 20 were comminuted (35.08%), 18 transverse (31.57%), 10 oblique (17.54%), two by compression (3.5%), two Salter-Harris (3, 5%), two longitudinal (3.5%), one splinter in (1.75%), one by avulsion (1.75%) and one coil (1.75%). Among the four incomplete fractures, 100% were fissures.

Discussion/Conclusions

There were a greater number of fractures in the appendicular skeleton, especially in pelvic limb. This incidence may be related to the giant anteater bipedal posture in threatening situations. There was also a higher rate of complete fractures, especially comminuted, highlighting the severity of trauma. This report aims to alert the authorities as to preserve the habitat of this species, guide veterinarians when conducting clinical examination in cases of trauma and report the main types of fractures while emphasizing the importance of radiographic examination for its diagnosis and classification.

RADIOGRAPHIC MONITORING OF RADIUS FRACTURE IN AMAZON MANATEE (*Trichechus inunguis*)

Lacreta Jr ACC, de Andrade MCM, Legatzki K, Trinta AF, Costa EMM. Universidade Federal Rural da Amazônia, Brasil, Belém-PA, CEP: 66.077-530

Introduction/Purpose

The Amazonian manatee is an aquatic mammal classified as threatened with extinction mainly due to hunting for subsistence. A pup of Amazonian manatee calf, was rescued on Marajo Island, state of Pará The animal had restriction of movement and abnormal positioning of the left pectoral fin, with crepitation on palpation.

Methods

After the rescue, the animal was sent to the Federal Rural University of the Amazon's veterinary hospital for radiographic evaluation. The radiographic examination indicated a complete oblique fracture in relation to the proximal-middle third of the diaphysis of the left radius bone, with loss of bone axis and overlap of the fracture fragments, radiolucent discrete point in correspondence to the cranial aspect of the distal metaphysis of the left humerus bone and irregularity of the bone surface in relation to the cranial aspect of the proximal metaphysis of the left ulna. The radiographic features suggested recent fracture. Conservative treatment was instituted, with restriction of space in the swimming-pool of 1,000 liters of milk diet enriched with calcium phosphate and vitamin D3.

Results

The monitoring of the fracture consolidation was done only utilizing radiographs. In the 21th day, regular periosteal reaction was visible in correspondence to the extremities of the fracture fragments of the left radius, cranial-medial aspect of the distal metaphysis of the left humerus and cranial aspect of the proximal metaphysis of the left ulna. In the 43th day, an intensification of the regular periosteal reaction was visible, with some evidence of bone lysis in the regions above (remodeling) and discrete filling of the fracture line by radiopaque content. In the 78th day and 106th day, the fracture's consolidation progress was visible with intensified radiographic aspects related to the process. In the 162nd day, it was possible to verify an ossified bone callus, absence of the fracture line, smooth and regular periosteal reaction, in correspondence to the cranio-medial aspect of the metaphysis of the distal left humerus bone and cranial aspect of the proximal metaphysis of the left ulna, suggesting bone remodeling. In the 319th day there was complete consolidation of the fracture with bone remodeling.

Discussion/Conclusions

The radiographic monitoring of this case offered an excellent parameter for evaluating the effectiveness of treatment, given the fact that, due to environmental and anatomical factors related to the species, it was not possible to carry out treatments other than conservative. This report has significant value for conservation, since the literature does not offer much information about fracture treatment and radiographic follow-up in this species.

COMBINED USE OF ULTRASONOGRAPHY AND COMPUTED TOMOGRAPHY IN ABDOMINAL EVALUATION IN DOGS: REVISION AND ILLUSTRATION OF TWO CASES. Bomfim, P.C.; Martins, M.C.; Mannheimer, E.G.; Pereira, J.J.; Amado, L.V.. CRV Imagem & Vet Care. Barra da Tijuca & Laranjeiras, Rio de Janeiro / RJ, Brazil. 22631-000 & 22240-000.

Introduction
With the growing population's access to different imaging techniques, especially ultrasound (US) and computed tomography (CT), witnessed a favorable scenario to obtain a diagnostic more accurate, specific and early, beyond the chance to perform the staging of diseases.

Case History Report
Illustrate two cases where both techniques were used to assess abdominal (US and CT). Dog 1, thirteen years-old, female, Poodle, presenting a large increase in abdominal volume, prostration and abdominal discomfort. Dog 2, nine years-old, female, mixed breed, had a history of occasional vomiting and diarrhea and abdominal discomfort on palpation.

Imaging
Dog 1: the US showed the presence of a large mass measuring approximately 11.0 cm, with heterogeneous and complex echotexture, predominantly solid, however with irregular cavernous areas represented by hypo/anechoic structures; the mass covers most of the abdominal cavity, displacing internal organs and in close contact mainly with liver, stomach and intestinal segments. Its spleen was not possible to identify. On CT there was very heterogeneous formation with well defined borders, heterogeneous uptake and presence of cavitary areas with liquefaction, measuring 11.7 x 10.9 x 7.6 cm, covering the entire region with mesogastric shift to the right, and moving the bowel caudally to the left. There is dorsal displacement of the spleen to the right, with loss of definition of cleavage between the mass and the spleen pole, suggesting splenic origin. There is also a new formation at the right and dorsally to mass, with greater attenuation measuring 1.7 x 0.9 x 1.4 cm, suggesting secondary lymphadenopathy. Dog 2: the ultrasound showed the presence of hypo/anechoic structures envolved by hyperechoic thin line at meso/hypogastric right topography, suggesting cystic structures; we could not identify the organ of origin. On CT an increased pancreas was observed with images nodular hypodense, peripheral uptake of intra-and peri pancreatic, suggesting pancreatic pseudocyst or neoplastic change.

Discussion / Conclusion
In these cases, similar images were viewed in both techniques, US and CT. However, more information were obtained on CT, as secondary lymphadenopathy in dog 1 and definition of the etiology of the structures seen in dog 2. It is concluded that the combined use of US and CT is a valuable tool for abdominal evaluation, as the correlation between the findings of imaging increases the diagnostic accuracy.

JOINT NEOPLASIA IN DOGS: 6 CASES (2006-2008). C.A.B. Lorigados, F. F. Calderaro, A. A. M. S. Rego, L.A. Giuffrida, H.M.G. Reis. Guarulhos University, Av. Anton Philips, n°1, Guarulhos, São Paulo, Brazil. 07192-140.

Introduction

Primary bone tumors are very common in dogs, although the ones that affect the joints are rare. They represent approximately 3% of the neoplasias that involves the skeletal system. Most of them are malignant. The most common is the synovial sarcoma. Other tumors have been reported with less frequency, as the fibrosarcoma, myxosarcoma, liposarcoma, rhabdomyosarcoma, osteosarcoma. The stifle is the most commonly affected joint in the dog, followed in decreasing order by the elbow, shoulder, antebrachiocarpal, talocrural and hip joints. They generally occur in middle-aged to older, medium-sized to large dogs. The objective of this report was to evaluate the radiographic aspect and the clinical evolution of dogs affected by joint tumors.

Methods

The cases of dogs presenting suggestive radiographic aspects of joint neoplasia and then confirmed though biopsy and histologic exam were reviewed at two veterinarian-school hospitals, between 2006 and 2008. All of the animals had radiographic exams of the thorax and ultrasound of the abdomen for research of metastasis. The dogs had as treatment the amputation of the affected member and because of the owners' motives, none of them received chemotherapy after the surgery. Periodical radiographic exams of the thorax were accomplished to monitor the appearance of metastasis after the treatment.

Results

Six cases of joint neoplasia were identified during this period. There were four synovial sarcomas, one mast cell tumor and one myxosarcoma. Relating the affected joint, four were in the talocrural, one in the stifle and one in the antebrachiocarpal. Regards the breed, an Akita, a Great Dane, a Poodle and two with no defined breed. The age varied from 6 to 12 years old. The most evident radiographic alteration was the permeative or punctate osteolysis, involving more than one articular face. The spiculated and irregular periosteal response was observed in only one case. No animal presented radiographic or ultrasound images of metastasis in the occasion of the diagnosis. The time gone between the diagnosis and the appearing of radiographicaly detectable metastasis in the thorax exam varied from 9 to 12 months.

Discussion / Conclusion

The small number of cases occurred in this period shows that the joint neoplasias really are of low frequency in dogs. Although the joint tumors are more frequent in large dogs, small dogs can also be affected, as well as animals with no defined breed. The talocrural joint was the most affected, but a study with a bigger number of cases shows that the stifle is generally the most involved articulation. All the articular neoplasias studied showed predominantly destructive alterations. In one of the cases of synovial sarcoma an in the myxosarcoma the lythic lesions were identical, characterized by punctate bone lysis, with a "moth-eaten" appearance. Although the radiographic presentation may be suggestive of neoplasia, the type of tumor can only be determined by the histopathological confirmation. Some authors state that the joint tumors have a slower course when compared to primary bone tumors and present a rate of metastasis between 25%-50% to the lungs and the lymph nodes. Then a precocious diagnosis is of fundamental importance so that to improve the surviving life of the affected animals.

DISORDERS OF THE SKELETAL SYSTEM IN BIRDS: A RADIOGRAPHIC STUDY

L.S. Arnaut, A.C.B.C. Fonseca Pinto, F.A. Sterman. Faculdade de Medicina Veterinária e Zootecnia da Universidade de São Paulo. Av. Prof. Dr. Orlando Marques de Paiva, 87, Cidade Universitária, São Paulo, SP, Brasil, 05508-270.

Introduction

Birds have become very popular as pets in recent years. A wide variety of diseases is seen in pet avian species. Skeletal diseases, however, are recognized as the most commom abnormalities. For the diagnosis of these diseases, radiography is one of the most important diagnostic tool available to the avian veterinarian. The purpose of this study was to investigate the frequency of skeletal diseases in birds.

Methods

A radiographic study of 201 birds, belonging to 10 orders, with skeletal disorders was performed. Radiographs were obtained from the archives of Radiology Service of the Veterinary Teaching Hospital, School Veterinary Medicine of University of São Paulo during the 60-month period. Skeletal radiographic alterations were reviewed.

Results

Psittacines performed the highest percentage (130/201, 64.68%) among the diverse avian orders, followed by passerines (33/201, 16.42%). The results are presented in Table 1.

Table 1. Disorders sustained by 201 birds

	Disorder	Number of birds	%
1	Traumatic disorders	94	46.77
2	Metabolic bone disease	48	23.88
3	Polyostotic hyperostosis	34	16.92
4	Inflammatory/Infectious	27	13.43
5	Degenerative	15	7.46
6	Localized osteopenia	13	6.47
7	Bone deformities	9	4.48
8	Aggressive bone alteration	4	1.99
9	Not specific alterations	2	1.00

Traumatic disorders were the most common alterations, detected in 94 of 201 birds (46.77%). Of these 94, 70 birds (74.47%) had fractures and 24 birds (25.53%) had luxations.

Discussion

The results of the present study support the opinion expressed in the literature that traumatic disorders are the most common in birds. Radiographic examination is a valuable diagnostic tool in the assessment of disorders of the skeletal system in birds and specific knowledge of normal avian radiographic anatomy is required for proper radiographic evaluation.

RADIOGRAPHIC STUDY OF THE THORAX TRAUMATIC DISORDERS IN 176 ANIMALS

F. L. Santos, S. M. Oliveira, F. A. Santos, C. O. Ghirelli Faculdade de Medicina Veterinária da Universidade de Santo Amaro, Rua José Portolano nº57, Jardim das Imbuias, 04829-300, São Paulo, SP Brasil.

Introduction and Purpose: The thoracic post-trauma radiography provides information about conditions of the thoracic wall such as cardiac size and shape, pulmonary parenchyma and vascular disorders and conditions compromising the pleura, mediastinum and diaphragm. The thoracic radiography helps in the confirmation or exclusion of diagnostic hypothesis as well as the follow up and evolution of disorders. As in any traumatized patient the hemodynamic stabilization and adequate analgesia come first and the animal should only be sent to the imaging diagnosis after the first assistance. The objective of this study is to bring up a retrospective research in a period of five years of the thoracic radiography exams of traumatized animal evaluating their main radiography changes.

Material and Methods: 176 dogs and cats exposed to different kind of traumas took thoracic radiographies at the hospital of the Universidade de Santo Amaro after emergency procedures in the laterolaterais projections, in the lateral right and left recumbency (when possible) and ventrodorsal or dorsoventral projections, according to the least uncomfortable position for the animal. In the suspicion of diaphragmatic rupture abdominal radiography in the laterolateral projection were included in the most comfortable recumbency for the animal. The animal did not take any tranquilizers to take these exams.

Results: The most often radiographys changes were: pneumotorax (36%); pulmonary contusion (25%); rib fractures (21%); subcutaneous emphysema (20%); diaphragmatic rupture (19%); pneumomediastinum (14%) and pleural effusion (10%). Found as mediastinal enlargement, microcardia, pulmonary cysts, and bullet shots were observed in less percentage. In the overall of the animals studied, 103 (58%) showed more than one radiographic change at the same time. The evolution of the cases was followed up through radiographies in 80% of the animals.

Discussion/Conclusion: The result of this study shows that the thorax radiography in traumatized animals is of great importance for the diagnosis analyzing the extension of the injuries as well as the follow up on the evolution of these disorders evaluating the success or failure of the treatments as long as the animal takes the first emergency assistance and adequate stabilization first.

EVALUATION OF TIMPANIC BULLAE OF DOGS WITH OTITIS MEDIA AND HEALTHY DOGS BY COMPUTADORIZED ANALYSIS. C.A.L. Leite, M.O. Salán, A.L.C.M. Fernandes, J. De Bortoli, A.C. Nepomuceno, D.G. Melo, T. Silveira, M.A.R. Feliciano. Universidade Federal de Lavras (UFLA), Campus Universitário, Departamento de Medicina Veterinária, Serviço de Diagnóstico por Imagem, Lavras, Minas Gerais, Brazil, 37200-000.

Introduction: Despite the otitis media is a common condition in dogs with chronic recurrent external otitis, its diagnosis by conventional methods available to the clinician is not always satisfactory. The conventional radiographs do not always provide a satisfactory image for the diagnosis, depending on the experience of the observer and the chronicity of the lesion. Aiming better diagnose this clinical apresentation, the purpose of this study was to evaluate the different nuances of intracavitary tympanic bulla in healthy dogs or patients with otitis media confirmed by means of radiographic digitization and subsequent analysis by ImageJ™ freeware (Wayne Rasband, National Institutes of Health, USA).

Methods: For this study, 63 radiographs were evaluated from 39 healthy dogs (control group) and 119 radiographs from 72 patients with otitis media confirmed by otoscopy or conventional radiography / contrast (test group). For better standardization, patients were divided into three groups according to the measurement of the tympanic rostrocaudal axis (small or <1cm, medium or between 1.0 and 2.5cm; and large or >2.5cm). Each patient underwent oblique dorsoventral projections right / left, providing excellent visualization of the anatomical area of both tympanic bulla. After processing and drying of conventional radiographs, it was performed scanning of the images by high-resolution photo. Each image was subjected to analysis by the software ImageJ™. The analysis was based on targeting the desired area by means of contrast thresholds and determination of the area corresponding to the intracavitary portion of the bullae (IPB). The contrast thresholds were adjusted for each image, which had a reference in size by a degree in centimeters. Comparisons were made among and between groups using non-parametric standard statystical tests.

Results: Data analysis indicated that for any of the bullae group analyzed, the IPB had a statistically significant difference ($p<0.01$) when compared healthy dogs and those with otitis media. The average IPB for healthy dogs was 2.46, 9.52 and 23.11 (small, medium and large, respectively), while in dogs with otitis media was 1.57, 6.62 and 17.30 (under the same conditions previously).

Discussion: A computer analysis of images of intracavitary tympanic bullae is useful, easily accessible and affordable for small animal clinician that works with radiographic images of tympanic bullae of dogs with otitis media. However, the clinician should screen for possible situations in which the intracavitary lesions not yet occurred, generating false negative results. Thus, it is advisable to use this computational analysis together with other techniques for routine diagnosis. It could be also infer that the joint analysis of multiple views of the same animal (as the rostrocaudal with open mouth) may improve the final diagnosis, reducing the number of false negative results.

RADIOGRAPHIC EVALUATION OF THE HIP JOINT IN PACAS (*Cuniculus paca*) RAISED IN CAPTIVITY

F.A.P. Araújo, S.C. Rahal, M.R.F. Machado, L.C. Vulcano, C.R. Teixeira, S.E.R.S. Lorena. School of Veterinary Medicine and Animal Science, Unesp Botucatu – Rubião Júnior s/n, Botucatu – São Paulo, Brazil, 18618-000

Introduction: Paca is the second largest rodent species found in the Neotropical zone, including South America and Central America. This mammal is frugivore that sleeps in burrows and has a nocturnal behavior. The maximum longevity reported in captivity is 16 years. Sexual maturity occurs from six to 12 months, and pregnancy lasts 115-120 days. This rodent has a heavy and robust appearance and thick strong limbs. The forefoot has four toes but the hindfoot presents five toes as an adaptation to swift movements. Due to the lack of knowledge about the locomotor system of this species, the aim of this study was to radiographically evaluate the hip joint in captive pacas.

Methods: This study was approved by the Veterinary School Ethical Committee. Nine intact adult pacas (*Cuniculus paca*) from a research breeding facility (3 females and 6 males) weighing 6.4-9.0 kg were used. Under dissociative anesthesia, traditional OFA-like and mediolateral radiographs were taken. For the ventrodorsal radiographs the paca was placed in dorsal recumbency with the hind limbs drawn out caudally and parallel to each other. The hind limbs were rotated inward so that the patellae would overlie the femoral trochleae. The radiographic features of the hip joint were observed and Norberg angles were measured using a transparent plastic goniometer. The Norberg angle values were submitted to Student's t-test for paired samples using the Minitab® 15 software. Differences were considered statistically significant for $p \leq 0.05$.

Results: Radiographically, in all animals, the femoral head had a hemispheric-like shape fitting more than 50% within the acetabulum. The acetabulum was deep and had semi-circular shape. The femoral neck was well defined and smooth. The Norberg angle was significantly different (p=0.002) between the right limb and left limb. The Norberg angle average was 132.33º (SD 2.29) on the right limb and 129.22º (SD 2.72) on the left limb.

Discussion: In general, rats and mice are used as animal models but the small size of these rodents may difficult some orthopedic procedures. Due to the ability to easily breed pacas and its considerable size, they could be used as animal model for studies that animal size is a limiting factor. The higher mean value of Norberg angles in pacas (total mean of 130.8º) compared to dogs (mean of 105 degrees or greater) indicates a good relationship between the center of the femoral head and the acetabular rim. In addition, the absence of signs of degenerative joint disease indicates that nutritional management and housing were adequate. Therefore, we suggest that paca could be used as animal model in hip joint studies.

RADIOGRAPHIC EVALUATION OF TRACHEAL COLLAPSE IN DOGS: 187 CASES (2001-2008)

SILVANA M. UNRUH[1], ANA CAROLINA B. C. FONSECA PINTO[1], FRANKLIN ALMEIDA STERMAN[1], STEFANO FELIPO HAGEN[1]

[1] Department of Surgery, University of São Paulo, Av. Prof, Dr, Orlando Marques de Paiva, 87 – Cidade Universitária, São Paulo – SP, 05508-900, Brazil

Address correspondence and reprint requests to Silvana Maria Unruh, at the above address. E-mail: unruh@usp.br

ABSTRACT

Tracheal collapse is a common cause of cough in mature, small-breed dogs but is rare in cats. This disease is defined either by narrowing of the lumen of the trachea, prolapsed of dorsal tracheal membrane, or a combination of those abnormalities. Tracheal narrowing is a multifactorial process that results from weakening of the tracheal cartilage. Pomeranians, Miniature and Toy Poodles, Yorkshire Terriers, Chihuahuas, and Pugs are most commonly affected. Tracheal collapse has been diagnosed in dogs of all age (i.e., 1 to 15 years) the condition typically affects middle-aged dogs 6 to 7 years of age. No sex predisposition has been observed. The clinical signs of tracheal collapse include a paroxysmal “goose honk” cough, which may lead to increasingly severe respiratory distress and cyanosis. Radiography has been reported to detect tracheal collapse in 59% to 84% of dogs. Radiography may be limited in confirming and determining the extent of tracheal collapse. The thoracic inlet was the area most commonly and severely affected with tracheal collapse in dog. Endoscopic evaluation of the airway can be an important step in both the diagnosis and grading of tracheal collapse and is considered by many to be the “gold standard”. Tracheal collapse is irreversible, but several medical and surgical options can help paliate clinical signs. The objective of this study was the retrospective evaluation of radiographs of 187 dogs with tracheal collapse and comparison with data from literature. Ninety-five (50,8%) dogs were female, and 92 (49,2%) were male; the age range was 1 to 16 years (being aged 11 to 15 years to more frequent). Among the dogs, breed dogs 77 (41,2%) Miniature e Toy Poodles, 38 (20,3%) 38 (20,3%) Yorkshire Terriers, 27(14,4%) mixed-breed dogs, 16(8,5%) Maltese, 12(6,4%) Fox Paulistinha. There was also 2-1(1%-0,5%) each of other breeds as follows: Schnauzer, Dachshund, Lulu’s Pomerania, Beagle, Chihuahua, Cocker Spaniels, and Fox Terrier. The prevalence of tracheal collapse was higher in Poodles, there was no sex predisposition of the animals and the elderly were most affected, as the literature. Remember the importance of endoscopy to confirm and establish the diagnosis of tracheal collapse.

SLIPPED CAPITAL FEMORAL EPIPHYSIS IN A CAT – RADIOGRAPHIC EVALUATION.

C.B. Amaral, M.A.P. Romão, A.M.R. Ferreira. Universidade Federal Fluminense. Vital Brazil Filho Street, 64. Niterói, Rio de Janeiro, Brazil, 24230-360.

Introduction: Slipped capital femoral epiphysis is a rare disease in veterinary medicine with few reported cases but it's a quite common disease in male obese young humans. Similarly, most of the affected cats are neutered, over weighted, young, male cats. An "apple-cored" metaphiseal lysis is frequently observed in one or both limbs. This report describes a slipped capital femoral epiphysis case in a female cat, with emphasis in the radiographic features of the lesion.

Methods: A 13-month-old, neutered female cat presented with acute, severe nonweight-bearing right hind limb lameness with no previous history of trauma. The cat weighted 4,1 kg and was kept indoors. Only commercial cat food was consumed and vaccination was performed annually. During clinical examination, pain was elicited upon palpation of the right hip area. No other abnormal finding was observed.

Results: On the basis of history and physical examination, a presumptive diagnosis of femoral luxation was made. Differential diagnosis included femoral fracture, hip dysplasia and aseptic necrosis of femoral head. Lateral and ventrodorsal pelvic radiographs were performed. Two semilunar lytic lesions were observed on the right femoral neck (metaphysic region) given an "apple cored" appearance with a slight lateral displacement of the epiphysis. The metaphysis line couldn't be identified. A closed physis was present on the left limb. Surgical excision of the right femoral head was proposed. Pre-surgery medication consisted in nonsteroidal anti-inflammatory meloxican, 0,2mg/kg daily on the first day and then reduced to 0,1 mg/kg one more day before surgery. Right capital femoral head was removed through a craniolateral skin incision. Histopathological diagnosis was not performed. Anti-inflammatory was continued after surgery for four more days along with antibiotic cephalexin, 20mg/kg twice a day for 7 days. The cat recovered well and by day 5 was using the right limb but walked with a limp, not bearing the whole weight on the right limb. Mild discomfort was elicited by palpation of the hip. Prognosis for return of the function was good and two months after surgery, only a slight alteration in gait could be observed, not preventing cat's deambulation or jumping.

Discussion: The lesion observed in radiographs seemed compatible with slipped capital femoral epiphysis, a rare condition affecting cats and dogs. It usually occurs in open physis and animals which have delayed growth plate closure. The pathogenesis is not fully understood and factors such as genetics, nutrition, obesity and endocrine imbalances may contribute to it. On the contrary of most cases, this cat was female and not over weighted (above 5 kg). The radiographic alterations differ from avascular necrosis where rounded lytic lesions are observed not only in the metaphyseal area but disseminated through the head itself and pathological fracture is hardly found. A histopathological diagnosis would show the condrocytes and connective tissue alterations although there's not a patognomonic lesion for slipped capital femoral epiphysis as happens in other chondrodysplasias. Radiographic identification of the lesion's pattern helps yielding a correct diagnosis directing the associated histopathological analysis. In this case, the establishment of the diagnosis was based on radiographic features compared with other cases of previously reported slipped capital femoral epiphysis and avascular femoral necrosis in cats. Although a rare condition, it seems to have a particular radiographic pattern and should be considered in differential diagnosis in young laming cats.

Mandible and Maxilla Osteomyelitis in *Panthera onca.* L. H. Silva, A. M. Fonseca, N. C. Borges, P. V. R. Gonçalves, A. G. Prego, J. C. Fávaro Júnior, A. M. Bogoevich, I. R. LIMA. Setor de Diagnóstico por Imagem – Escola de Veterinária – Universidade Federal de Goiás, Campus II - samambaia - Caixa Postal 131 - CEP: 74001- 970 Goiânia - Goiás – Brasil. E-mail: luyzhenryque@hotmail.com

INTRODUCTION: The prevalence of oral lesions in *Panthera onca* kept in captivity is high, probably due to the bad adaptation and nutritional problems. One of the frequent processes is the osteomyelitis by teeth infection; it can show swelling, pain, fistulas, osseous sequestrum, teeth loose and pathological fracture. Microorganisms are commonly introduced by trauma, contiguity or hematogenous route. The diagnosis is given by local inspection, radiographs and laboratorial exams, and the treatment requests antibiotics use and surgery intervention.

METHODS: A jaguar female specimen with approximately 15 years and 50 pounds was seized by IBAMA and sent to the Zoo Park of Goiânia. During the time it was in particular captive, was submitted to a “disarming process” in which the claws of the chest members were extracted and the four canine teeth were sawn and covered with acrylic. The feline had inappetence and bilateral fistulas on the belly area of the mandible with putrid odour and mucopurulent secretion. The animal was sent to the Veterinary Hospital of the Universidade Federal de Goiás where it was chemically contained and submitted to radiographic exam of the cranium in laterolateral right, left and dorsoventral projections. During 45 days before the surgery the animal was treated with amoxicillin and clavulanato of potassium. The teeth extraction of the lower canines was realized under general anesthesia and loco-regional block with lidocain at 2%.

RESULTS: The radiographic exam allowed the visualization of the maxilla and mandible osteomyelitis process with first focus on top and low canines region (picture 1-A). The extraction of the low canine teeth (picture 1-B/B’) removed the local contamination spot and the animal had pain released and started to eat again.

Picture 1-(**A**) Radiograph of *Panthera onca* cranium in laterolateral projection. (**B**)-Radiograph of cranium indicating the place of fistula. Osteomyelitis-filled arrow. Canine sawed-red arrow.

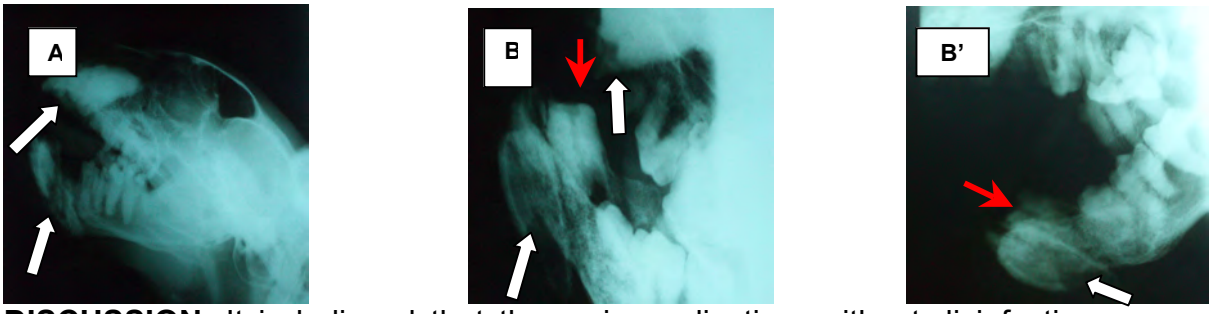

DISCUSSION: It is believed that the resin application, without disinfection on amputees canine teeth predisposed the development of the infection and consequently osteomyelitis. Radiographically the osteomyelitis was diagnosed by the visibilization of areas with bigger radiolucency with uniform and dotted default, irregular limits and with one or more radiopaque focus representing scleroses by the cronic infection. The use of radiographic techniques was essential to diagnose the osteomyelitis and helped on deciding treatments. The antibiotic therapy established before the surgery eased the infection process with consequently improvement of the general state of the animal. The specific treatment established by the extraction showed itself effective and permitted total solving of the fistulas in 15 days.

COMPARATION BETWEEN RADIOGRAPHIC AND ELECTROCARDIOGRAPHY METHODS FOR ASSESSING DIMENSION IN CARDIAC FELINE. A.R.S. Silva[a], M. Marcondes[b], M.F. Zanette[c], C.N. Rossi[c], L.D.R.P. Ciarlini[b]
[a, b]College of Veterinary Medicine Integrado from de Campo Mourão -PR
[b]Departament of Clinical, Surgery and Animal Reproduction, College of Veterinary Medicine, São Paulo State University, Araçatuba (SP)
Correspondence and reprints: alexandreredson@grupointegrado.br

Introduction

Feline cardiomiopathy is the result of miocardic disfunction and can be presented under various forms, being the hipertrophic the most common one. Complementary evaluations of low cost can assist in the diagnosis and prognosis of cardiomiopathy. Between them, there are electrocardiography (ECG) and radiologic evaluation. The ECG is used as the initial choice in the diagnosis of cardiac arrhythmias. Radiographic evaluation supplies informations suchs as alterations in size, shape and positioning of the heart. The VHS method (vertebral heart score) can be used to quantify the presence and degree of cardiomegaly.

Methods

For the present study there were selected 30 healthy adult cats, disregarding gender or breed, originated from Araçatuba, São Paulo, Brazil. All of them were submitted to thoracic radiographies and electrocardiographic evaluation. Thirty six percent were male, and 63% were female, with age varying between 12 and 72 months. The electrocardiography records were made in the six standard frontal leads (DI, DII, DIII, AVR, AVL, AVF) and in precordial leads CV5RL, CV6LL, CV6LU and V10, at 50 mm/s. Amplitude and duration of the waves were measured at DII. Data obtained for VHS were submitted to Pearson's correlation analysis, and considered significant when $p< 0.05$.

Results

Data from electrocardiographic and radiologic interpretations were used to subdivide the animals in three ways. Initially considering one group of 30 cats (G1) without clinical signs, independent of radiographic or electrocardiographic alterations; then, considering 24 cats without clinical, radiographic and electrocardiographic alterations (G2); and finally, considering six cats without clinical alterations, however with discrete electrocardiographic and radiographic alterations (G3). VHS values for G1 group had been: LR (9,72 $\pm$ 0,64), LF (9,62 $\pm$ 0,46), DV (9,82 $\pm$ 0,69) and VD (9,84 $\pm$ 0,66); G2: LD (9,65 $\pm$ 0,62), LE (9,59 $\pm$ 0,43), DV (9,75 $\pm$ 0,67) and VD (9,82 $\pm$ 0,66); G3: LD (10.01 $\pm$ 0,67), LE (9,73 $\pm$ 0,60), DV (10,2 $\pm$ 0,69) and VD (9.91 $\pm$ 0,71).

Discussion

Linear correlation was extremely significant for VHS and LR and LF, and for VHS and DV and VD projections, for G1 and G2. Nevertheless, although VHS in cats can be useful for heart radiographic evaluation, this method does not seems to be useful as the first choice in the initial radiographic asses of the heart. In these cases it is better to evaluate heart position and size qualitatively, once in cats there are great influences of size, shape, position of the heart and trachea because of thoracic flexibility. However, VHS can assist the study in sequential x-rays of the same animal, when evaluating the evolution of the disease.

RADIOGRAPHIC EVALUATION OF THE STIFLE JOINT IN PACAS (*Cuniculus paca*) RAISED IN CAPTIVITY

F.A.P. Araújo, S.C. Rahal, M.R.F. Machado, L.C. Vulcano, C.R. Teixeira, F.A. Oliveira. School of Veterinary Medicine and Animal Science, Unesp Botucatu – Rubião Júnior s/n, Botucatu – São Paulo, Brazil, 18618-000

Introduction: The complex interaction of the distal femur, proximal tibia, patella, and proximal fibula allows the stifle joint to withstand tremendous forces during locomotion. Differences in the anatomical structures may occur among the animals. Pacas are herbivores that do not climb trees. These large rodents have thick strong limbs, and four toes on their front paws and five on their back feet. Due to the few reports about the locomotor system of this species, the aim of this study was to radiographically evaluate the stifle joint in captive pacas.

Methods: This study was approved by the Veterinary School Ethical Committee. Nine intact adult pacas (*Cuniculus paca*) from a research breeding facility (3 females and 6 males) weighing 6.4-9.0 kg were used. Under dissociative anesthesia, craniocaudal and mediolateral radiographs of both stifle joints were taken. For the craniocaudal radiographs the paca was placed in dorsal recumbency with the hind limbs drawn out caudally and rotated inward so that the patellae would overlie the femoral trochleae. Mediolateral views were made with the stifle placed at an approximate angle of 140°.The radiographic features of the stifle joint were observed. The length of the patella was measured using lateral radiographic views. The values were submitted to Student's t-test for paired samples using the Minitab® 15 software. Differences were considered statistically significant for $p \leq 0.05$.

Results: In craniocaudal view the lateral condyle was larger than the medial condyle, and next to it there was a small sesamoid bone. The patella was long and wide, with base proximal and distal apex. There were no significant differences between the limbs or among pacas for patella length. Overall ± SD mean of length of the patella was 27.26 ± 1.93 mm (range, 24.0 to 30.2 mm, 95% CI, 26.36 to 28.14 mm). The fibula was lateral to the tibia and the shaft was completed defined. In mediolateral view the small sesamoid bone was observed at the caudal aspect of the condyles. The patella had a drop-like aspect, with a thin distal apex, and concave caudal aspect. Two radiopaque structures with triangular aspect were observed cranially at femorotibial joint. There were no signs of degenerative joint disease.

Discussion: The absence of radiological signs of degenerative joint disease suggested that nutritional management and housing were adequate. The patella shape of the pacas was very similar to the sheep's patella. Different from the sheep the fibula was not vestigial. On the other hand, the pacas had one small sesamoid bone that suggesting be a fabella. Some mammals, such as the dogs, have two sesamoid bones in the tendon of the lateral head of the gastrocnemius muscle. In addition, the two radiopaque structures observed cranially at femorotibial joint may be associated to meniscus. More studies are necessary to determine the effect of these anatomic particularities in the dynamic articular.

APPENDICULAR CHONDROSARCOMA IN A TEN-CASE SERIES OF JAMSHIDI NEEDLE-BIOPSIED BONE TUMORS IN DOGS. C.B. Amaral, M.A.P. Romão, A.M.R. Ferreira. Universidade Federal Fluminense. Vital Brazil Filho Street, 64. Niterói, Rio de Janeiro, Brazil, 24230-360.

Introduction: Chondrosarcoma accounts for around 10% of all primary bone tumors in dogs, affecting mostly large breeds. The most common sites are ribs, skull (mainly nasal cavity) and appendicular skeleton. Biopsy often provides definitive diagnosis. In this study, bone tumors in ten dogs were biopsied with Jamshidi needle; eight diagnosed as osteosarcoma and two as chondrosarcoma, both occurring in the appendicular skeleton and at the same site.

Methods: Ten dogs between 3 to 18 years of non-specific breed and Rottweiler, English Bulldog, Siberian Husky, German Shepard and Doberman breeds presented radiographic image suggestive of primary bone neoplasm. In order to confirm it, all of them were submitted to bone biopsy with Jamshidi needle 11 gauge under general anesthesia or right after euthanasia was performed.

Results: In eight cases, biopsy yielded diagnosis of osteosarcoma. In the two cases left diagnosis was chondrosarcoma. Both chondrosarcomas were localized in proximal epiphysis of the tibia. The dogs were of non-specific and Siberian Husky breed, with 10 and six years old respectively. In both cases, biopsy was performed under general anesthesia. Only the Siberian Husky dog had the limb amputated. Both dogs were euthanasiated five and six months after diagnosis with respiratory distress and radiographic image compatible with pulmonary metastasis. In both cases, biopsy diagnosis was confirmed at necropsy.

Discussion: In this series of ten primary bone tumor cases, chondrosarcoma accounted for 20% of the cases, a higher percentage than previous reported studies and osteosarcoma accounted for 80% of the cases, similarly with most studies reported. No other primary bone tumor were identified. These results imply that osteosarcoma and chondrosarcoma still are the most common primary malignant bone tumors in dogs. It's possible that having more cases, the chondrosarcoma share would decrease and rarer kinds of bone tumors should appear. Yet, the ribs are described as the most common site for chondrosarcoma to develop, followed by nasal cavity. Interestingly, neither of the cases reported here were at these sites; both were from appendicular skeleton and coincidently affecting the same bone (tibia) and region (proximal epiphysis). Chondrosarcoma is known to have lower metastatic rate compared to osteosarcoma. Both chondrosarcoma metastatic rate reported in this study were similar to osteossarcoma one (around six months). This can be true concerning appendicular chondrosarcomas. When compared to rib or skull cases, it might be more aggressive. More appendicular chondrosarcoma cases should be gathered to confirm this hypothesis. Therefore, through this study, it can be concluded that chondrosarcoma is an important primary malignant bone tumor, that Jamshidi needle is an important tool to confirm diagnosis of radiographic lesions suggestive of primary bone tumors and that appendicular site may be implied in a more aggressive chondrosarcoma behavior and could lead to a presumptive diagnosis of osteosarcoma if only supported by radiographic images, considering the fact that proximal tibial epiphysis is a common site for osteosarcoma development.

COMPUTED RADIOLOGY SYSTEM IMPLEMENTATION IN A SMALL ANIMAL REFERRAL CENTER

Rômulo Caldas Braga[1], Alex G. Adeodato[2], Francielle Fernandez Shinkai[3], Mauro Caldas Martins[4], Elcio Hiromi Ogata[5]

1 MV, CRV- Imagem romulobraga@crvimagem.com.br Av.Americas 505 Lj M Rio de Janeiro – RJ Brasil CEP 22631000
2 MV, PhD CRV Imagem
3 MV, CIAV
4 MV, CAD, CRV- Imagem
5 field engineer, NDT, Fujifilm

Introduction

The digital radiography systems recently produced great impact on your introduction in veterinary medicine, bringing several advantages to exotics and small animals practice and radiology routine. It brings a new challenge for veterinarians absorb new technology. Some recommendations for the use of digital radiology systems have been reported and are being implemented as the committee and working group for DICOM standardization from Association of Electrical and Medical Imaging Equipment Manufacturers (NEMA *) and American College of Veterinary Radiology (ACVR) for veterinary medicine (working group-26). The aim of this paper is to report the needs, problems and solutions in the deployment of a computed radiology (CR) system in small animal referral center in Brazil.

Material and Methods

Accidents and facts about introduction, routine work and observations about processes were cited as a reference. Data related to exam time duration and release of reports, number and causes of losses (repetitions of the series) from each study of images were collected in the first 10 months of the new referral service in computed radiology and compared to other conventional radiology center already established in the same period and in previous time.

Results

Reducing the time of completion of radiograph exam, but extending the period for the release of reports was significantly important in the comparison of data. Suggestions and recommendations for implementation and considerations about selection of equipment and its requirements, structural requirements, technical and logistics are made on this initial experience, approaching the transition, implementation of systems, training, integration methods, errors and critical operational procedures employees.

Conclusion

The use of computed radiology has advantages and benefits superior to conventional radiology but require the acquisition of knowledge, application of systematic and implementation of "software" such as programs for archiving and communications (PACS) and other integration with information from patient and their medical records (RIS) to facilitate the workflow and reduce the problems related to the greater number of procedures implemented.

RADIOGRAPHIC AND TOMOGRAPHIC EVALUATION OF THE LUMBOSACRAL JUNCTION IN GERMAN SHEPHERD DOGS: COMPARATIVE STUDY.

Silva, T. R. C.[1]; Guirelli, C. O.[1], Hayashi, A. M.[1], Sant'Ana, A. J.[2], Matera, J. M.[3], Pinto, A. C. B. C. F.[3]

Introduction: The cauda equina syndrome defines the clinical signs that come from the sensory and or motor neural dysfunction caused by the terminal part of the spinal cord and adjacent nerve roots damages. Normally happens to large breed dogs, without preference of gender or age. The stenosis lumbosacral is the most frequent cause, correlating to the alterations of the soft tissues and or the bone tissues in the lumbosacral segment.

Methods: The aim of this study was to analise the contribution of diagnostic imaging of the lumbosacral region of 30 German shepherd dogs. There were thirteen animals that belonged to the group (A) without clinical signs and X-Ray alterations in the lumbosacral segment; twelve animals to the group (B) without clinical signs, with X-Ray alterations; five animals to the group (C) with clinical signs and X-Ray alterations. All exams had radiographic measurements: lumbosacral angle, endplate angle, articular process angle, ventral displacement of S1 to L7, the point of intersection of the measured angles and the mobility of the lumbosacral junction.

Results: The ventral displacement of S1 related to L7 was present in most of the animals not only in the extension position, raising the hypothesis about the racial standard established, a certain degree of ventral displacement of the sacrum might be part of the expected for the lumbosacral segment. It was noticed a statistical difference among the variables: endplate angle L7 – S1, the point of intersection of the endplate angle L7 – S1, lumbosacral angle and the mobility of the lumbosacral junction.

Discussion: The CT examination showed being superior in the evaluation of the vertebral canal, intervertebral foramen and the articular processes. It was concluded that the two modalities of images complement each other, becoming important tools in the clinical-surgical evaluation in the lumbosacral segment, helping in the diagnosis, prognostic and therapeutic to be adopted.

[1] Pos-Graduation, Department of Surgery, Faculdade de Medicina Veterinária e Zootecnia (FMVZ), University of São Paulo (USP), Av. Prof. Orlando Marques de Paiva 87, São Paulo, SP 05508-900, Brasil. * e-mail author: thelmacintra@yahoo.com.br
[2] Pos-Graduation, Department of Surgery. Faculdade de Medicina (FM), University of São Paulo (USP), São Paulo, Brasil. Av. Dr. Arnaldo 455, 2º andar, 2120, Cerqueira César, São Paulo, SP, Brasil Code: 01246-903.
[3] Department of Surgery, veterinary Hospital, FMVZ, USP, São Paulo, SP.

MEGAESOPHAGUS: RETROSPECTIVE RADIOGRAPHIC STUDY OF 40 CASES.

P.M.M. MATAYOSHI, P.A. BARNABÉ, E.D. OLIVEIRA, L.D.R.P. CIARLINI Departamento de Clínica, Cirurgia e Reprodução Animal da Faculdade de Medicina Veterinária, Universidade Estadual Paulista, Rua Clóvis Pestana 793. Araçatuba, SP 16050-680, Brasil. E-mail: lupinoti@fmva.com.br

Introduction: The pathological dilation of the esophagus is defined as megaesophagus, but this is a complex, with different origins, may be called megaesophagus syndrome. The disorder is characterized by moderate to severe dilation of the esophagus due to its inefficient peristalsis. There are various known forms of megaesophagus syndrome: the congenital and acquired idiopathic and secondary acquired. The diagnosis of the syndrome is made by clinical signs and radiographic findings. This study aimed to evaluate the patients with megaesophagus and subjected to radiographic examination, evaluating them as to species, breed, sex, age, radiographic methods used in diagnosis, lesion topography and main clinical signs appear.

Methods: Small animals with clinical suspicion of megaesophagus were studied, and sent to the sector of Veterinary Radiology of Veterinary Hospital "Luiz Quintiliano de Oliveira " - UNESP, Campus of Araçatuba, during the period 2003 to 2008. The patients were evaluated and classified as to species, breed, sex, age, radiographic methods used in diagnosis, lesion topography and main clinical signs presented, and determined the frequency of each occurrence. The radiographic exam were made on the right side, ventrodorsal of cervical and thoracic regions. When esophagogram was necessary for diagnostic confirmation, administration of oral radiopaque contrast of barium sulphate, at a dose of 2 to 6 mL / kg.

Results: 40 cases of megaesophagus were diagnosed radiographically during the period 2003 to 2008, 38 (95%) animals were dogs and 2 (5%) cats. The mixed breed were the most affected (10, 26.32%), the same happened with all the cats. The canine pure breeds most affected were the Yorkshire Terrier (4, 10.53%), Pinscher, Pastor Rottweiller and Belgian (3 of each race, 7.89% each). Of dogs**,** 25 (65.79%) were male and 13 (34.21%) females. All the cats were females (2, 100%) and younger than 1 year (100%). The ages of the dogs ranged between one month and 11 years, 16 (42.11%) were younger than 12 months and 22 (57.89%), older than 12 months. The survey radiographic allowed the diagnosis of 6 cases (15%) and 34 (85%) need contrasted exam. The cervical megaesophagus was diagnosed in 6 dogs (15.79%), the thoracic in 19 (50%) and 13 (34.21%) showed the cervical and thoracic disease. In cats, one occurrence was cervical (50%) and another was cervical and thoracic (50%). The main clinical signs were related were regurgitation (18, 45%), emesis (8, 20%), pneumonia (13 / 32.5%) and dyspnea (5 / 12,5%).

Discussion: The survey and contrast radiographic examination showed to be of great importance in the diagnosis of megaesophagus and in determining the location and extent of the injury. The incidence of esophageal disease was much lower in cats than in dogs. According to the literature, the most affected dogs were younger than 12 months without sexual predisposition, what is different of the results of this study.

EFFECTS OF PROBIOTICS IN THE ULTRASONOGRAPHIC FINDINGS OF THE GASTROINTESTINAL TRACT IN BEAGLE DOGS. M.A.R. Feliciano, C.A.L. Leite, T. Silveira, A.C. Nepomuceno, W.R.R. Vicente. Universidade Estadual Paulista (UNESP), Campus Jaboticabal, Departamento de Reprodução Animal, Via de Acesso Prof. Paulo Donato Castellane, s/n°, Jaboticabal, São Paulo, Brazil, 14884-900.

Introduction: Lactate-producing bacteria as *Lactobacillus* and *Bifidobacterium* are the most commonly used as probiotics. None of the commercial probiotic products for dogs have microorganisms of canine origin. Beneficial bacteria, as Bifidobacterias and *Lactobacillus*, are resistant to acid environment, while the harmful bacteria, as *Clostridium*, *E. coli*, *Listeria*, *Shigella*, *Salmonella* and others, are sensitive to this environment. The reference to the use of ultrasound in the gastrointestinal tract of small animals is recent. The first reports started since 1989. In human medicine, this image modality is well recognized as a diagnostic method in gastrointestinal diseases, with the main purpose to complement other diagnostic methods. The great advantage of ultrasound over other imaging techniques is to allow the evaluation of the architecture of the tissues and of the structures of a non-invasive way, without the need of tranquilizers and anesthetics, with minimal preparation of the patient. The purpose of this research was to verify the effects of probiotics in the ultrasonographic findings in the gastrointestinal tract of Beagle puppies.

Methods: We used 18 dogs distributed randomly into three treatments: (1) control; (2) diet + probiotic A; (3) diet + probiotic B. The research was divided into two phases according to offered diets: 1) Standard and 2) Super Premium. Dietary changes and fasting were used as nutritional challenge for the dogs. Ultrasonographic evaluations were performed before and after the administration of probiotics. Probiotics were administered after fasting of one day and for three days of the exchange of the diets Super Premium to Standard (first phase) and Standard to Super Premium (second phase). At ultrasound examination were evaluated thickness and characteristics of the wall of the intestinal loops. For the examination, was used Toshiba SSH-140A equipment, with transducers of 3.75 and 7.5MHz. The design was completely randomized with split plot in time, being the probiotics plots and the dates subplots. The averages were evaluated by analysis of variance and the separation of averages by Tukey test and t Student with a significance level of 1 to 5%, depending of analyzed variables.

Results: The medium values of thickness of the intestinal wall at phase 2 of the research, characterized by the exchange of diet, a Standard commercial diet to a Super Premium diet, compared by t Student test with a nominal level of significance of 5%, showed an increase in the thickness of the wall of the intestinal loops in the groups of treatments with probiotics than the control group in the phase 2, relating to the time of action of the probiotic. However no echogenic changes were observed in the characteristics of the wall of these intestinal loops.

Discussion: The use of probiotics can increase the thickness of the intestinal loops of the dogs, not changing their echogenic characteristics, suggesting an increase of the villous and other structures of their anatomy.

ULTRASONOGRAPHIC EVALUATION OF PORTOSYSTEMIC VASCULAR ANOMALY IN A POODLE TOY DOG - A CASE REPORT. M.A.R. Feliciano, C.A.L. Leite, T. Silveira, A.C. Nepomuceno, W.R.R. Vicente. Universidade Estadual Paulista (UNESP), Campus Jaboticabal, Departamento de Reprodução Animal, Via de Acesso Prof. Paulo Donato Castellane, s/n°, Jaboticabal, São Paulo, Brazil, 14884-900.

Introduction: Portosystemic vascular anomaly is a venous malformation that causes anastomosis of the systemic circulation to the hepatic portal system. Its prevalence is unknown, being reported only in North America, Japan, England and Australia. At ultrasonographic examination, in general, intra-hepatic deviations are easier to visualize that the extra-hepatic deviations. Through ultrasound is visualized subjective micro-hepatia, hipervascularity, deviation and dilation of hepatic blood vessels and portal vascular structures changed. The purpose of this study was to report the ultrasonographic detection, using the color Doppler, of portosystemic vascular anomaly in a Poodle Toy dog.

Methods: A Poodle Toy dog, with two years old and weighing 5.0kg, had dry cough and episodes of dyspnea since puppy. At this time, it was radiographed and was given diagnosis suggestive of collapse of trachea and chronic obstructive pulmonary disease. The animal was treated and showed clinical improvement. After one year of therapy, it returned to present the episodes of dry cough and dyspnea. At the last consultation and after clinical evaluation, were measured the levels of alkaline phosphatase (AP), alanine aminotransferase (ALT) and direct bilirubin (DB). Ultrasonographic examination was indicated for evaluation of the gastrointestinal tract and liver. It was performed other radiographic exam too.

Results: At abdominal palpation was verified thickening of bowel with presence of net content. Serum biochemical evaluation for this patient showed an increase of ALT (360UI/L) and maintenance of the serum levels of AP and DB within the normal range for the species. During lung auscultation was noted the presence of fine, discrete and diffuse crackles in the left lung lobe. At cardiac auscultation, mesosystolic murmur was detected in the mitral valve of grade I/VI. At laterolateral thoracic radiographic examination were visualized asymmetry of trachea and mixed lung pattern (interstitial and bronchial), suggesting the presence of collapse of trachea and pulmonary edema. At the ultrasound findings were visualized dilated and tortuous portals vessels, suggesting the establishment of portosystemic vascular anomaly.

Discussion: Biochemical evaluation of the animals presenting portosystemic vascular anomaly provides low dosage of urea, creatinine, glucose and cholesterol, and variable activity of ALT and AP (usually high in young patients) and level of DB within the reference values. Some animals with portosystemic vascular anomaly present moderate pulmonary edema and ascites, due to hypoalbuminemia, agreeing with the findings of thoracic radiography. Through color Doppler was assessed the presence of the vascular anomaly and the turbulence of the vessels. Color Doppler images showed a communication of flow between the portal vein and the hepatic vein, observing blood turbulence too. Through ultrasound evaluation, associated with clinical and laboratory findings, was possible the detection of portosystemic vascular anomaly in the patient in question and this is the first report in Brazil.

MENSURATION OF THE PODOTROCHLEAR BURSA IN TWENTY TWO QUARTER HORSES (*EQUUS CABALLUS*) WITH NAVICULAR DISEASE. C.I.C. PEIXOTO; L.C. VULCANO; V.M.V.MACHADO; A. C.S. AGUIAR**.** FMVZ-UNESP**.** Department of Animal Reproduction and Veterinary Radiology, São Paulo State University, Brazil. Distrito de Rubião Jr., s/n – 18.618-000 – Botucatu/SP

Introduction: Navicular disease is considered to be the main cause of one third of lameness affecting athlete horses, it mostly affects the thoracic limbs and it is characterized by intermittent lameness. The diagnostic, in most cases, is based only on clinical symptoms and radiographic findings. This study aimed to improve the technique of diagnosis for this disease by evaluating and measuring alterations in the podotrochlear bursa in equines with navicular disease using ultrasound, specifically the transcuneal approach.

Materials and methods: Twenty two American Quarter Horses from the region of Bauru and Botucatu, São Paulo State, Brazil were examined. There were 8 mares and 14 males, ages between 3 and 20 years, training in different sport modalities: roping, barrel racing and race horses. The ultrasonographic exam was performed on both thoracic limbs using a Honda HS-2000 device for the evaluation (thickness and echogenicity) of the podotrochlear bursa. Before the procedure, cleaning and foot-bath for 60 minutes were fulfilled. The examinations were performed with a HONDA 7.5 MHz linear transducer, and transmission gel[4] placed at the central region of the frog with the flexed limb. The images were obtained and registered on sagittal plane. No sedatives were used.

Results: The mean thickness of the podotrochlear bursa for the right thoracic limb was of 3.26 ± 1.68mm and 3.84 ± 0.88mm for the left one. The evaluation was made through alterations in echogenicity and the presence of cellularity, indicatives of acute or chronic bursitis.

Discussion: The mensuration of the bursa using an ultrasound scans shows that the mean values obtained are different from the ones reported by Grewal et al. (2004), that were 2.03 mm thickness for the podotrochlear bursa. The alterations found are indicatives of bursitis.

IMAGING DIAGNOSIS: ULTRASONOGRAPHY OF AN INTRA-ABDOMINAL CAVITARY LIPOMA IN A DOG.

P.J.R. Frazão, G.S. Godoy, M.J.B. Prado. Spécialité – Diagnóstico Veterinário. Av. João Paulo Ablas, 465, Cotia/SP, Brazil, CEP 06711-250.

Introduction: Lipomas are the most common mesenchymal tumors in dogs. Breeds with a predilection for lipomas include Labrador Retrievers, Doberman pinschers, and miniature Schnauzers. Most lipomas are subcutaneous, although they can appear in other regions of the body, such as abdominal cavity. Intra-abdominal lipomas are rare and usually become large before clinical signs of a space occupying mass or evidence of necrosis is seen.

Case Report: An 8-year-old spayed female Labrador Retriever woke up lethargic, inappetent, and had an episode of vomiting with streaks of blood. Streaks of blood were also found with feces. Blood analisys was unremarkable and at ultrasound examination was observed few amount of echogenic fluid content in some bowels and an echogenic homogenous well-defined mass at the caudal pole of the left adrenal gland, measuring about 1.7 cm in diameter, which had been observed previosly during a routine ultrasound exam six months before. No clinical sign was related to this mass. At night the animal had an episode of melena and all syntoms disapeared. Three months later, an abdominal mass was palpated near to the spleen. Another ultrasound exam was performed and was observed the presence of a multi-cavitary well-circumscribed mass in mesentery at the left mesogastric region, caudal to the stomach, cranial to the left kidney and medial to the spleen. Its wall was echogenic and dense, cavitations were full-filled with anecogenic fluid, and the whole mass measured about 5.97 cm in diameter. The mass at adrenal gland had no difference comparing to previous exams. A fine needle guided aspiration of the mesenteric mass was performed, which showed the presence of great amount of bacterias and inflamatory cells (neutrophils). Cefalexin was administraded three times per day, during ten days, when another ultrasound exam was executed. The mass had the exactly same apperance than the first exam but it was measuring 6.75 cm in diameter.

Outcome: The mass was then surgically excised and sent to histopathologic analysis. At gross its size was aproximattely 6 cm in diameter, was fleshy at palpation, and white with cavitations at the cut surface. Histologicaly it was observed proliferation of neoplastic adipocytes with mild anisocytosis and anisocariosis. Besides, inflammatory infiltrated, composed by macrophages, lymphocytes and giant cells, was associated to the neoplastic proccess. Based on these finding the mass was caracterizated as lipoma.

Discussion: In this case, different from what has been reported, the intra-abdominal lipoma was diagnosed at early stages without any other complication, such as intestinal obstruction. Besides, at first it had been diagnosed as an abscess due the presence of cavitions. Therefore, lipoma must be considered as differential diagnosis when intra-abdominal cavitated masses are visualized during ultrasound exam.

IMAGING DIAGNOSIS: ULTRASONOGRAPHY OF HUMERAL HEAD OSTEOCHONDROSIS DISSECANS IN A DOG. P.J.R. Frazão, Prado. Spécialité – Diagnóstico Veterinário. Av. João Paulo Ablas, 465, Cotia/SP, Brazil, CEP 06711-250.

Introduction: Osteochodrosis occurs when articular cartilage of the epiphysis fails to form subchondral bone, which results in thickened cartilage. Following, this cartilage can be fractured and form a cartilage flap, known as osteochondrosis dissecans, usually causing clinical problems. Osteochondrosis dissecans can be diagnosed by conventional radiographic exam, once the cartilage flap is mineralized or by positive contrast arthrography when nonmineralized cartilage flap is present. Few studies have been reported on the assessment of osteochondorsis using ultrasound of this joint in dogs, but only one has shown its helpness on detecting ostechondrosis dissecans.

Case Report: An 8-months-old male Rottweiller presenting mild lameness of the left front limb showed irregularities of the caudal aspect of the humeral head in a medio-lateral radiograph. Osteochodrosis was suggested. Radiography and ultrasound of the contra-lateral joint was proposed. No radiographic signs of any disorder were found on the right. Ultrasound exam showed cartilage thickening over a concave defect in the hyperechoic subchondral bone on the caudal part of the humeral head, when the limb was adducted. The bottom of the defect was covered with a second hyperechoic line. This image was valued as an ultrasonographic image of the presence of a cartilage flap and subchondral erosion.

Outcome: The animal was submitted to arthrotomy, the presence of a cartilage flap at the caudal aspect of the humeral head and the subchondral erosion were confirmed, and the flap was removed.

Discussion: In this case, as previously reported, the use of ultrasonography for humeral joint assessment showed to be a helpful diagnostic aid. When compared to positive contrast arthrography, ultrasound can be performed without anesthesia or sedation, and is not invasive. However, an experienced ultrasonographer is required. The full potential of this diagnostic procedure has not been explored.

OSTEOSARCOMA CONFIRMED BY ULTRASOUND-GUIDED FINE-NEEDLE ASPIRATION BIOPSY: CASE REPORT.

M.C.F.N.S. Hage, G.V. Peixoto, P.R.S. Costa, L.G. Conceição, J.C.L. Moreira, T.S. Duarte, A.C. Prandi. Departamento de Veterinária, Universidade Federal de Viçosa, Av. P.H. Rolfs, sem número, Viçosa, Minas Gerais, Brasil, 36.570-000.

Introduction:

Ultrasound-guided fine-needle aspiration biopsy is the most common procedure used to obtain cytological samples from abdominal organs and superficial lesions. The aim of this abstract is to report a case of an ultrasound-guided fine-needle aspiration biopsy of a bone lesion confirming osteosarcoma in a Rottweiler.

Methods:

A case of a twelve-year-old female Rottweiler presenting pain, lameness and soft tissue swelling of the right forelimb is described. The radiographic exam detected a monostotic lesion extending from proximal epiphysis to distal diaphysis of the right humerus showing bone lyses, loss of the fine trabecular pattern, cortical thinning, no clear margin distinction, sunburst effect and soft tissue swelling. It was proceeded the ultrasonographic exam of the area with a 5- to 10-MHz transducer identifying sites of cortical bone discontinuity. The area was aseptically prepared and a 22-gauge needle was advanced percutaneously through the defect. A freehand aspiration biopsy technique was used. Suction was applied with a 10-cc syringe until material was identified within the needle hub. The sample was evaluated for cellularity.

Results:

The cytological findings revealed spindle and polygonal cells, with occasional bi and multinucleation, large nucleoli, anisokaryosis, large and usually well defined basophilic cytoplasm with occasional vacuolization, atypical mitosis and an osteoid substance. This cellularity is consistent with the diagnosis of osteosarcoma.

Discussion:

These radiographic bone lesions were suggestive of neoplasia, however, the definitive diagnosis depends of histopathologic evaluation. A tissue sample core biopsy is the most common procedure performed, but requires anesthesia. Ultrasonographic exam of the bone lesion was used to detect defects in the humeral cortex what turn able the collection of a cytologic sample by ultrasound-guided fine-needle aspiration biopsy that confirmed osteosarcoma. The use of this technique showed advantages over tissue core biopsy. Aspiration biopsy was quick and easy to perform and didn't require any sedation. Although the cytological result was obtained quickly, it depended of the cytologist experience to evaluate the sample. What we learned about this case is that ultrasound-guided fine-needle aspiration biopsy seems to be a promising technique for diagnosis of bone lesions.

MORPHOMETRIC EVALUATION OF THE PORTAL VEIN, CAUDAL VENA CAVA AND ABDOMINAL AORTA IN HEALTHY DOGS OF DIFFERENT BODY WEIGHTS.

R. SARTOR; M. J. MAMPRIM. FMVZ-UNESP - São Paulo State University - Departament of Animal Reproduction and Veterinary Radiology – Distrito de Rubião Jr. s/n - Botucatu-SP-Brazil 186180-000.

Introduction The diameters and areas of portal vein, caudal vena cava and abdominal aorta in dogs of different weights are important measurements to establish a standard for these animals, since portosystemic shunts are frequent in small dogs and may lead to either an increase or a decrease in the portal vein and vena cava calibers. Right-sided heart failure has also been described as an important cause of caudal vena cava dilatation. The measurements of these areas and the knowledge of normal values **for dogs of different sizes** are also required to make and to interpret the Doppler evaluation of the hepatic vessels, in humans, an increase in portal vein diameter is one of the main signs of portal hypertension. The aims of this study were to measure the diameter and area of portal vein, caudal vena cava and abdominal aorta of healthy dogs, which were divided into three groups according to body weight, to assess whether these data are influenced by the animal weight.

Methods Thirty healthy dogs of several breeds were evaluated. They were divided into three groups according to weight range: Group A ≤ 10kg; Group B 10.1–20kg; and Group C ≥ 20.1kg. To measure the diameters and areas of portal vein, caudal vena cava and abdominal aorta, the animal was kept in left lateral decubitus position and the transducer was placed on the right lateral abdominal wall, at approximately the 10^{th} or 11^{th} intercostal space, in the *porta hepatis* region. For caudal vena cava, when only an ovoid format of the vessel was obtained through transversal section, measures were done in both directions and the diameter was estimated based on a mean. After diameters were determined, vessel areas were calculated through the following formula: $A = D^2.\pi/4$ Data were analyzed through F-test and means compared by Tukey's test, at 5% significance.

Results According to the statistical analysis, the diameters and areas of portal vein, caudal vena cava and abdominal aorta were significantly ($P<0.01$) smaller in Group A and similar between Groups B and C. As regards the relationships among the diameters of such vessels, values were similar among the three groups (Table 1).

TABLE 1 - Description of the means (± SD) diameter (D) and area (A) obtained from evaluation through B mode Ultrasonography of Portal Vein (PV), Caudal Vena Cava (CVC) and Abdominal Aorta (AA), according to groups.

Weight (kg)	PVD (cm)	CVCD (cm)	AAD (cm)	PV/CVC	PV/AA	PVA (cm²)	CVCA (cm²)	AAA (cm²)
≤ 10,0	0.65 ± 0.11	0.65 ± 0.12	0.61 ± 0.11	1.01 ± 0.08	1.07 ± 0.09	0.34 ± 0.12	0.34 ± 0.14	0.30 ± 0.12
10,1 - 20,0	0.90 ± 0.08	0.98 ± 0.12	0.90 ± 0.07	0.93 ± 0.18	1.01 ± 0.08	0.64 ± 0.12	0.77 ± 0.19	0.64 ± 0.09
≥ 20,1	0.97 ± 0.12	1.04 ± 0.08	0.95 ± 0.07	0.93 ± 0.11	1.02 ± 0.09	0.76 ± 0.18	0.88 ± 0.22	0.72 ± 0.11

Discussion As observed in the present study, the diameters and areas of these vessels vary with the animal size, and reference values must be specific according to the weight range, especially for animals weighed less than 10kg, which had significantly lower values, relative to the remaining dogs.

FLOW EVALUATION OF THE PORTAL VEIN IN HEALTHY DOGS OF DIFFERENT BODY WEIGHTS.

. R. SARTOR; M. J. MAMPRIM. FMVZ-UNESP - São Paulo State University - Departament of Animal Reproduction and Veterinary Radiology – Distrito de Rubião Jr. s/n - Botucatu-SP-Brazil 186180-000.

Introduction: Portal hemodynamics are evaluated by Doppler ultrasonography measuring of average velocity, flow volume and portal vein congestion index. For this evaluation the insonation angle must be kept below 60º, but a difficulty in obtaining such angle, in the main portal vein, is described in both dogs and humans. Thus, in humans is suggested that the measurements are making at the right branch of portal vein, in which smaller insonation angles could be more easily obtained, allowing a more accurate velocity measurement. This study aimed to make the Doppler fluxometric analysis of the right branch of the portal vein of healthy dogs divided in groups according to body weight, to assess whether the data are influenced by animal weight and if the right branch could be used in the portal hemodynamic evaluation as an alternative to the main portal vein.

Methods: Thirty healthy dogs of several breeds were evaluated. Animals were divided into three groups according to weight range: Group A ≤ 10kg; Group B 10.1–20kg; and Group C ≥ 20.1kg. The transducer was placed on the right lateral abdominal wall, at approximately the 10^{th} or 11^{th} intercostal space to locate the main portal vein, then the transducer was moved approximately one intercostal space cranially and the angle was set according to the visualization of a longitudinal image of the portal vein right branch. Mean velocity (Vmean) was assessed through the uniform insonation technique. For each animal, all measurements had three replicates, from which a mean was calculated. Based on the obtained data, portal congestion index (CI) and average portal blood flow (PFBV) were assessed. Data were analyzed through F-test and means compared by Tukey's test, at 5% significance.

Results: Table 1- Description of the means (± SD) variables obtained from Evaluation through Duplex Doppler Ultrasonography of the right portal vein, according to groups.

WEIGHT (kg)	Vmean (cm/s)	PBFV (ml/min/kg)	CI (cm.s)
≤ 10,0	16.95 ± 5.79 a	51.37 ± 20.55 a	0.022 ± 0.01 b
10,1 - 20,0	16.98 ± 3.04 a	38.28 ± 8.15 ab	0.039 ± 0.009 a
≥ 20,1	17.39 ± 4.77 a	32.19 ± 13.23 b	0.043 ± 0.009 a

a, b – in each column, means followed by same letter do not differ by Tukey's test (P>0,05).

Discussion: The portal right branch was easily found in all evaluated animals, as well as insonation angles lower than 60º. Also an important similarity between the obtained values for portal vein right branch and those reported in literature for the main portal vein was observed in dogs presenting similar body weights, which evidences the viability of using such branch in Doppler ultrasonography of dog portal system as an alternative to the main vessel segment, mainly in those animals in which an ideal insonation angle for examination is hardly obtained. The flow portal vein average velocity doesn't show any variation with the animal weight, but in the flow volume and congestion index a significant difference was noted among the groups demonstrating thus that body weight can influence such values and must be considered in the evaluation of the results.

ULTRASONOGRAPHIC ASPECT OF THE TREMATODA *Fasciola hepatica* ISOLATED IN ACOUSTIC GEL. W.G. Santos, D.C. Oliveira, I.V.F. Martins, C.C. Bernardo, F.S. Costa. Universidade Federal do Espírito Santo, Centro de Ciências Agrárias, Departamento de Medicina Veterinária. Alto Universitário s/n^{o}, Alegre – ES, Brazil. Postal Code: 29500-000.

Introduction: Fascioliasis is caused by the digenetic trematoda *Fasciola hepatica*. This parasitosis occurs mainly in ruminants, but it can infect humans and others species too, parasitizing primarily the liver and the biliary tract. The diagnosis in humans has been based in regional epidemiological aspects, associated to laboratorial exams. Imaging techniques like magnetic resonance, computed tomography, retrograde colangiohepatography and ultrasound have been employed to the diagnosis and follow-up of the patient with fascioliasis, however, the sensibility and specificity indexes for these techniques have been controversial and varied. Ultrasonographic findings of human fascioliasis are unspecific, and the literature has no details about the direct visualization aspect of the parasite during the examination.

Methods: Livers of bovines infected by *Fasciola hepatica* were collected in Atilio Vivacqua's municipal slaughterhouse, south of Espirito Santo State, Brazil. The livers were removed right after the slaughter, and 30 living parasites were collected immersed in a recipient filled with acoustic gel in order to enable a detailed ultrasonographic visualization.

Results: All of the evaluated trematodas presented a similar ultrasonographic image after subjective analysis, in which was observed a clear image with a hyperechogenic periphery and a hypoechogenic interior. The parasites were observed as thin structures with thickness varying from 1 to 2 mm and they didn't produce distal acoustic shadow.

Discussion: Just a few studies demonstrate the ultrasonographic aspects of *Fasciola hepatica*, and generally they describe findings caused by the alterations in the hepatic parenchyma and biliary tract due to the parasitic infection. The ultrasonographic image of this trematoda in humans is referred as a structure with vermiform aspect, or as echogenic particles floating in the gallbladder and common biliary tract, without acoustic shadow formation. Despite the existent descriptions, its ultrasonographic direct visualization is frequently difficult, and only in some cases it's possible to visualize the parasites inside dilated biliary ducts, mainly when they are moving. This study enabled more detailing of the parasite, once the acoustic gel allowed more contrast and eased its observation. Basing in the knowledge of *Fasciola hepatica* ultrasonographic anatomy, it's possible to direct the diagnosis of fascioliasis in humans, ruminants and other hosts, mainly when the parasite is in the gallbladder wrapped by bile.

QUANTITATIVE ULTRASONOGRAPHY OF LIVER IN CATS TREATED WITH PREDNISOLONE. W.G. Santos, J.N.M. Monteiro, D.C. Oliveira, D.C. Borlini, L.A. Vescovi, F.M. Machado, S. Martins Filho, F.S. Costa. Universidade Federal do Espírito Santo, Centro de Ciências Agrárias, Departamento de Medicina Veterinária. Alto Universitário s/n°, Alegre – ES, Brazil. Postal Code: 29500-000.

Introduction: The use of corticosteroids can unchain series of collateral effects in dogs and cats. In the liver, there are described alterations such as hepatomegaly and vacuolar hepatocyte degeneration, with glycogen and/or lipid accumulation. The ultrasound evaluates the intra-hepatic anatomy in a secure and non-invasive way; however it can present divergences in the interpretation of its findings, due to the individual and subjective analysis. Some techniques can be used to minimize the subjectivity of the exam, quantifying the echogenicity and echotexture of the evaluated regions. The aim of this study was to evaluate quantitatively the echotexture and echogenicity of the hepatic parenchyma of cats submitted to corticotherapy, by the use of grey-levels histogram.

Methods: Nine healthy cats with no race or sex distinction, and with none clinical or laboratorial alterations were studied. All animals received oral tablets of prednisolone (6 mg/kg body weight) during 14 days. All the ultrasonographic variables were measured immediately before and by the end of the experimental protocol. Hepatic parenchyma histopathologic samples were obtained by ultrasound-guided biopsy using a Tru-Cut needle, both before and after the experiment. The statistic analysis of the variables was made with the non-parametric test of Wilcoxon ($P<0,05$). This study was realized under the approval of the *Comitê de Ética em Experimentação Animal* of the *Universidade Federal do Espírito Santo* – Brazil.

Results: The grey-levels histogram technique proved an increase in the hepatic parenchyma echogenicity due to a significant elevation of the LMEAN variable between the experiment's initial and final moments. However, the hepatic ultrasonographic echotexture, characterized by the values of the NMOST/NALL variable, didn't vary statistically. The hepatic samples' histopathologic analysis demonstrated the presence of a cytoplasmic microvacuolization, suggesting intracellular accumulation of glycogen.

Discussion: The accumulation of lipids and glycogen in the hepatocytes increases the hepatic parenchyma echogenicity in cats and in other species. The histopathology proved that the ultrasonographic alterations caused by the corticotherapy were due to glycogenosis, demonstrating the quick occurrence of collateral effects in the liver of cats treated with high doses of prednisolone. The prednisolone in the dose used in this research, even in a short time period, induces adverse effects in the cat's liver, for this reason, some prudence is needed when using this drug in cats. The quantitative evaluation of the hepatic parenchyma allows an accurate evaluation and enables a better sequential follow-up of a patient that needs to be submitted to a corticosteroid treatment.

ECHOCARDIOGRAPHY AND TISSUE DOPPLER IMAGING OF THE MYOCARDIUM OF CATS WITH INDUCED THYROTOXICOSIS. D.C. Oliveira, D.C. Borlini, W.G. Santos, J.N.M. Monteiro, L.A. Vescovi, A.Q. Araújo Sobrinho, T. Roesler, S.V.S.G. Barros, S. Martins Filho, M.J.L. Cardoso, F.S. Costa. Universidade Federal do Espírito Santo, Centro de Ciências Agrárias, Departamento de Medicina Veterinária. Alto Universitário s/n^{o}, Alegre – ES, Brazil. Postal Code: 29500-000.

Introduction: Hyperthyroidism is the most frequent endocrine disease in cats. The most common cardiac alterations caused by the excessive serum concentrations of thyroid hormones include elevation of heart rate, increase in the left ventricle, diastolic dysfunction and arrhythmias. Tissue Doppler imaging (TDI) is a relatively new technique, which allows the quantitative evaluation of the myocardial motion. The aim of this paper was to study the physiologic aspects of thyroid hormones excessive serum concentrations over the cardiac function in cats by the echocardiographic examination and the TDI technique.

Methods: Nine healthy adult cats (no sex or race distinction) were studied. The thyrotoxicosis was achieved by the administration of sodium levothyroxin oral tablets (150μg/kg body weight) once a day, during 10 weeks. The exams were realized immediately before the induction and by the end of the experimental protocol. A few minutes before the realization of the exams, the cats were anesthetized with tiletamin and zolazepam. The statistic analysis of the variables was made with the non-parametric test of Wilcoxon ($P<0,05$). This study was realized under the approval of the *Comitê de Ética e Bem Estar Animal* of the *Universidade Estadual Paulista*, Botucatu Campus - Brazil.

Results: The pulsed TDI results proved the occurrence of cardiovascular effects during the experimental protocol, with an increase in the myocardial motion velocity in the interventricular septum. The values of septal Ea and septal Sa suffered a significant increase, however, there was no alteration in the Ea and Sa variables in the lateral corner of the mitral annulus. The conventional echocardiographic examination verified a statistically significant reduction of the left ventricular chamber in systole and diastole. No statistical variation was verified in the other echocardiographic parameters, but there was a significant elevation of the heart rate in the experimental group animals.

Discussion: The experimental protocol was responsible, in a short time period, by alterations in the myocardial motion, but with no damage to the diastolic function. In a general way, thyrotoxicosis increased the heart rate and the cardiac motion velocity of all the cats. Pulsed TDI values suggest a major influence of the thyroid hormones over the interventricular septum than over the left ventricle free wall, during the initial stage of the disease. One cat of the experimental group presented a severe hypertrophy in the left ventricle free wall and interventricular septum, surpassing the normal ranges pre-established for healthy cats. This fact demonstrates concentric hypertrophy occurrence possibility in cats with thyrotoxicosis non-concomitant to idiopathic hypertrophic cardiomyopathy. The TDI technique has proved to be an exam with higher sensibility and efficacy than the conventional echocardiography in the diagnosis of diastolic dysfunction, helping in the early diagnosis of cardiomyopathies, and in the monitoring of hyperthyroid cats.

ULTRASONOGRAPHIC PERCUTANEOUS ANATOMY OF CAUDAL LUMBAR REGION IN NORMAL DOGS AND US-GUIDED APPROACH FOR LUMBAR SUBARACHNOID PUNCTURE

Etienne A.-L.*, Jacquemot O.**, Bolen G.*, Snaps F.*, Busoni V.*
*Diagnostic Imaging Section, **Anatomy Section, Faculty of Veterinary Medicine, University of Liège, Boulevard de Colonster, 20, Bât. B41, Sart-Tilman, 4000 Liège, Belgium

Introduction/Aims

The use of ultrasound (US) to identify lumbar landmarks is a technique commonly used in human medicine, in particular in the emergency department and at the time of unsuccessful blinded procedure. In the dog US of the lumbar region has not been described. The aims of this poster are: 1. to present the percutaneous US anatomy of the caudal lumbar region in dogs, 2. to present the US landmarks that can be used for US guided subarachnoid puncture in dogs.

Methods

Five normal dogs were used to illustrated normal US anatomy of the caudal lumbar region. Images were obtained by a percutaneous approach with a linear 7.5MHz transducer, a microconvex 7.5MHz and/or a convex 5MHz transducer depending on dog size and fatness. Adjust of the US-guide subarachnoid puncture was done on 3 cadavers and in 2 anesthetized dogs.

Results

The top of the dorsal spinous processes is easily seen as a curved hyperechoic line very close to the transducer surface. Articular processes are seen in a parasagittal position compared to the spinous processes. The degree of visibility of the different muscular planes and the ease in visualization of the articular processes greatly depend on the amount of fat present. A longitudinal parasagittal US view was obtained to visualize the intervertebral space between two contiguous articular facets. The space between the facets was used as a landmark. The vertebral canal was visible between the articular facets and the sagittal plan. The needle was directed US guided toward the space between the articular processes were the vertebral canal was visible to obtain entering of the subarachnoid space.

Discussion/Conclusion

Visibility of the anatomical structure of the lumbar region at percutaneous US mainly depend on the fatness of the dog. Parasagittal images can be used to localize by US the site for entering the vertebral canal and obtaining a lumbar subarachnoid puncture.

ECHOCARDIOGRAPHIC CHANGES OF LEFT VENTRICULAR END-DIASTOLIC VOLUME IN A MODEL OF CANINE HYPOVOLEMIC SHOCK.

J. Ko, H. Kang, S. Heo, H. Lee, M. Kim, K. Lee, N. Kim. College of Veterinary Medicine, Chonbuk National University, 664-14, 1 ga, DuckJin-dong, Jeonju 561-756, Republic of Korea..

Introduction; The objective of this study was to document echocardiographic changes of left ventricular end-diastolic volume with other left ventricular performances in an experimental canine model of severe hypovolemic shock.

Methods; Twenty mature healthy male beagles were used in severe hypovolemic shock. All experimental groups were divided into BL (Base Line) groups (n=10) and PH (Post Hemorrhage) groups (n=10). During the experiment, we evaluated the result of left ventricular end-diastolic volume and cardiac performances in non-induced shock and severe hypovolemic shock in anesthetized beagles. The LVEDV using four apical chamber view was also assessed by modified Simpsons rule in triplicate for more accurate LVEDV evaluation. After being anesthetized, all experimental animals were instrumented with an arterial catheter and a thermodilution cardiac output catheter. The measurements were performed at BL and PH. Approximately 40% of the dogs' blood volume (total blood volume: 85 mL/kg), was withdrawn from the right carotid artery over 30 minutes until an MAP of about 50 mmHg was reached. Additional small amounts of blood were drawn to maintain the arterial blood pressure at 50 mmHg for 60 minutes. At the end of the hypovolemic period (PH), All measurements were performed at PH.

Results; The mean arterial blood pressure (ABPm) decreased from 107.70 to 44.15 mmHg, was associated with the following changes. Left ventricle end-diastolic volume (LVEDV) decreased from 12.14 ml to 5.33 ml. Stroke volume (SV) decreased from 18.65 to 5.50 mL/bpm, Cardiac output (CO) decreased from 2571 to 834 ml/min.

Discussion; Left ventricular end-diastolic volume measurement was conventional technique in veterinary medicine. In terms of emergency ultrasonographic diagnosis, LVEDV measurement as noninvasive and quick technique could be efficient for patient monitoring in severe hypovolemic shock without cardiac instrumentation.

Key words: echocardiography, left ventricular end-diastolic volume, hypovolemic shock, dog.

DOPPLER VELOCIMETRICS PARAMETERS OF RENAL VASCULATURE AND ABDOMINAL AORTA OF HEALTHY PERSIAN CATS.

C.F. Carvalho, M.C. Chammas. INRAD-HCFMUSP. Travessa Leon Berry, 122, São Paulo, São Paulo, Brazil, 01402-030.

Introduction: Renal failure has high morbidity in cats, especially the older ones. Decreased renal blood perfusion may be the first sign that indicates dysfunction. Ultrasonography is a routine method of imaging diagnostic in animals with renal diseases, but a few reports are available describing values for hemodynamic renal vasculature derived by Duplex Doppler Ultrasonography in normal cats. The purpose of this research was evaluating normal dopplerfluxometrics parameters of renal arteries (RA), interlobar arteries (IA) and abdominal aorta artery (AO) in adult healthy Persian cats.

Methods: Fifty renal units of 25 Persian cats (13 females and 12 males ranging in 12 to 60 months of age) were selected for normal renal function by clinical and biochemical examination (complete blood count, serum biochemical for renal and hepatic function, urinalysis, urine protein/creatinine ratio); for normal systemic blood pressure, and normal anatomy using a triplex Doppler ultrasonography unit, with a 7 to 10 MHz linear transducer. It was performed B-mode ultrasonography, color mapping of renal vasculature and pulsed Doppler of both AR, AI in both kidneys at three sites (cranial, media, caudal), and AO with special attention to the insonation angle. All vessels were measured maximal systolic peak velocity (VPS), minimum end diastolic velocity (VDF) and resistive index (RI). Based on obtained data, and to establish normal values, 95% confidence intervals were calculated. It was also obtained ratio indices between AR/AO, and AI/AR velocities. A paired *t* test was performed to determine if any significant differences ($P<0.05$) existed between each artery for both kidneys and for intrarenal velocimetric values.

Results: Results of AO measurements were VPS 53.17±13.46cm/s and mean diameter of 0.38±0.08 cm. The mean RA diameter of fifty renal units was 0.15±0.02 cm. Considering velocimetric values in both renal arteries the mean obtained was VPS 41.17±9.40cm/s and RI 0.53±0.07. Correlations between renal and aortic velocities were verified with Pearson's coefficient calculations. Renal-aortic ratio mean obtained was 0,828±0,296. Results of IA measurements were VPS 32.16±9.33cm/s and RI 0.52±0.06. Positive correlations between renal and interlobar velocities were verified with Pearson's coefficient calculations, as IA themselves. Renal-interlobar ratio mean obtained was 1.45±0.57.

Discussion: This research performed with selected cats as normal, healthy and same ranging of age, RI was slightly smaller than others referred in literature. It is known that neonates and infants can have normal RI values considered elevated by adult standards. Maybe this occurs with cats, but further studies are needed to determine if age have an effect on these values. According with other studies VPS mean values of AO were higher than RA, and in these vessels were higher than those obtained at IA. To our knowledge, no reports are available describing values of normal Doppler velocimetric parameters of RA in Persian cats. Beside this, we suggest an index renal-aortic ratio and renal-interlobar ratio similar as used in humans to monitoring renal hemodynamic parameters.

OBSTETRIC ULTRASOUND IN A FREE-RANGING GIANT ANTEATER (*Myrmecophaga tridactyla*)

Lacreta Jr ACC, Cruvinel TMA, Cruvinel CAT, Regonato E, Monteiro FOB. Universidade Federal Rural da Amazônia, Brasil, Belém-PA, CEP: 66.077-530

Introduction/Purpose

The Giant anteater belongs to the Order Xenarthra, previously classified as Edentata, and now contains anteaters, armadillos and sloths. The Family Myrmecophagidae is composed by three genus and four species, and only one does not occur in Brazil, where, the species occurs in all biomes. It is the largest member of its order, with total length of 2 meters and 18 to 40 kg of weight in the wild. Giant anteaters pregnancy ranges from 130 to 190 days, however, little is known about reproductive aspects of this species.

Methods

The present study describes the case of a free-ranging female Gian anteater, probably run over by a car, admitted in May 18 th at the "Dr. Halim Atique" Veterinary Hospital, UNIRP, São José do Rio Preto, São Paulo, Brazil, for medical care. On physical examination pelvic instability was identified. Biological material was collected for routine examinations and the animal was sent to the diagnostic imaging department for radiographic and ultrasound examinations. A fracture of the right acetabulum was confirmed, and pregnancy was diagnosed.

Results

The ultrasound examination was performed with a Medison equipment Sonoview 9900 model. The following means of the fetal measurements in B-mode were obtained: left femur = 2.6cm, right femur = 2.69cm, left tibia = 2.34cm, right tibia = 2.31 cm, left foot = 3.69 cm, right foot = 4.22cm, left humerus = 1.90cm, right humerus = 1.87 cm, abdominal diameter = 5,59cm, thoracic diameter = 4.48 cm, biparietal diameter = 2.88 cm, nasal bone diameter = 5.51 cm, frontal-occipto diameter = 3.99 cm, nasal-occipto diameter = 8,03cm, cranial circumference area = 10.73 cm, abdominal circumference area = 16.65 cm. The initial Heart rate during clinical examination was 103bpm and final was 102bpm. The values obtained in the umbilical artery Doppler spectrum were: PSV = 29.07 cm/s, EDV = 4.85 cm/s, TAM = 7.46 cm/s, Vmean = 15.75 cm/s, Gmean = 0.11 mmHg, Gpeak mmHg = 0.34, RI = 0.83, PI = 1.54 and S/D = 5.99. 23days after admission the animal suffered spontaneous abortion. The weight of the aborted fetus was 420 grams, at the estimated gestational age of 120 days. On 42th day after admission, the animal was clinically recovered and then returned to its natural habitat.

Discussion/Conclusions

In giant anteaters, little is known about fetal development and fetal ultrasound parameters, especially free-ranging individuals. This report aims to demonstrate these parameters and collaborate with future obstetric studies in the species.

DIAGNOSIS OF FETAL HYDROCEPHALUS BY ULTRASOUND IN A RAGDOLL CAT: A CASE REPORT. Bomfim, PC; Veiga, CCP. Imagem Veterinária. Botafogo, Rio de Janeiro / RJ, Brazil. 22280-090.

Introduction
Hydrocephalus is a neurological disorder characterized by an abnormal accumulation of cerebrospinal fluid (CSF) within the ventricles and subarachnoid spaces. Due to its complex and multi-etiologic nature, the pathogenesis of the hydrocephalus has no definitive explanation. When it is a congenital condition, it may be caused by structural defects. It seems to be relatively rare in cats.

Case History Report
A one year old Ragdoll cat, vaccinated in her early pregnancy, was submitted to ultrasound evaluation during labor. No prior ultrasound had been performed therefore the number and viability of the fetuses were previous unknown. Four fetuses were normal; three were hydrocephalus and died just after the cesarean section. One was already dead with evidences of decomposition.

Imaging
The dead fetus was in cephalic position. It had no heartbeats, no structural definition and small size if compared to the others. Three fetuses showed enlarged ventricles with different degrees characterized by visualization of anechoic crescent-shaped structures. Only a small amount of residual neural tissue remained in the ventral calvarium in one of them. The other fetuses had normal aspect.

Discussion/Conclusion
The dead fetus was the probable cause of dystocia. The lesions of hydrocephalus were so evident that probably would have been detected before. We recommend an early ultrasound evaluation and constant monitoring during the pregnancy. The cause of hydrocephalus in this case was not determined, however, is possible to be related to vaccination during the early pregnancy. Young cat with cerebellar hypoplasia due to intrauterine infection by panleukopenia virus may have a concomitant hydrocephalus and hydranencephaly. This possibility must be considered in this case.

ULTRASONOGRAPHIC FEATURES OF GRANULOMATOUS MENINGOENCEPHALITIS IN DOGS. R.B. Perez, C.F. Carvalho, M.C. Chammas. Instituto de Radiologia - Faculdade de Medicina da Universidade de São Paulo. (Rua Campinas 143, São Bernardo do Campo, São Paulo, Brasil, 09751-420).

Introduction: Granulomatous meningoencephalitis (GME) is an acute, progressive inflammatory disease, specific of the central nervous system (CNS) of dogs and it can cause depression, tremor, generalized seizure, hyperesthtesia ataxia and blindness. It affects mainly small breed, 5-years-old dogs and its incidence is higher in females. According to the distribution, the degree of histological lesions and the course of the disease, GME has been classified in three different categories: disseminated or multifocal, focal and less common ocular. The clinical diagnosis is based on history, clinical signs, cerebrospinal fluid analysis, computed tomography or magnetic resonance studies. The purpose of this study was to evaluate the sonographic aspects of Transcranial Color Doppler Sonography (TCDS) in B-Mode, color Doppler and pulsed Doppler in eleven dogs with clinical signs of GME confirmed at necropsy and histopathologycal findings.

Methods: Eleven dogs with neurologic signs and a presumptive diagnosis of GME were submitted to TCDS without any sedation. All examinations were performed with a triplex Doppler ultrasound unit with mechanical convex transducer (2-5 MHz), using a temporal and/or rostral fontanel approach, and sagittal, coronal and axial planes were performed. The encephalic parenchyma aspects were evaluated, as well as the presence of focal lesions (echogenicity, location and extension), ventricular diameter, color mapping detection of Willis circle and the measurement of the resistive index (RI) of anterior, middle and caudal cerebral arteries as described in literature.

Results: This study correlated the necropsy and histopathologycal findings with the ultrasonographic aspects, since there are no veterinary reports about color Doppler aspects of GME in dogs. The reduction of echogenicity (45%) was correlated with mild to severe congestion and hemorrhage of the encephalic parenchyma found at necropsy. Dilatation of the ventricular system was associated with lateral ventriculomegaly detected on ultrasonography (63%). Granulomas were associated with parenchymal focal lesions on ultrasonography (45%). The evidence of Willis circle detected by color Doppler (72%) could indicate dilatation of cerebral vessels and seems to be related to congestion and edema of CNS. A significant correlation between the resistive index and cerebral perfusion pressure is described in literature, and pulsed Doppler showed normal to higher values of IR indicating that intracranial pressure can be normal to elevated in GME.

Discussion: TCDS is a noninvasive, rapid, low cost method to evaluate the brain parenchyma through the intact skull. Further studies must be performed, but these results suggested that TCDS can be an additional tool when CT and MR can not be performed, providing information about the encephalic parenchyma and hemodynamic aspects of cerebral vasculature.

DIFFUSE LIVER DISEASE IN DOGS: COMPARATIVE STUDY BETWEEN ULTRASONOGRAPHY, LABORATORY TESTS, BIOPSY, AND FINE-NEEDLE ASPIRATION.

M.J. Mamprim, N. S. Rocha, R.S. Lopes, F.A.M. Santos, A.C.A. Zablith, C.F., Carvalho, I. F. C. Santos. Faculdade de Medicina Veterinária e Zootecnia – Universidade Estadual Paulista - Departament of Animal Reproduction and Veterinary Radiology – Distrito de Rubião Jr. s/n - Botucatu-SP- Brazil 186180-000.

Introduction: The diseases that most frequently affect dogs are chronic inflammatory hepatic diseases, which in most cases progress to hepatic cirrhosis. Clinical diagnosis of these diseases poses challenges because in the early stages they do not show specific symptoms. However, when characteristic symptoms appear, the liver parenchyma is already severely compromised. Laboratory tests only show alterations when more than 70% of the parenchyma is compromised. Inflammatory diffuse diseases are also difficult to detect by ultrasonography. In humans, however, using ultrasonographic patterns, it is now possible to distinguish between fatty infiltration and fibrosis. The aim of this study was to classify diffuse hepatic alterations and compare them with results from laboratory tests, biopsy, and fine-needle aspiration (FNA) in order to contribute new information that may be useful in differential diagnosis of chronic diffuse hepatic diseases.

Methods: Sixty-two dogs of different sexes, ages, and breeds were used. Ultrasonography enabled the classification of the diffuse alterations of liver parenchyma into the following patterns: homogeneous hypoechoic (H); heterogeneous hyperechoic, micronodular (HH type IIIa) and macronodular (HH type IIIb); and heterogeneous nodular of mixed echogenicity (HM) correlated to the neoplasias. FNAs were performed with 25-gauge spinal needles and the biopsy with 14-gauge *Tru-cut* needles.

Results: After biopsy, mild hemorrhage was seen in 5.2% of the animals. Collected samples were of diagnostic quality in 95.38% of the biopsies and 98.38% of the FNAs. There was 75.81% positive correlation between histological and ultrasonographic results. There was positive correlation between cytological results and ultrasonographic patterns: H - 90%, HH - 29.55%, and HM - 100%. Pattern H was mainly related to acute hepatitis, . Pattern HH type IIIa suggests chronic hepatic diseases, such as active chronic hepatitis, and mild cirrhosis (grades I and II). Pattern HH type IIIb confirms chronic hepatic diseases, such as active chronic hepatitis, chronic hepatitis, and severe cirrhosis (grades II and III). Transmissible venereal tumors (TVT) may show H, HH type IIIa and IIIb, and HM ultrasonographic patterns. Liver parenchyma with diagnosis of mastocitoma showed H pattern. The animals with liver carcinoma showed HM pattern of hyperechoic and mixed nodules. The animals with diagnosis of liver hemangiosarcoma showed HM pattern with anechoic areas.

Discussion: Alterations in the liver parenchyma were diagnosed by ultrasonography earlier than laboratory tests could confirm them, especially in chronic and acute inflammatory hepatic diseases. FNA has shown to be a safe, low cost, fast, and efficient technique to differentiate inflammatory from neoplastic processes. Therefore, FNA with 25-gauge should be used as routine in liver ultrasound examination to allow differential diagnosis of neoplasias. Biopsy should only be used when FNA is not conclusive.

ULTRASONOGRAPHIC IMAGES OF MAMMARY GLANDS IN DAIRY HEIFERS AT DIFFERENT STAGES OF GROWTH

M. Nishimura[1,2], T. Yoshida[1], M. Miyoshi[1], K. Miyahara[1,2]
[1]Veterinary Medical Teaching Hospital, Obihiro University of Agriculture and Veterinary Medicine, Inada-cho, Obihiro, Hokkaido 080-8555, JAPAN; [2]United Graduate School of Veterinary Sciences, Gifu University, 1-1 Yanagido, Gifu, Gifu 501-1193, JAPAN

Introduction

Ultrasonography is a useful tool for diagnosis or screening of human breast diseases. In farm animals, the use of ultrasonography for examination of mammary gland has been developed for ruminant animals; however, there has been no report on ultrasonographic images of heifer mammary gland. The objective of this study was to describe the ultrasonographic findings in normal mammary glands of dairy heifers at different stages of growth.

Methods

A total of twenty clinically normal Holstein heifers were used. Heifers were divided into five groups by stage of their growth; two months of age, five months of age, postpuberty, second trimester of pregnancy and three weeks prepartum (n=4 per group).The two left quarters of each heifer were scanned by B-mode using a portable instrument with a convex array transducer operating at 5.0MHz. Structure, echogenicity and homogeneity of the each tissue were assessed.

Results

Ultrasonographic images varied at the different stages of growth. In two months of age, mammary glands were oval, homogeneous hypoechoic and surrounded by heterogeneous hyperechoic area. In other age groups, the mammary tissues had a coarse-grained structure and medium echogenicity including poor-defined hypoechoic area mostly in superficial part to various degrees. In five months of age, mammary glands generally showed a thickness of 1 cm, however, the hypoechoic area was different in extent. The characteristic finding in postpuberty was that the irregular hypoechoic area spread into depth. In both groups of pregnant heifers, superficial hypoechoic area spread into depth more extensively than postpuberty. Six of eight pregnant heifers had irregular and very hypoechoic or anechoic areas in the tissue. In the last trimester, tubular structure was seen in transverse section from lateral.

Discussion

This study showed that the morphological changes of heifers mammary glands at different stages of growth could be visualized by ultrasonography. Ultrasonography is possible to be a useful tool for study of mammary gland development in cows, and thus comparing ultrasonographic images with anatomical and histological findings of mammary glands is needed.

CORRELATION BETWEEN ULTRASOUND IMAGE OF THICKENED URINARY BLADDER WALL AND THE PRESENCE OF CYSTITIS IN GERIATRIC BITCHES. V. R. BABICSAK; M. J. MAMPRIM; A. B. OLIVEIRA; I. F. C. SANTOS. Faculdade de Medicina Veterinária e Zootecnia – Universidade Estadual Paulista - Departament of Animal Reproduction and Veterinary Radiology – Distrito de Rubião Jr. s/n - Botucatu-SP-Brazil 186180-000.

Introduction: Veterinary Medicine has advanced concerning technology and knowledge of several diseases, leading to an increase in the life expectancy of animals. Today, 40% dogs reach the old age; thus, the geriatric animal has become a frequent patient in routine ultrasound examinations, mainly of the abdominal region. During the ultrasonography of geriatric bitches bearing mammary tumor, a large number of these animals were observed to have thickened urinary bladder wall. Thus, the aim of this study was to verify whether thickened urinary bladder wall is a normal alteration in geriatric females (similarly to other organs and systems) or should be considered chronic cystitis.

Methods: In this retrospective study, ultrasonographic findings from the Radiology Service of the Veterinary Hospital, School of Veterinary Medicine and Animal Sciences, São Paulo State University-UNESP, Botucatu, São Paulo State, Brazil, were analyzed from 2000 to 2008. Females presenting >2mm urinary bladder wall under optimal conditions of bladder repletion (i.e. moderate repletion) were selected. Animals with uroliths, microuroliths, crystals, and confirmed neoplasm diagnosis were discarded. Of the remaining dogs, those presenting urine test results of 1 day before or after the ultrasound were included in this study, accounting for 33 animals. Thus, the bitches with 2 or more leukocytes per field in the sedimentation test were considered to have cystitis.

Results: Thirteen females (39.39%) had the disease, whereas 20 animals (60.1%) did not present cystitis. All animals of the breeds Fila Brasileiro, Rottweiler, Fox Paulistinha, German Shepherd, Lhasa Apso and Poodle presented cystitis (100%). As regards age, middle aged (6 years) and the eldest females (11 and 12 years) presented the highest frequency of the disease. Bitches with cystitis (88.08 months) had higher age mean than the group without the urinary disease (67.6 months). Considering the geriatric animals, cystitis frequency was 5 of 6 geriatric bitches with the disease (83.33%) and only 1 animal without cystitis (16.66%).

Discussion: The highest cystitis frequency was found in middle aged and the eldest females which, according to literature, are more predisposed to such disease due to the existence of other urinary lesions favoring the infection. Considering breeds, many of them presented 100% cystitis; however, breed predisposition to cystitis is not cited in literature. Relative to the aim of this study, the presence of thickened urinary bladder wall is not physiological in geriatric bitches; it is caused by cystitis. This could be inferred since only 1 geriatric animal did not present cystitis, representing 16.66% of the population.

EARLY BONE REGENERATE IN EXPERIMENTAL BONE LENGTHENING IN SHEEP – COMPARISON OF US, RX AND MORPHOLOGICAL RESULTS

W. Atamaniuk, P. Kuropka*, R. Henklewski, A. Krawczyk**
Environmental University of Wrocław, Faculty of Veterinary Medicine, Department of Surgery, pl. Grunwaldzki 51, 50-366 Wrocław, Poland
*Environmental University of Wrocław, Faculty of Veterinary Medicine Institute of Histology and Embryology,
**Orthopaedic Clinic of Wrocław Medical University

Introduction

The objective of this experiment was to evaluate early stages of bone regenerate formation in distraction osteogenesis by means of US and to compare it with radiography to histological examination, SEM and superficial x-ray microanalysis (EDX).

Methods

Twenty-three, two-year-old, pure bred Merynos sheep were divided into three test groups. Each group represented a different method of tibial corticotomy with compromised blood supply in the operating field (open corticotomy, Cattaneo corticotomy and osteoclasia).
Ultrasound scans were taken postoperatively, again on the sixth day and then every fourth day respectively through the experiment. Pre and post operative radiographs were taken under premedication on the day of operation, then every two weeks throughout the experiment. For further data collection, three representatives of each group were humanely euthanized at the fifth, ninth, and fourteenth week of experiment to collect bone regenerates for microscopic study.

Results

In all cases we observed normal bone regenerate filling the distraction gap. Sonolucent gaps at the site of osteotomy was clearly seen on US scans. At the beginning of distraction, echogenic foci were visualized at these sonolucent gaps. On longitudinal scans, these foci elongated into parallel longitudinal lines. Ultrasonographically, we noted two types of bone regeneration, called *hypertrophic* (seen in all regenerates in osteoclasia group) and *normotrophic.* Histologically, hyperechogenic foci which evolved into to parallel lines in the distraction gap represented fibrous osteogenic tissue while hyperechogenic lines at the ends of the bone fragments are likely due to periosteal bone reaction. SEM examination and x-ray microanalysis indicated the most advanced osteogenesis process in the osteoclasia group.

Discussion

Excessive damage of the periosteal and endosteal vasculature in experimental group operated by open osteotomy resulted in a slowing of new bone formation on the 14-th post operative week for about 2-3 weeks, comparing sheep operated with osteoclasia method. However, full regeneration appeared in every case regardless of the extent of vascular compromise. Ultrasound exam was valuable method to predict type of regenerate seen later on radiographs.

PHYSICAL RESTRAINT PROTOCOL TO PERFORM GYNAECOLOGICAL AND OBSTETRIC EXAMINATION BY ULTRASOUND IN OWL MONKEYS

Monteiro FOB, Coutinho LN, Pompeu ESS, Castro PHG, Maia CE, Lacreta Jr ACC, Vicente WRR. Universidade Federal Rural da Amazônia. Av. Presidente Tancredo Neves, 2501 CEP: 66.077-530, Belém-Pará-Brasil.

Introduction/Purpose

The anesthetic drugs and capture method used for gestation ultrasonographic monitoring in owl monkeys contributed to abortion, and establishing conditioning methods may be a solution. The objective of this study was to establish a physical restraint protocol for the gynaecological and obstetric ultrasound examination.

Methods

The study was conducted at the National Primate Center (Ananindeua, PA, Brazil), with adult owl monkey (*Aotus azarai infulatus*) couples, evaluated in two different time periods. In the first period (P1), the females (n = 10) were kept isolated from the males during four months. The second period (P2), starting 30 days after P1, involved mating and non pregnant females (n = 6) and pregnant females (n=3) were examined once a week, during seven consecutive months. The exams were performed using the ultrasound equipment Medical SonoAce 9900® with a multifrequential linear array probe (5-12 MHz). The females were manually restrained and fruits were offered before, during and after the procedure. Initial and final heart rates (HR1 and HR2) of each female were calculated based on the interval between systolic peaks, obtained in Spectral Doppler Mode at the iliac arteries. The average heart rate (HRA) of each exam was obtained through the arithmetic mean between HR1 and HR2. The time spent on the exam (TE) was obtained through the difference between final and initial time. The correlation and mean tests were considered statistically significant ($p<0.05$).

Results

Gynaecological and obstetric exams presented HR2 lower than HR1 during the two periods evaluated ($p<0.01$). The comparison established between the gynaecological exams in P1 and P2 demonstrated that HR1 and HR2 obtained in P2 were lower than those obtained in P1. Only the comparison between HRA presented $p<0.05$. Obstetric exams in P2 demonstrated higher heart rates than those observed in the gynaecological exams in P1 and P2. Significant differences ($p<0.05$) were only observed in the comparison established between HR2 and HRA of the gynaecological exams performed in P2. The correlation tests (r) applied for TE and HR2 indicated low intensity correlations. The gynaecological exam in P1 presented $r = - 0.1249$ ($p = 0.1937$). When the same exam was performed in P2, $r = - 0.1740$ ($p = 0.0130$) was observed and, during the obstetric exam in P2, $r = - 0.01352$ ($p = 0.9265$) was verified. This indicates that there was a tendency of HR2 to decrease while TE increased.

Discussion/Conclusions

The stress caused by the initial restraint increased the sympathetic activity and elevated HR1. Offering fruits and habituating the animals favored the parasympathetic modulation that would justify the decrease in the HR2. This was observed in gynaecological and obstetric exams.

OBSTETRIC ULTRASONOGRAPHY IN CAPTIVE OWL MONKEYS

Monteiro FOB, Coutinho LN, Pompeu ESS, Castro PHG, Maia CE, Silva KSM, Lacreta Jr ACC, Vicente WRR. Universidade Federal Rural da Amazônia. Av. Presidente Tancredo Neves, 2501 CEP: 66.077-530, Belém-Pará-Brasil.

Introduction/Purpose

Ultrasonography is a method that enables the monitoring of embryonic/fetal development and viability in humans and nonhuman primates (NHP). Even though it requires anesthesia in NHP, ultrasonography is both safe and non-invasive. It can be used to determine the date of conception and gestational age, estimate the date of parturition, and detect placental and fetal abnormalities. This study monitored the gestation of owl monkeys by ultrasound without chemical restraint, attempting to answer questions related to the gestational physiology of this species.

Methods

The study was conducted at the National Primate Center (Ananindeua, PA, Brazil). The obstetric exams were performed using the linear probe of 5-12MHz. Embryonic and fetal biometric data were obtained throughout pregnancy on three owl monkey (*Aotus azarai infulatus).* Measurements included mean sac diameter (MSD), crown-rump length (CRL), biparietal diameter (BPD), occipito-frontal diameter (OFD), head circumference (HC), head area (HA), abdominal circumference (AC), abdominal area (AA), and femur length (FL). The first third of gestation comprised the period between the first and the sixth weeks. The second third began in the seventh throughout the twelfth week and the last third included the period between the thirteenth and the nineteenth weeks, when parturition occurred. The determination coefficients (R^2) were individually calculated for each regression model, with a significance level of 5% probability.

Results

Three positive gestations were analyzed, from which two were carried out to its final stage and one was spontaneously interrupted at the end of the second third. It was only possible through the developmental signs visualization that began in the third week, with the appearance of the anechoic GS in the uterine fundus region. During the second third, it was possible to measure the MSD (until the eighth week) and CRL (until the tenth week). The measurements related to the BPD, OFD, HC and HA were obtained from the eighth week, the AC and AA were measured from the ninth week and the FL was only measurable from the tenth week. Twenty nine BPD, OFD, HC, and HA measurements were performed during three pregnancies (between 8th and 19th weeks of gestation). This data analysis indicated that parameters increased with gestational age in weeks according to linear and quadratic models. There was a progressive increase in size of the parameters with gestational age, which appeared to slow towards the term. The determination coefficients (R^2) were high for all variables analyzed. However, R^2 values were higher for the quadratic model, and that would justify its utilization.

Discussion/Conclusions

The female restraint and conditioning methods were important to allow the gestation ultrasonographic monitoring, enabling the study of chronological events related to the embryonic/fetal development in owl monkeys.

CORRELATION BETWEEN ULTRASONOGRAPHY AND CYTOLOGY EXAMS OF CERVICAL MASSES IN DOGS C.D. SCHAEFFTER, C.O.GHIRELLI, F.A.M. SANTOS, F.P. MEDEIROS, S. BURANELLO Núcleo Diagnóstico Veterinário, São Paulo, Brazil, 04708-001

Introduction/Purpose Ultrasonography of the ventral neck represents an especial challenge due to the complexity of the regional anatomic and the relatively small size of the structures and organs. The main clinical indication to perform neck ultrasound includes the evaluation of palpable masses in this region to identify its source, aspect and extension. In the Brazilian veterinary, cervical ultrasound still corresponds to small number of cases and few veterinarians are capable to perform this kind of exam, thus it isn't considered a routine exam. The aim of this study was to use ultrasonography to characterize cervical lesions and to correlate them with cytological findings.

Material and Methods The medical records of 11 dogs with ultrasonographic diagnosis of cervical mass and cytological report were included in this retrospective study. The ultrasonographic lesions were reviewed for lesion description including vascularization. All dogs had final cytological diagnosis.

Results

Ultrasound	Cytology
Well-defined, coarser texture, hypoechoic elongate structure in the submandibular region.	Salivar gland
Well-defined, mixed echogenicity heterogeneous multinodular mass. Mild central vascularization.	Malignant epithelial neoplasm
Multinodular coarsed hypoechoic structures in the submandibular region. Mixed vascularization, especially at the periphery	Lymphoma
Well-defined,oval structures with hypoechoic contents presenting little moviment involving the trachea.	Sialocele
Multinodular hypoechoic coarsed mass in the submandibular region. Intense mixed vascularization.	Melanoma
Oval heterogeneous mass sidewards to trachea, with cavities. Mixed intense vascularization.	Malignant epithelial neoplasm
Irregular mass with anechoic contents	Chronic inflamatory process
Multinodular hypoechoic masses in the left submandibular region. Intense mixed peripherical vascularization.	Lymphoma
Well-defined coarsed rounded structures. Intense vascularization	Malignant epithelial neoplasm
Hypoechoic heterogeneous mass sidewards to trachea. Intense vascularization. Oval hypoechoic coarsed area sidewards to trachea.	Malignant epithelial neoplasm
Heterogeneous mass sidewards to trachea. Small nodular structures with hyperechoic central areas. Intense vascularization.	Malignant epithelial neoplasm

Discussion/Conclusions The association between ultrasound and fine needle cytology contribute to the final diagnoses of cervical masses. The information collected in this study should be useful for ultrasonographers who do not have extensive experience scanning cervical region.

ULTRASONOGRAPHIC AND RADIOGRAPHIC APPEARANCE OF BILATERAL ECTOPIC URETEROCELE IN A DOG. Finardi J. C., Backes M. A. V., Backes F. S, Jabin V. C. P, Miranda M. D. Bionostic. Machado de Assis 218, Curitiba, Paraná, Brazil, 80330 370.

Introduction Primary ureteral disease is a relatively uncommon diagnosis in small animal practice. Abnormalities affecting the ureters may cause potentially serious secondary effects such as renal function impairment.
Contrast radiography used to be the main diagnostic imaging modality used for detecting abnormalities affection the ureters in small animals. However, the difficulties associated with the radiographic diagnosis are well recognized. It is somewhat difficult to visualize normal canine or feline ureters ultrasonographically. Conversely, diagnosis of various ureteral abnormalities is certainly possible in many instances. Ultrasonography is now becoming established in small animal practice as a useful diagnostic modality for the ureters, kidneys and bladder, and is tending to replace contrast radiography.
This report describes a case of bilateral ectopic ureterocele that was diagnosed with ultrasonography with validation with contrast radiography.

Methods A 2-month-old female Labrador retriever was presented with a history of urinary incontinence. On physical examination the dog was alert and in overall good health condition, except by the presence of urine dermatitis around the vagina. The blood urea nitrogen concentration was 7.6 mg/ dl and serum creatinine concentration was 0.55 mg/ dl. Abdominal ultrasonography was performed using 8.5 and 10 MHz linear probes. An intravenous urography was performed under general anesthesia. Contrast medium (ioexol) was administered by rapid intravenous *bolus* at a dose of 850 mg/ kg. Serial lateral and ventrodorsal radiographs were obtained immediately after injection of contrast.

Results The ultrasonographic findings included moderate dilatation of ipsilateral renal pelvis and ureters, absence of ureteral jets and ureters passing caudal to the bladder trigone. A rounded and thin-walled cavitary structure was seen inside the urinary bladder and a communication between this structure and the ureters was visible. Contrast radiography revealed bilateral hydronephrosis, tortuous and enlarged ureters passing caudal to the bladder trigone and a “cobra head sign” appearance within the urinary bladder.
A bilateral ectopic ureterocele was suspected and confirmed by exploratory laparotomy. Only the orifice of the right ureter was located normally at the lateral angle of the bladder trigone and the ureterocele was resected. The dog died postoperatively when returning from anesthesia.

Discussion In this case, there was a close correlation between the ultrasonographic and contrast radiographic findings for ureterocele. However, recent reports favors ultrasonography comparing with contrast radiographic for examination of certain ureteral lesions. Besides being a quicker and less costly method, ultrasonography does not involve use of contrast media or ionizing radiation and usually requires no sedation or anesthesia.
Although further studies are needed, this study suggests that ultrasonography should be considered as the first choice imaging modality for ureterocele diagnosis.

RETROSPECTIVE NEUROIMAGENOLOGICAL DIAGNOSTIC STUDY IN 45 DOGS WITH NEUROLOGICAL DEFICITS SUBMITTED TO BRAIN COMPUTED TOMOGRAPHY BETWEEN 2004 AND 2008 IN A REFERENCE CENTER OF SANTIAGO, CHILE.

E. Bosco, M.C. Gómez. Instituto Neurológico y Especialidades Veterinarias. Pepe Vila 25, La Reina, Santiago, Chile, 7880024.

Introduction Computed tomography (CT) it is a helpful tool for the diagnosis of many cases of neoplastic and nonneoplastic brain disorders in dogs. The advantage of CT relies on the ability to describe normal and abnormal anatomy, which facilitates the identification of neoplastic disorders, developmental anomalies, vascular disorders, inflammatory and degenerative diseases.
The main purpose of this paper is to present a retrospective study that was performed to 45 patients with neurological deficits in which a brain CT was undertaken. The study took place between 2004 and 2008 in the reference center of Santiago, Chile.

Methods The methodology used in this study, is a descriptive cadastre to the neuroimaging findings, after which different neuroimagenologic diagnosis groups where conformed. On a second stage, the relation between variables such as age, breed and sex was established. Also, the relevance of medium contrast administration was evaluated in order to determine the importance of such a procedure in effectiveness of such a technique on the detection of intracranial pathologies.

Results From the 45 analyzed computed tomographic imaging, 66,7% presented visible injuries, which were classified in the following groups: neoplasia/MEG, inflammatory, hydrocephalus, and vascular sequels, representing 30%, 20%, 36,7%, and 13,3% of the cases respectively.
The study didn't showed any significant statistical correlation between the analized variables ($p>0,05$).
In the pre-contrast images, the results showed the following results: 36,4% corresponded to vascular injuries, 36,4% to inflammatory and 27,2% to neoplastic injuries. In the post-contrast images, 75% were neoplastic and only 25% were inflammatory injuries.
In all the images that presented neurological anomalies, it was noticed that the tomographic findings were compatibles with some of the pre-diagnosis established before.

Discussion This technique was capable to identify injuries in 2/3 of the patients and the computed tomographic findings were compatibles with four groups of the neuroimageneologic diagnosis.
There was no statistical significance correlation between the analyzed variables.
In pathologies such as neoplasia/MEG, the administration of medium contrast was of significant importance, while in inflammatory pathologies was less relevant.
After concluding the study and the results were analyzed, it was shown that CT is an effective technique to corroborate the suspicion of intracranial injuries.

MRI FINDINGS OF MUSCULOTENDINOPATHY OF THE LATERAL HEAD OF THE GASTROCNEMIUS MUSCLE IN HERDING DOGS

C. Stahl[1], C. Wacker[3], U. Weber[3], F. Forterre[2], J. Lang[1], P. Hecht[3], D. Gorgas[1].
[1]Clinical Radiology, and [2]Division of Surgery, Department of Clinical Veterinary Medicine, Vetsuisse Faculty Berne, Länggassstrasse 124, 3012 Berne, Switzerland; [3]Tierärztliches Überweisungszentrum, Hauptstrasse 21, 4456 Tenniken, Switzerland

Introduction
Pelvic limb lameness without trauma history clinically localized to the lateral gastrocnemius head has not been described in dogs. The aim of the study was to describe magnetic resonance imaging (MRI) findings of this condition.

Methods
Medical records of two referral centers were reviewed for dogs that underwent MRI of the knee joint. Cases with MRI findings in the gastrocnemius muscle were selected and signalement, clinical signs, radiographic findings, and MRI findings were recorded. MR images were subjectively assessed for location, extend and border definition of altered signal intensity (SI), and contrast enhancement in the gastrocnemius muscle including the sesamoid bones, in the femur, knee joint and surrounding soft tissues.

Results
Nine dogs were included; all of them were herding dogs (eight Border Collies and one Australian Shepherd). Three dogs were male (one spayed) and six female (four spayed), with a mean age of 5.3 years (range 0.3 to 8.3 years) and a mean weight of 15.8 kg (range 9.5 to 22.5 kg). All dogs were presented with chronic right (5 dogs) or left (4 dogs) pelvic limb lameness, which was most obvious during the first steps of walking. The lameness was clinically localized to the region of the lateral gastrocnemius head; no signs of stifle joint effusion or instability were present. All dogs underwent MRI examination of one or both (2 dogs) knee joints. In all dogs altered SI was seen in the lateral head of the gastrocnemius muscle located around the sesamoid bone, reaching up to the origin at the femur and tapering distally with a high SI in T2-, T2*-w and STIR sequences and a iso- to mildly hyperintens signal to the surrounding musculature in T1-w sequences with marked contrast enhancement. Two dogs with bilateral MRI examination had mild changes in the clinically normal contra lateral limb as well. The majority of dogs showed abnormality of the lateral sesamoid bone including mineralization in the surrounding tissue. Contrast enhancement in the center of the sesamoid bone was seen in two skeletally immature dogs and in the dog with the most extensive lesion. No other changes in the musculature, bones, knee joint and surrounding tissues were recorded.

Discussion
The focal altered signal intensity located in the lateral head of the gastrocnemius muscle most likely represents a myotendinous strain and has not been described in dogs before. In human medicine it is reported to typically occur in superficial muscles at the myotendinous junction due to distraction or shearing forces, and is characterized by diffuse bleeding and interstitial edema, leading to the abnormal MRI findings. The gastrocnemius muscle is prone to strain injury due to its action across two joints and its superficial location. In humans, strain injuries in the medial head of the gastrocnemius muscle are well described and termed “tennis leg” due to their common association with this sport. The breed affiliation to Border Collies is striking, and a relation to biomechanical forces or motion pattern may be possible.

THE EFFECT OF A SALINE CHASER FOR CONTRAST ENHANCEMENT OF MULTIDETECTOR-ROW COMPUTED TOMOGRAPHIC ANGIOGRAPHY IN CATTLE

K. Lee, M. Kishimoto, J. Shimizu, T. Iwasaki, Y. Miyake, K. Yamada. Obihiro University of Agriculture and Veterinary Medicine, Obihiro, Hokkaido 080-8555, Japan.

Introduction

In bovine practice, no studies have concentrated on the condition of the contrast injection or dosage of contrast material. The purpose of this study was to evaluate experimentally the effect of a saline chaser for enhancement in contrast enhancement CT.

Methods

Nine calves were imaged in a crossover method for CT angiography. The calves were divided into two groups. The first group was administered a contrast injection (600 mgI/kg at 4 mL/s) followed by 50 mL of a saline chaser at the same rate as the contrast material. The second group was administered a contrast injection without a saline chaser. Attenuation values of the right and left maxillary arteries and dorsal sagittal sinus were measured. Analysis of differences with the paired t test was used to evaluate the statistical significance of the difference in attenuation between the two groups.

Results

The addition of the saline chaser to the contrast material resulted in a higher peak attenuation in the maxillary artery (244.45 ± 36.19 vs 202.20 ± 27.07, $p < 0.05$) and dorsal sagittal sinus (241.21 ± 31.51 vs 198.88 ± 21.09, $p < 0.05$).

Discussion

Results indicate that a contrast injection followed by saline chaser increased uptake in contrast enhanced CT.

COMPUTED TOMOGRAPHY IMAGING IN THE INVESTIGATION OF DOG HEADS- RETROSPECTIVE STUDY

Cardoso L.A., Teixeira M.A., Witz M.I., Fischer C.D., Pinto V.M. Universidade Luterana do Brasil – ULBRA Faculdade de Medicina Veterinária, Canoas, RS, Brasil CEP 92425-900

Introduction

Among the methods of image diagnosis the computed tomography (CT) is distinguished by its power of resolution and in the last 10 years it has increasingly been used. The objective of this study was to relate the changes found in CT dogs heads and it´s efficiency in such cases.

Method

During the period of 1 year, 110 CT of dog heads with clinical indication were performed. The animals were anesthetized for such exam and the axial tomography model GE CT Pace brand was used. There were two sequences of cuts, a simple and one with intravenous contrast medium in the transverse plane.

Results

Of the 110 examinations, 76% of cases had CT changes. In 42 cases (38%) were found hyperdense mass lesion and the other 42 cases (38%) were classified as other changes. The 42 cases of mass-type lesions were associated with neoplasic or inflammatory processes, 20 (48%) of them located in the upper respiratory tract; 15 (36%) in the central nervous system, probably intra-axial tumors; 7 (16%) cases of extra-axial tumors, involving soft tissues or skull bones. In the 42 animals that were classified having other changes, it was observed brain edema or hidroencefalia in 20 cases (48%), skull fractures in 9 (21%) and otitis in 6 (14%) dogs. In the 26 cases (24%) which there were no changes in the CT, 20 (77%) exams were to search brain lesions, 4 (15%) were specifically to the pituitary gland, two (8%) were for dentition evaluation and one was to evaluate the ear.

Discussion/Conclusion

This survey showed that CT was effective in identifying the type and location of dog’s head lesions in 76% out of 110 clinical cases in small animal practice.

TYPE I PROTRUSION WITH MIGRATION AND SEQUESTRATION IN DOGS: CORRELATIONS BETWEEN CLINICAL, RADIOLOGICAL AND MRI FINDINGS. N. Tudor[1], A. Mangrau[2], F.E. Grosu[1], H. Elefterescu[1], C. Vlagioiu[1]. [1]Faculty of Veterinary Medicine, Splaiul Independentei 105, Bucharest, Romania, 050097; [2]Phoenix Diagnostic Clinic, Calistrat Grozovici 1, Bucharest, Romania, 021105.

Introduction

Chondroid disc degeneration is often seen in chondrodystrophic breeds and it is characterized by dehydration and mineralization of the pulpous nucleus of the intervertebral disc. Annulus fibrosus tearing may occur leading to the dorsal extrusion of the dehydrate nucleus material into the vertebral canal and it compresses dura and the spinal cord in different percentages and determinates the Type I protrusion. The migrated disc may sometimes move away cranially or caudally into the vertebral canal with different clinical signs. This study describes some correlations between clinical, radiographic and MRI aspects of the Type I protrusion with cranial and caudal migration and sequestration of the calcified disc material into vertebral canal.

Methods

12 dogs between 5 and 9 years old (6.42 years average), 9 females and 3 males, with sensibility and motor neurological disorders of the hind limb in different degrees have been neurologically, radiographically and MRI evaluated. Radiographic exam has been performed at lateral and ventro-dorsal positioning. We obtained T1 TSE and T2 TSE MRI images in 3 perpendicular imaging planes using a 1.5 Tesla machine. The subjects were anesthetized and placed in sterno-abdominal recumbency.

Results

4 dogs were discovered with hindlimb monoparesis, 3 dogs with paraparesis and 5 dogs with paraplegia. Only one dog the radiological exam revealed an increased radio-opacity occupying 70% of the vertebral canal at the L5 cranial vertebra. Disc mineralization and narrowed disc space was seen at all the dogs. MRI established dorso-cranial migration with sequestration at 5 dogs (3 median-left paramedian and 2 right paramedian-median-left paramedian) and dorso-caudal migration with sequestration at 7 dogs (1 right paramedian, 3 left paramedian and 3 left and right paramedian-median).

Discussion/Conclusion

A strict correlation between neurological signs and radiographic showings couldn't have been made because almost the same radiographic changes were shown in all cases but they were with different symptomatology (from lameness to paraparesis and paraplegia). Only one dog with right hind limb lameness made an exception in radiography which revealed a fragment of the disc migrated caudal in medullar canal L5. MRI confirmed caudal disc migration and sequestration of the L4 disc material into L5 vertebral canal. Secondary there were right lateral recesses and foraminal stenosis. MRI also confirmed disc mineralization/degeneration, different degrees of narrowed disc spaces shown by radiography. MRI diagnosis is tightly related to each case's simptomatology. MRI's anatomic high fidelity characteristics and multiplanar capability makes it an useful technique for diagnosing and describing Type I disc protrusion with migration (cranial and caudal) and sequestration of the degenerated disc material into the vertebral canal.

COMPUTED TOMOGRAPHY ASPECTS OF CATS WITH RHINITIS AND SINUSITIS

R. Zanatta , J.C. Canola , V. Páfaro, T.C.F. Cintra
Current address: Universidade Estadual Paulista “Júlio de Mesquita Filho”, Campus Jaboticabal. Via de Acesso Prof. Paulo Donato Castellane, s/n, Jaboticabal, São Paulo, Brazil, 14884-900

Introduction

Sinonasal diseases are common in small animals, however is difficult to establish a definitive diagnosis due clinical signals are similar in different diseases of nasal cavity and paranasal sinuses and the diagnostic methods are limited. Computed tomography (CT) is a technique that allows the study of the body in slices, generating images without overlapping of anatomical structures.

Methods

Ten adults mixed-breed cats, with chronic signals of rhinitis and sinusitis were anesthetized and positioned in ventral recumbency for CT examination of the head. Transverse scans were completed at 3 mm intervals from the rostral extremity of the head until the atlanto-occipital articulation.

Results

The main findings in CT images in this study were opacification of frontal sinuses (ten cats) and opacification and the nasal cavity (nine cats). In six animals were observed extrasinonasal involvement, like increased opacification of tympanic bullae and lack of some teeth. Nasal septal deviation was observed in four cats. One cat had turbinate destruction and other nasal bony changes.

Discussion

Cats with inflamatory and neoplasic sinonasal diseases commonly had opacification of nasal cavity and paranasal sinuses. Septal deviation is observed in cats with chornic rhinitis, while destruction of nasal septal involvement occurs in cases of neoplasia. Turbinate osteolysis and extrasinonasal involvement are findings in rhinitis and neoplasia cases. The tomographic images acquired determine the localization and extension of the described alterations.

INTRAHEPATIC PORTOSYSTEMIC SHUNT IN DOG. COMPARISON OF ULTRASOUND AND COMPUTED TOMOGRAPHY FINDINGS – CASE REPORT.

Mauro Caldas Martins[1], Márcia Salomão[2], Juliana Jorge[3], Alex G. Adeodato[4], Marcelo A.Pinto[5]
1 MV, CRV- Imagem maurocaldas@crvimagem.com.br Av.Americas 505 Lj M Rio de Janeiro – RJ Brasil CEP 22631000
2 MV, PhD Universidade Federal Fluminense
3 MV, PhD CRV Imagem
4 MV, MSc CRV Imgem
5 MV, PhD, Fiocruz

Introduction

Portal venous anomalies result in reduction of total hepatic blood flow and inability to extract toxins from the liver of portal blood from the digestive tract and spleen. The clinical signs are growth retardation, lethargy, gastrointestinal disorders and hepatic encephalopathy with ataxia, depression, behavioral changes and seizures. The diagnostic image can be achieved by using portography, scintigraphy, ultrasonography (USG), computed tomography (CT) and magnetic resonance imaging (MRI). The portography is an effective study, but with greater technical difficulty and risk to the patient. Scintigraphy and MRI examinations are of limited availability in veterinary by technical and financial questions. The USG is a safe technique, and has been widely used in screening for liver injury but is operator dependent and not always characterizes
the change in sufficient detail to guide appropriate treatment. The angiography is a quick method, painless and minimally invasive with high efficiency and excellent vascular anatomical detail for surgical planning, the only drawback being the need for anesthesia. The objective of this study is to compare the images obtained by the techniques of USG and CT in a dog with suspected liver disease.

Material and Methods.

A one year old female Rottweiler with retarded development, anemia, apathy and elevated plasma concentrations of liver enzymes was referred to the CRV Imagem with suspected liver disease. The animal was initially subjected to USG examination with high-resolution Doppler, using an equipment P5 GE Logic ® and then to the spiral CT examination in HISPEED GE ® LXi in helical cut of 3.0 mm with a table increment of 3,0 mm, 180 MA, 0.8 seconds, 20 Kv without contrast and in portal phase with non-ionic iodinated contrast (662 mgI ioversol / kg) in soft-tissue algorithm (Std +) under inhalational anesthesia.

Results:

The USG showed a small liver and the presence of tortuous anomalous vessel in right hepatic lobe from the caudal vena cava and porta, with size of 1.3 cm and the turbulent color Doppler flow, compatible with the diagnosis of shunt portosystemic. In portal phase contrasted CT there showed a large caliber vessel connecting the portal vein to the intrahepatic vena cava flow forming an arc with length of 137mm, giving 16 mm in its length and 8mm thick at the most thin in the right lateral lobe, showing single intrahepatic shunt. The patient showed improved with dietary treatment. Surgery treatment is currently been discussed by owners.

Conclusion

The USG examination was an appropriate technique for the diagnosis of this intrahepatic portosystemic shunt , but the CT showed in greater detail the location, origin, destination, route and size of the shunt, therefore providing critical information to the therapeutic approach in the case reported.

SPLENIC VEIN THROMBOEMBOLISM IN DOGS - REPORT OF 2 CASES SUBMITTED TO CT EXAMINATION

Mauro Caldas Martins[1], Márcia Salomão[2], Alex G. Adeodato[3], Ana Luiza Pereira Brito[4], Alexandre Marques de Oliveira[4].
1 MV, CRV- Imagem maurocaldas@crvimagem.com.br Av.Americas 505 Lj M Rio de Janeiro – RJ Brasil CEP 22631000
2 MV, PhD Universidade Federal Fluminense
3 MV, PhD CRV Imagem
4 MV,

Introduction:

Splenic and portal vein thromboembolism is poor documented in dogs. The most common causes of this disorder in humans are related to pancreatitis, pancreatic cancer, gastric cancer, cirrhosis and hematopoietic changes. The thromboembolism of the portal system leads to the symptomatology of portal hypertension, which is described as increased pressure in the hepatic portal system with reduction of blood flow through the portal vein to the liver and possible leakage of ascites and other sings of liver failure. The diagnosis is usually made by ultrasound (USG) or by the necropsy findings. Computed tomography (CT) is the diagnostic method of choice for imaging in humans. The objective of this study is to report two cases of dogs with liver disease and ascites who were submitted for CT, with USG before, and the CT enabled the diagnosis of thromboembolism of the portal vein.

Material and Methods.

Dog 1: 9 years old male Labrador presenting with moderate ascites symptoms of liver failure and gastrointestinal changes with emesis. USG showed a liver with increased size and echogenicity, suggesting lipidosis or hepatitis, severe ascites and splenomegaly Dog 2: 8 years old female , with ascites, USG showed ascites, and an abdominal mass was observed near the left kidney. In both dogs the USG not viewed thrombi.. Both were referred to the CRV Imagem for CT scan. A Hispeed GE ® LXi in helical cut of 5.0 mm with a table increment of 5.0 mm, 180 MA, 1.0 seconds, 120 Kv without contrast and in portal phase with non-ionic iodinated contrast (662 MGI ioversol / kg) in soft-tissue algorithm (Std +), were used. The dogs were under inhalational anesthesia.

Results:

The portal phase contrast CT showed , ascites and splenomegaly in both patients, with increased size of the splenic vein and obstruction of its flow to the portal vein by thrombus, in Dog 1 the thrombus was in terminal portion of splenic vein and the Doq 2 in medium portion. Dog 1 was observed thickening of gastric mucosa and increase of pancreatic dimensions suggestive of congestive process. The patient evolved to death before the surgery of splenectomy and biopsy of the gastric mucosa, with the owner not allowing postmortem examinations.

Dog 2 presented heterogeneous and irregular mass, with high opacification in contrasted fase, around the cranial mesenteric artery, suggesting neoplasy. Splenectomy was performed. but the mass could not be removed surgically.

Conclusion

The use of Doppler examination in the USG should be increased in patients with symptoms of portal hypertension. CT proved to be an efficient method for diagnosis of thromboembolism of the portal system in animals should be evaluated and suggested as a method for further evaluation

MEASUREMENT OF BODY SURFACE AREA IN LIVING MICE USING MULTIDETECTOR-ROW CT

M. Miyoshi[1], M. Nishimura[1,2], K. Miyahara[1,2]
[1]Veterinary Medical Teaching Hospital, Obihiro University of Agriculture and Veterinary Medicine, Inada-cho, Obihiro, Hokkaido 080-8555, JAPAN; [2]United Graduate School of Veterinary Sciences, Gifu University, 1-1 Yanagido, Gifu, Gifu 501-1193, JAPAN

Introduction

Body surface area (BSA) is an important parameter for evaluation of physiological functions and for administration of anticancer drugs in both human and animals. Unfortunately, BSA is difficult to measure because of the complex architecture of the body. Therefore, the BSA (cm^2) of animals is generally estimated by multiplying the Meeh constant (k) by the 2/3 power of the body weight (BW, g). Dead animals can be skinned and the area of the skin measured, but it is difficult to determine how much to stretch the skin. Multidetector-row CT (MDCT) offers important advantages over conventional CT for three-dimensional (3D) data acquisition of subjects affected by respiratory movements. The purpose of this study was to measure the BSA of living mice using MDCT and to determine the k value for mice.

Methods

One hundred and ninety-two (96 male, 96 female) healthy mice at 4 to 19 weeks of age were used. Each mouse was anesthetized and positioned in ventral recumbency for whole-body CT scanning. All scans were performed on a 4-slice MDCT scanner with a slice thickness of 0.5mm. The BSA was determined from the CT images using high-speed 3D analysis software. After the BW and BSA were determined, the k value was calculated as the ratio of BSA (cm^2)/BW $(g)^{2/3}$.

Results

The overall BW was 35.2 ± 6.4g (18.1–48.1g). However, the overall BSA was 103.8 ± 12.7cm^2 (65.0–128.3cm^2). Therefore, the overall k value was 9.7 ± 0.2 (9.0–10.3).

Discussion

MDCT can noninvasively provide information about the BSA of living mice. Our method of measuring BSA and the data obtained in this study may be useful particularly in physiological, pharmacological and toxicological studies.

CHANGES DURING TIME IN MR IMAGES OF ISOLATED EQUINE LIMBS REFRIGERATED AT 4°C .

G. Bolen[1], D. Haye[2], R. Dondelinger[2], V. Busoni[1]
[1]Medical Imaging Section, Department of Companion Animals and Equidae, Faculty of Veterinary Medicine, University of Liège, Boulevard de Colonster, 20, Bat B41, 4000 Liège, Belgium. [2]Medical Imaging Section, Department of Clinical Sciences, Faculty of Medicine, University of Liège, CHU, Bat B35, 4000 Liège, Belgium.

Introduction: The use of magnetic resonance (MR) imaging is increasing to evaluate the equine digit. The majority of these clinical examinations are made on anesthetized horses which cause some risks for the horses. Therefore, a lot of experimental studies are made on cadaver limbs. The purpose of this work was to assess the MR signal changes of anatomical structures of the equine digit on cadaver limbs stored at 4°C to establish a simple protocol for preservation of the digit between the death of the animal and the MR examination.
Methods: Eight equine cadaver feet were scanned with a 1.5T MR unit within 12h after death (T0) and then after 1, 2, 7, 14 days (d) of refrigeration. After the last examination, 4 feet were warmed at room temperature for 24h and rescanned (TRT). The feet were preserved at 4°C in a fridge between each examination. The sequences used were Turbo Spin Echo (TSE) T1-weighted in transverse plane, TSE T2-weighted in sagittal plane, Short Tau Inversion Recovery (STIR) in sagittal plane and Double Echo Steady State (DESS) in dorsal plane. Qualitative analysis: Images at T0 were subjectively compared side by side for image quality and signal changes to images at T1d, T2d, T7d, T14d. Quantitative analysis: Signal to noise ratio (SNR) was measured and compared between examinations for bones, palmar proximal recesses of the DIPJ, digital cushion, deep digital flexor tendon. A linear model with a mixed procedure was done to test the SNR changes.
Results: A mild reduction of the synovial recesses size was subjectively detected. Visibility and margination of the anatomical structures of the digits and overall image quality were subjectively considered unchanged in all feet. No signal change was detected except for bones in STIR and in TSE T2 sequences. At T1d, bones were slightly hypointense and remained the same for the following examinations in TSE T2 sequence. At T1d, bones appeared homogeneously slightly hyperintense and remained the same for the following examinations in STIR sequence. Quantitative analysis showed significant SNR changes in bone marrow of refrigerated limbs compared to T0 in STIR and TSE T2 sequences. Warming at room temperature produced a reverse effect on SNR compared to refrigeration with a significant increase in SNR in TSE T2 sequence. After 14 days of refrigeration a trend to decreased SNR was found in bone marrow in TSE T2 and DESS sequences. The SNR in the deep digital flexor tendon showed no significant change.
Discussion: As the feet were not warmed at room temperature (except at TRT), these initial signal changes most likely reflect a lower temperature of the limbs between T0 and the following examinations after refrigeration and thus a decrease in T1 and T2 relaxations times. A reverse trend toward an increased SNR of bone marrow in T2w images and a decreased SNR in T1w images between T14d and TRT supports this hypothesis. Changes between T1d, T2d, T7d and T14d and changes between T0 and TRT more likely represent changes related to *post-mortem* interval and degradation of tissues and a trend to a decreased SNR was seen in most instances in bone marrow and the synovial recess. No change in images quality occurs in refrigerated limbs. Results of *post-mortem* studies should be interpreted considering temperature changes and length of *post-mortem* interval.

CT-DACRYOCYSTOGRAPHY OF THE NORMAL CANINE NASOLACRIMAL DRAINAGE SYSTEM. P.A. Rached, C. Nöller, G. Oechtering, J.C. Canola, E. Ludewig. Faculty of Veterinary Medicine, Department of Small Animal Medicine, University of Leipzig – An den Tierkliniken, 23, 04103 Leipzig.
Faculty of Veterinary Medicine, Department of Small Animal Medicine, São Paulo State University (Unesp-Jaboticabal), Via de Acesso Prof. Paulo Donato Castellane, s/n, Jaboticabal, Brazil. paula_rached@yahoo.com.br

***Introduction**:* Conventional radiographic cannulation dacryocystography is the most commonly used technique for evaluation of the nasolacrimal system (NLS). Recently, CT-DCG has been extensively employed in human patients. Systematic investigations of these techniques in dogs are not frequently observed in veterinary literature. The objectives of this study were to develop CT-DCG protocols for the evaluation of NLS structures in dogs and to evaluate the usefulness of 3D reconstruction techniques for visualization of this system.

***Methods**:* The superior lacrimal canaliculi of 32 cadavers of dogs were bilaterally canulated and contrast media was injected (Imeron®). Four scans were obtained, using a combination of two different slice thickness values (0.8mm and 2mm) and two different mAs values (300mAs and 50mAs), each one in two different slice orientations: perpendicular to the hard palate and 60° to 70° oblique to the hard palate. Sequences were blindly evaluated by two radiologists, who were instructed to determine the degree of visibilization of contrast media inside NLS structures, using a four-point scale (1–very good, 2-satisfactory, 3-unsatisfactory, 4- inadequate). For the comparison between slice orientations, the Wilcoxon matched-pairs signed-ranks test was used. Three-dimensional images were reconstucted using Volume Rendering (VR) and Maximum Intensity Projection (MIP).

***Results**:* All the structures obtained a high percentage of grades 1 and 2, especially the lacrimal sac and the nasolacrimal duct (>79%). Perpendicular slice orientation was significantly better ($p \leq 0.05$) for evaluation of superior and inferior lacrimal canaliculi and lacrimal sac. No difference between slice orientations ($p \geq 0.05$) was observed for the evaluation of the nasolacrimal duct. No difference on image quality was observed when the above mentioned slice thickness and mAs values were used. MIP allowed biometric evaluation of the NLS structures, such as measurement of the nasolacrimal duct length. For providing different contrast windows for visualization of NLS structures, VR allowed easier and faster differentiation between cranial structures, turning two-dimensional images into a realistic 3D anatomical portrayal.

***Discussion**:* CT-DCG is considered an acurate technique for evaluation of the nasolacrimal system in dogs. Bony and soft tissue structures can be easily differentiated. Without affecting image quality, all mAs and slice thickness tested in this study can be used for evaluation of the nasolacrimal system. We recommend the perpendicular slice orientation for evaluation of all structures of the NLS. Three-dimensional reconstructions were easily performed in all patients. MIP and VR techniques provide aditional information that can be important for anatomical studies and surgical planning.

MR-DACRYOCYSTOGRAPHY OF THE NORMAL CANINE NASOLACRIMAL DRAINAGE SYSTEM. P.A. Rached, C. Nöller, G. Oechtering, J.C. Canola, E. Ludewig. Faculty of Veterinary Medicine, Department of Small Animal Medicine, University of Leipzig – An den Tierkliniken, 23, 04103 Leipzig.
Faculty of Veterinary Medicine, Department of Small Animal Medicine, São Paulo State University (UNESP), Via de Acesso Prof. Paulo Donato Castellane, s/n, Jaboticabal, Brazil. paula_rached@yahoo.com.br

***Introduction**:* Conventional radiographic cannulation dacryocystography is the most commonly used technique for evaluation of the nasolacrimal system. Recently, MR-DCG has been extensively employed in human patients. Systematic investigations of this technique in dogs have not been described yet. The aim of this study was to develop MR-DCG protocols for the evaluation of NLS structures in dogs.

***Methods**:* The superior lacrimal canaliculi of 32 cadavers of dogs were bilaterally canulated and contrast media was injected (Omniscan®). MR protocol included transverse images obtained by T1W/3D/FFE, T1W/TSE and PDW/TSE sequences, each one in two different slice orientations: perpendicular to the hard palate and 60° to 70° oblique to the hard palate. Sequences were blindly evaluated by two radiologists, who were instructed to determine the degree of visibilization of contrast media inside NLS structures, using a four-point scale (1–very good, 2-satisfactory, 3-inadequate, 4- no visibilization). For the comparison between slice orientations, the Wilcoxon matched-pairs signed-ranks test was used.

***Results**:* MR showed a high tissue contrast definition. MR sequences required long scanning time (up to 9 minutes). For the evaluation of all structures, T1W/3D/FFE offered better results when compared to PDW/TSE and T1W/TSE. Evaluation of superior and inferior canaliculi showed high porcentages of grades 3 and 4 (>73%) in all sequences, whereas evaluation of the lacrimal sac and nasolacrimal duct showed high porcentages of grades 1 and 2 (>73%) when sequence T1W/3D/FFE was used. Oblique slice orientation was significantly better ($p \leq 0.05$) for evaluation of nasolacrimal duct. No difference between slice orientations ($p \geq 0.05$) was observed for the evaluation of the lacrimal canaliculi and lacrimal sac.

***Discussion**:* MR-DCG is not indicated for evaluation of small drainage structures, such as the lacrimal canaliculi. T1W/3D/FFE showed to be more indicated for evaluation of the NLS, as it allows the acquisition of a larger number of thin slices, providing more information than sequences T1W/TSE and PDW/TSE. Sequence T1W/3D/FFE can be indicated for evaluation of the lacrimal sac (perpendicular slice orientation) and of the nasolacrimal duct (oblique slice orientation), especially when adjacent soft tissue injury is suspected, due to its high contrast definition between cranial tissues.

STUDY OF ARTERIAL BRAIN VASCULARIZATION OF NORMAL DOGS USING MAGNETIC RESONNANCE ANGIOGRAPHY TECHNIQUES. O. Jacqmot, M.P. Heinen, A. Gabriel, F. Snaps. University of Liège, Faculty of Veterinary Medicine, Boulevard de Colonster, 4000 Liège Belgium Europe

Introduction: A good interpretation of many physiological and pharmacological experiments made on laboratory animals requires accurate data concerning the pattern of vascular supply of the brain, including information about the distribution, lengths and internal calibers of the various major arteries. The study of the vascularization of the canine brain could be done by classical angiography or as in human medicine by a less invasive procedure: Magnetic Resonance Angiography (MRA). To insure the results we have used the casts technique utilizing a synthetic resin.

Methods: Three normal healthy dogs of different breeds have been euthanized two hours before injecting the cerebral arteries with a synthetic resin (acryle and methylmetacrylate , Flowing type II, classe I manufactured by Biolux International, Belgium). The casts obtained of the cerebral vascular system were helpful to corroborate the results of the MRA. For the MRA experience, six normal female Beagle dogs premedicated 20 minutes before the test with 200µg/kg of butorphanol IV injected followed by an IV injection of 10µg/kg of medetomidine were used. The dogs were forced to fast 24 hours before the test and were injected with a paramagnetic contrast agent into the vena cephalic using a catheter. The paramagnetic contrast agent: Gadovist® (gadobutrol 1mmol/ml) is bolus injected at the dose of 0,1ml/kg at the speed of 2 ml/sec. The visualization is realized with care bolus and a phased array radio frequency (RF) coil acquisition (the dog is laying on ventral decubitus). The FLASH (Fast low angle shot) acquisition sequenced every 20 seconds with 0, 7 mm slice thickness and T1 weighted with a short flip angle (20°), needed contrast agent while the TOF (Time off flight) acquisition is based on flow related enhancement of spins entering into an imaging slice and calculates arterial results without contrast agent and with a better resolution but with longer sequences (300 seconds). The post processing tool is a Siemens Magnetom Trio (3 Tesla) Erlagen, Germany using a VB15 software and a 3D MIP (maximum intensity projection) graphic card.

Results: The Flash acquisition gives us a very accurate image of the cerebral arteries as well as of the veins, venous sinuses and venous plexus of the brain. The Tof acquisition is less accurate but gives only the imaging of the main cerebral arteries.

Discussion: Up to now, the diagnosis of the vascular brain diseases of dogs were post-mortem diagnosis, so no treatments were proposed. With the new techniques like MRA, a non invasive rapid technique, the clinicians have now the opportunity to study the arterial vasculature of the normal canine brain and also to give a diagnosis of brain diseases dragging modifications of the brain vascularization like tumors, hemorrhages,...

CORTICOTROPH ADENOMA IN DOGS WITH CUSHING′ S DISEASE: MORPHOLOGICAL AND FUNCTIONAL ASPECTS

Waldhorn J.G [(*)], Gallelli MF. [(**,*)], Castillo V. [(**, 1)] [(**)] Unit of Veterinary Endocrinology and * grant scholarship UBACyT Veterinary School Hospital. Universidad de Buenos Aires. Argentina. [(*)] Unit of Veterinary Radiology. Veterinary School Hospital. Universidad de Buenos Aires. Argentina.[1]corresponding address: vcastill@fvet.uba.ar

Introduction

Corticotroph adenoma is the most frequent pituitary tumor in dogs. Currently cut off values in order to discriminate between micro to macro adenoma have not been defined in veterinary medicine. In human medicine tumor sizes lower than 2,0 mm by Nuclear Magnetic Resonance Imaging (NMRI) are considered micro adenomas. Conversely in veterinary medicine this denomination is defined by less than 10 mm by Scan Computerized Tomography (SCT). Until recently, image diagnosis in dogs has been done with SCT. However NMRI would be the most precise image diagnosis method for detecting pituitary tumors

ACTH and α- MSH secretion pattern has not been established at the moment neither the differences between micro and macro adenoma in relation to hormone production in dogs with Cushing´s Disease(CD).

The aim of the present study was to determinate a cut off value to discriminate micro vs. macro adenomas as well as their hormone secretion pattern.

Material and methods

107 dogs with CD were studied. According to their tumor size (height), by NMRI on sagital slice, were divided into two groups: intraselar (IS) and extraselar (ES). A limit was established considering Turkish Chair top in the above mentioned slice.

ACTH and α- MSH were measured by IRMA (immune radio metrical assay). These hormone concentrations were analyzed in order to find if they were related to the adenoma size. Values of tumor size are expressed as median and range, and hormone values are expressed as mean ± SD. A multiple linear regression was used to evaluate if ACTH and α-MSH secretion was related to the size of the adenoma and its IS and ES projection. $P<0.05$ was considered significant

Results

2/3 of tumors were ES and 1/3 IS. Considering every tumor (107) median was 6 mm (3 – 115). ES size tumor was 7.2 mm (6 – 115) and IS tumor was 4 mm (3 – 5.5).

Respect to hormones, equimolar secretion of ACTH and α-MSH was observed in 50.5% of cases, ACTH secretion was greater in 16,8% while α-MSH predominated in the remaining 32,7%. Correlation was found between ACTH vs. tumor size ($r=0.37$; $p<0.05$) while α-MSH did not present significant differences.

Discussion

There are differences between ES and IS respect to ACTH secretion but not to α- MSH production. NMRI is a certain method to show differences between micro and macro adenomas, taking account Turkish Chair on sagital slice limit independently of dog size, being classified as IS and ES.

Acknowledgements

Research grant from UBACyT V009

THREE – DIMENSIONAL ASSESSMENT OF SARCOMAS IN CATS, USING COMPUTERISED – TOMOGRAPHY COUPLED WITH DESIGN-BASED STEREOLOGY– A CASE REPORT. C.S. Carneiro[1], A.A.C.M. Ribeiro[2], T.A. Costa[1], S.P. Gomes[2], F.R. Oliveira[2], A.C.B.C. Fonseca Pinto[1], J.M. Matera[1]. University of São Paulo, College of Veterinary Medicine and Animal Science, Department of Surgery[1]. Laboratory of Stochastic Stereology and Chemical Anatomy[2], Av. Prof.Orlando Marques de Paiva, 87 CEP 05508-270 - Cidade Universitária "Armando de Salles Oliveira" – São Paulo/SP – Brasil.

Introduction

The unbiased estimation of sarcoma volume in cats is useful to determine animal therapy. More recently, new imaging techniques i.e. computerised tomography (CT) plays an important role helping oncologists improve the diagnosis of several neoplasias. Increasingly, CT-scan is associated with cutting-edge design-based stereology, which uses stochastic methods to estimate sizes of biological structures, irrespective of their shape, distribution or orientation.

Methods

One seven-year-old male cat weighing 6.6kg was diagnosed with a sarcoma through two computerised tomography (CT), pre and post-chemotherapy. Subsequently, the animal was subjected to a four-cycle chemotherapy, i.e. doxorubicin (1.5mg/kg/IV) each 21 days. Finally, the sarcoma volume was estimated using state-of-the-art design-based stereology, i.e. Cavalieri's principle intermingled with computerised tomography, giving all parts of sarcoma the same chance of being sampled: systematic, uniform and random sampling (SURS).

Results

The first CT depicted a two-node irregular mass, extending from vertebra L5 to the proximal third of the right femur. Mass length, thickness and width were: 10 cm, 4.2 cm and 3 cm, respectively, and compromised some abdominal muscles: *m obliquus abdominal externus, m. sartorius* and tensor fascia lata (TFL) muscles. The patient has not side-effects during treatment. After the chemotherapy was finished, a 60%-decrease was observed when palpating the tumour, although a second CT-scan depicted no reduction in the tumour dimensions. Stereological estimates are given below as value (CE), where CE is the coefficient of error of the estimate. The pre-chemotherapy sarcoma volume was 2.23 cm^3 (0.04). After a four-cycle treatment, the post-chemotherapy sarcoma volume was 1.60 cm^3 (0.05).

Discussion

CT-scan per se did not show any change in sarcoma dimensions, especially in the tumour volume. However, when CT-scan was combined with design-based stereology, a chemotherapy-induced 28%-decrease in the sarcoma volume was observed. The reduction in the sarcoma volume matched the previous clinical finding, which suggests that the chemotherapy scheme was effective. By the same token further studies are warranted using imaging diagnosis techniques and design-based stereology to unbiasedly and accurately assess tumour dimensions during animal therapy.

BIOMEDICAL PROTOTYPING BASED ON COMPUTERIZED TOMOGRAPHY (CT) OF THE MAXILLOFACIAL REGION OF THE DOG

E.P. Freitas, S.C. Rahal, L.C. Vulcano, *J.V.L. Silva, *G.H.L. Paschoal, *A.M. Silva. School of Veterinary Medicine and Animal Science, Unesp Botucatu – Rubião Júnior s/n, Botucatu – São Paulo, Brazil, 18618-000. * CTI (Centro de Tecnologia da Informação Renato Archer) – Rodovia D. Pedro I, Km 143,6 - Campinas – São Paulo, Brazil, 13069-901.

Introduction: The importance of rapid prototyping (RP) in the biomedical sector has been increasing steadily during the past decade in human medicine, however, little known in veterinary medicine. Rapid prototyping is a technique used to produce stereolithographical models based on digital images such as computerized tomography (CT). Good results are highly dependent on the acquisition of computed tomography images and their subsequent manipulation by means of specific softwares. Whereas there are few studies about the rapid prototyping in veterinary medicine, the aim of this study was to evaluate the acquisition and manipulation of computed tomography images of the maxillofacial region of the dog for biomedical prototyping.

Methods: This study was approved by the Veterinary School Ethical Committee. A computerized tomography (CT) examination was performed on the head of a adult male dog cadaver. Sequential transverse images were acquired on a helical Scanner (Shimadzu SCT-7800CT) with the head placed in a dorsal position. The scanning parameters were 120kVp, 110 mA, 1.0 mm slice thickness, pitch of 1.0, and 1 s/rotation. The images were reconstructed in 3D format with the software InVesalius. The InVesalius software was also used to edit and measure the original 3D virtual model obtained directly from CT scan, and the Magics® X SP2 was used to generate the final model to the prototype machine. This physical model was used to evaluate the quality of reconstruction of the anatomy of a dog's head.

Results: The acquisition and manipulation of CT images of the maxillofacial region of the dog allowed the following advantages: excellent reproduction of thin structures, good dimensional accuracy, bone verisimilitude and autoclave sterilizable of the biomedical prototyping.

Discussion: Biomedical prototyping from CT images has shown to be an innovative solution in the preoperative planning and to minimize the time of the surgery. The rapid prototyping model allows the construction of physical objects reproducing anatomic structures, however only is possible by means of an integration of medical images acquisition and manipulation with computer-aided design (CAD) and rapid prototyping (RP) techniques, therefore involving multidisciplinary teams. The disadvantage in veterinary medicine is that the utilization of such prototypes is still restricted, because of the high production costs involved. However, it is probable that this limitation will be overcome by the interdisciplinary utilization of this method, increasing the accessibility to biomedical prototypes.

STANDARIZED UPTAKE VALUE (SUV) OF 2-DEOXY-2-[^{18}F] FLUORO-$_{D}$-GLUCOSE (^{18}FDG) WITH POSITRON EMISSION TOMOGRAPHY /COMPUTERIZED TOMOGRAPHY (PET/CT) IN NORMAL CAT. Y. Cho, J. Kim, J. Ko, H. Lee, M. Kim, N. Kim, K. Lee. Department of Veterinary Radiology, College of Veterinary Medicine, Chonbuk National University, 664-14, 1 ga, DuckJin-dong, Jeonju 561-756, Republic of Korea.

Introduction; PET/CT could be becoming available in veterinary medicine and science. The normal biodistribution of 2-deoxy-2-[18F]fluoro-D-glucose (^{18}FDG) in normal dog's major organs was reported. To the author's knowledge, no study in normal cats using PET/CT was established.

Methods; Dynamic PET data was acquired in list-mode acquisitions with transaxial field-of-view (FOV) PET/CT scanner with a 605mm, lutetium oxyorthosilicate(LSO) in five normal cats. Regions of interest (ROIs) were manually drawn over left ventricular free wall, left ventricular blood pool, liver, spleen, left and right renal cortices. Standardized uptake values (SUVs) of these organs were calculated for 5-min frames over the 95 min acquisition.

Results; Uptake of ^{18}FDG within the major organs except left ventricle and blood pool showed declining tendency gradually. Uptake of ^{18}FDG within both renal cortices was high at beginning of study (right kidney: SUV 5.27±0.74, left kidney SUV 4.58±0.49) which were highest level among organs examined. The decrease in SUV was rapid after injection with a plateau occurring after 30 minute (right kidney: 0.5-h SUV 2.65±0.25, 1-h SUV 2.04±0.21, 1.5-h SUV 1.69±0.29; left kidney: 0.5-h SUV 2.63±0.13; 1-h SUV 2.008±0.34, 1.5-h SUV 1.78±0.32). Uptake of ^{18}FDG within the hepatic parenchyma was low (SUV 2.86±0.62) compared to the kidney at the beginning of study. A steady decline in SUV was quite similar to the kidney (0.5-h SUV 1.45±0.29; 1-h SUV 1.00±0.20, 1.5-h SUV 0.78±0.14). SUV of ^{18}FDG within the spleen was low (injection SUV 1.54±0.83; 0.5-h SUV 1.04±0.28; 1-h SUV 0.82±0.21, 1.5-h SUV 0.66±0.14). Uptake of ^{18}FDG within the myocardium was minimal.

Discussion; This SUV data from parenchymal organs of normal cats compares positively with those of normal humans and dogs, and will be used as a reference data in feline studies using PET/CT. Additionally; PET/CT can provide higher quality images over shorter examination times than conventional PET.

Key words: standardized uptake value (SUV), PET/CT, ^{18}FDG, cat.

MULTIDETECTOR CT CEREBRAL ANGIOGRAPHY AIDS DIAGNOSIS OF INTRACRANIAL NEOPLASIA IN A DOG. R. Hagen, F. DelChicca, L. Galeandro, F. Steffen, M. Hilbe, M. Makara. Division of Diagnostic Imaging and Radio-oncology, Vetsuisse-Faculty, University of Zürich, Winterthurerstrasse 260, CH-8057 Zürich, Switzerland.

Introduction: CT is well established to diagnose intracranial disease in both human and veterinary medicine. Even though MRI is superior in depicting the intracranial structures, many institutions do not have access to MRI. Iodinated contrast medium improves soft tissue contrast and highlights areas of impaired blood- brain barrier. In the case presented here, a CT cerebral angiography and contrast study were performed using a multidetector CT unit[@]. Since multidetector CT allows for fast scanning time, a cerebral arteriogram could be recorded, which demonstrated a space-occupying lesion that did not show convincing delayed contrast enhancement.

Materials and Methods: An 11-year old male castrated Airedale Terrier presented to the Veterinary Hospital of the University of Zürich for investigation of an acute episode of seizure. Standard clinical and neurological examinations lead to suspicion of an intracranial lesion. Pre- and post-contrast CT scans of the head were performed under general anaesthesia. 2ml/kg iodinated high-osmolar contrast medium* was administered via a cephalic catheter, using a power injector. A pre-contrast, an arterial phase and a 120s delayed post-contrast study were recorded. Scanning was started when contrast medium was visible in the carotid artery. Contiguous transverse images were obtained and reconstructed in algorithms for bone and soft tissue detail with a slice thickness of 0.75 and 3mm.

Results: No bony abnormalities were detected. Mineralization of the cartilage of the external ear canals was present. The right lateral ventricle was not clearly delineable and there was moderate midline shift to the left side with deviation of the falx cerebri. During contrast administration, common carotid artery enhancement was clearly visible and image acquisition was started without delay. Branches of the carotid artery, intracranial and meningeal vessels enhanced well. The midline shift became more obvious, partially outlined by the enhancing cerebral and meningeal vessels. Almost complete obliteration of the right lateral ventricle was present. The inter-thalamic adhesion was poorly visible. The choroid plexus of the 4th Ventricle did not show contrast enhancement, suggesting increased intracranial volume/ pressure and a mild degree of cerebellar herniation was suspected. In the post-contrast images, no distinct abnormal enhancement was seen. An intracranial, intraaxial mass was diagnosed and the owners elected euthanasia. On post-mortem examination, a midsagittal section of the frozen skull confirmed mild cerebellar herniation. Histopathological diagnosis was gliomatosis cerebri in the area of the thalamus.

Discussion: Diagnosis of this intraaxial neoplasia that did not demonstrate convincing contrast enhancement was aided by CT angiography, which showed the location and extent of the lesion more clearly. CT angiography also indicated increased intracranial volume/ pressure by lack of contrast accumulation in the choroid plexus, suggesting its compression. CT angiography is relatively easy to perform with a multislice helical CT scanner. Since scan time is quick, a pre-contrast and two contrast studies can be performed within reasonable time. In this case we could demonstrate an intracranial space-occupying lesion, which was at post mortem confirmed to be a tumour, diagnosed as gliomatosis cerebri.

[@] Somatom Sensation Open, Siemens AG, Medical Solutions, Erlangen, Germany; * Telebrix®, 350mgI/ml, Guerbert, Zürich, Switzerland

ENDOSCOPIC AND HISTOPATHOLOGY'S USE IN AID OF DUODENITIS IN DOGS .

F.A.B. Auler, J.F. Godoy, F.N.Yoshitoshi. Provet. Av.Divino Salvador,774 04078-012 São Paulo BRAZIL.

Introduction: Enteritis is common in routine veterinary clinic. The most common clinical manifestation is diarrhea, other symptoms such as vomiting, weight loss and inappetence are commonly associated. Laboratory tests and imaging are indicated for this diagnosis. Many cases respond to usual therapy, but in some chronic cases, the answer is not expected, requiring diagnostic tests with more specific, and its confirmation comes from intestinal biopsy followed by histopathological analysis. As techniques for collecting intestinal material are shown in open surgery, laparoscopy and endoscopy. Each technique has its advantages and disadvantages, and the endoscopic procedure is little traumatic, little invasive, fast and the aspect of the intestinal mucosa can be viewed.

Materials and methods: Data collection was performed in São Paulo, Brazil, in the year 2008. Endoscopy were selected from 17 dogs of various breeds, all presenting emesis and just some dogs with diarrhea , but the duodenitis were diagnosed by histopathology. All dogs were submitted to general anesthesia inhalation. We used a fiberendoscopic of 9.8 mm, image capture, halogen light source, surgical aspirator, forceps for endoscopic biopsy. Were collected from three to ten fragments in the stomach and duodenum of dog and preserved in formalin to 0.9% being sent to histopathology. Of the 17 dogs, 11 were males and six females, 12 to 144 months of age (mean 57.2 months). In all 17 procedures was seen to macroscopy endoscopic gastritis and duodenal mucosa in 11 patients showed images suggestive of duodenitis as hyperemia and granularity.

Discussion: In this study, six of the selected patients showed no change in the macroscopy duodenal mucosa, but the histopathological analysis of 17 cases confirmed duodenitis proving to have greater diagnostic accuracy compared with endoscopic imaging, corroborating with other authors. The results from this study, certainly demonstrate that gastroduodenoscopy is safe and effective in collecting material and direct evaluation of the mucosa, but the image quality of the fiberendocopy is limited, is still incomplete in the diagnosis of duodenitis, but perhaps with the advent of video-endoscopy with magnification image of up to 50 times and high resolution, to complement the endoscopic diagnosis with higher specificity to allow the image expansion with villi and crypt's standard definition of intestinal mucosa pattern.

RADIOLOGIC IMAGES AT THORACIC CAVITY OF GOLDEN RETRIEVER DOGS AFFECTED BY MUSCULAR DYSTROPHY

F. R. Alves, D. K. Abreu, M. P. Brolio, R. A. Fernandes, C. C. Souza, C. V. Wenceslau, Carlos Eduardo Ambrósio, Ricardo Romão Guerra, Maria Angélica Miglino, F. R. Alves.
Department of Surgery - Faculty of Veterinary Medicine and Zootechnics, University of Sao Paulo. Av. Prof. Dr. Orlando Marques de Paiva, 87, Sao Paulo, SP, Brazil, 05508-270.

Introduction: The Duchenne's muscular dystrophy (DMD) in humans is a recessive X-linked neuromuscular disease, caused either by the absence or dysfunction of the dystrophin. Clinically it is characterized by severe alteration in the skeletal musculature, resulting in precocious death of the affected patient. In Golden Retriever dogs, the mutation that determines the muscular dystrophy occurs spontaneously and the extensive homology among the pathogenesis of DMD and of Golden Retriever muscular dystrophy allows qualifying the dog as the main substitute of humans in the clinical tests of new therapies. Other systems can be changed in dystrophic humans and animals.

Methods: Therefore, for identifying internal organs abnormalities in twelve GRMD dogs were made examinations by radiography of thoracic cavity.

Results: These examinations revealed this tissue predominantly to be interstitial and alveolar pattern of the lung, developing pneumonia and pulmonary edema. Cardiomegaly was observed with a principal circulatory disorder in thoracic cavity. Displacement of the trachea and heart silhouette was caused by thoracic mega esophagus. Morphological modifications in the diaphragmatic cupola identified with cranial protrusion into the thoracic cavity and hiatal hernia characterized by stomach protruded upward into the caudal mediastinum. Necropsy founds revealed pleural effusion, pulmonary emphysema and injuries compatible like a degenerative and metaplasic process of the diaphragmatic and intercostals muscles.

Discussion: Radiography examination was considered an essential auxiliary diagnostic for identification of cardiac and respiratory disease in golden retriever dogs affected by muscular dystrophy, availing to identify primary pulmonary process, providing the establishment of suitable therapeutic treatment, a hardest problem in an advantage course of this pathology.

Key word: Muscular Dystrophy, Duchenne, golden retriever dog, radiology.

APPLICATION OF FLUOROSCOPY IN THE TREATMENT OF A BITCH URETRAL STENOSIS USING CORONARY STENT

Witz MI, Raudales JC, Cardoso LA, Teixeira MA, Fischer CD, Allgayer MC. Universidade Luterana do Brasil – ULBRA Faculdade de Medicina Veterinária, Canoas, RS, Brasil CEP 92425-900

Introduction

Interventional radiology procedures are minimally invasive, and cause less pain, morbidity and mortality than conventional open surgery. Interventional radiology is in constant evolution; however the techniques are less standardized than surgical techniques.

Method

A three month-year-old, Chow Chow female dog, with a run over record of three weeks showing progressive difficulty to urinate. The cystography of the vagina demonstrated stenosis in the distal urethra. A retrograde cystourethrogram was carried out with the animal under general anesthesia, where the bladder was filled with physiologic solution and iodine contrast in the same proportion. After manual compression of the bladder forcing the passage of the contrast through the urethra, it was verified moderate dilatation of the proximal urethra, with a severe and long obstruction in the transition segment from medial to distal, with minimal passage of the contrast solution. An attempt of dilatation using balloon catheter (2.5 X 15 mm 8 atm) was carried out, however the result was not satisfactory. Then, there was the option of implanting a coronary metallic stent *Tsunami Gold** (Terumo Co., Japan) expanded to nominal pressure of 10 atm, followed by the optimization of the implant with balloon catheter (3.5 X 18 mm) at high pressure (20 atm).

Result

A new retrograde cystourethrogram was carried out which demonstrated reconstruction of the urethral canal with adequate passage of the contrast solution. Laboratory evaluations indicated the return to a normal renal function. Soon after this procedure, the animal urinated normally.

Discussion/Conclusion

Due to potential benefits gained for the patient through state-of-the-art interventional radiology procedures associated to the use of the stent is an alternative for the treatment of other pathologies related to hollow organs. Although having a satisfactory result using the implant of the coronary stent in this stenosis urethral case, further studies should be carried out in order to confirm the viability of the technique as well as the attendance of the patient for a longer period.